Application of GIS for modelling of the spatial distribution of rainfall. October l996.

Author:
Luk, K. C.; Ball, J. E.

Publication details:
Report No. UNSW Water Research Laboratory Report No. 191
0858240149 (ISBN)

Publication Date:
1996

DOI:
https://doi.org/10.4225/53/57a400a89062e

THE UNIVERSITY OF NEW SOUTH WALES
water research laboratory
Manly Vale N.S.W. Australia

APPLICATION OF GIS FOR MODELLING OF THE SPATIAL DISTRIBUTION OF RAINFALL

by

Kin C Luk and James E Ball

Research Report No. 191
October 1996

THE UNIVERSITY OF NEW SOUTH WALES
WATER RESEARCH LABORATORY

APPLICATION OF GIS FOR MODELLING OF THE SPATIAL DISTRIBUTION OF RAINFALL

by

Kin C Luk and James E Ball

https://doi.org/10.4225/53/57a400a89062e

Research Report No. 191
October 1996

BIBLIOGRAPHIC DATA SHEET

Report No. 191	Report Date: October1996	ISBN: 0/85824/014/9

Title

APPLICATION OF GIS FOR MODELLING OF THE SPATIAL DISTRIBUTION OF RAINFALL

Author (s)

Kin C Luk, MEngSc, MIEAust, MHKIE
James E Ball, ME, PhD, MIEAust, MASCE, MIAHR

Sponsoring Organisation

Australian Research Council (ARC)

Supplementary Notes

The work reported was carried out and published under the direction of the Director of the Water Research Laboratory.

Abstract

This report describes a generic procedure developed in a geographic information system (GIS) for the estimation of spatial distribution of rainfall over an urban catchment. Five different techniques, namely, Thiessen Polygon, Inverse Distance Weighted, Kriging, Trend and Spline, were implemented in the GIS to estimate point values at ungauged sites as well as average values for subcatchments. The basic principles of the techniques were outlined. In comparing the alternative techniques, both visual and arithmetic comparisons were established. It was found that using spline surfaces within a GIS produced robust and accurate estimates of rainfall and enabled real-time estimation of spatially distributed patterns. The use of a generic GIS for rainfall modelling enables the more accurate and sophisticated techniques to be used by a wide range of users.

Distribution Statement

For general distribution

Descriptors

Generic; Geographic Information System (GIS); Spatial Distribution of Rainfall

Identifiers

Number of Pages: 90	Price: On Application.

ACKNOWLEDGMENT

The authors wish to acknowledge the Australian Research Council (ARC) for providing the funding and support for this study.

In addition, the authors would like to express their sincere thanks to the people who contributed to this project. Dr Stephen Lee and Mr Stephen Lynch of the Upper Parramatta River Catchment Trust are gratefully acknowledged for providing data for this study. Thanks also go to Mr Andrew Hee and Mr Richard Beecham of the Department of Land and Water Conservation for their encouragement and for providing useful literature papers for this project.

SUMMARY

Since their development, Geographic Information Systems (GISs) have attracted much attention in many fields of science and technology, such as natural resources management, transportation planning, and water management, due to their capability for handling spatial information.

Initially, the application of GIS was mainly for storing and organising spatial information in digital format. Following the rapid development of computer technology, the capability and functionality of the GIS have been much enhanced. Consequently, the GIS has gained a much wider scope of applications; notably the GIS can now be used to analyse and correlate spatial information from different sources.

The present study explores a new application for GIS; this application is the modelling of the spatial distribution of rainfall. This is demonstrated using a commercially available GIS package, ARC/INFO. A set of powerful and general-purpose programs written in the ARC/INFO macro programming language was developed in this study to automate the rainfall modelling. With some modifications, these programs can be applied for real-time estimation of spatially distributed rainfall patterns. These programs can be used by any ARC/INFO user and the programs can be made applicable to any catchment configuration.

These programs utilised five ARC/INFO functions to estimate the spatial distribution of rainfall on an urban catchment in Western Sydney, Australia based on algorithms using Thiessen Polygons, Inverse Distance Weighted, Kriging, Trend (polynomial) and Spline Interpolation. The background theory of these algorithms were explained and their merits and shortcomings highlighted. These algorithms were evaluated and compared for both artificial and real rainstorm events.

The primary aim of the comparison was to develop general guidelines for use of the alternative algorithms. It was aimed also at promoting the application of the more accurate and sophisticated algorithms. With the automated procedure developed in this study, the use of such sophisticated algorithms can be as easy as the simpler algorithms.

CONTENTS

1. INTRODUCTION 1

1.1 General 1
1.2 Outline of the Study 5

2. THE UPPER PARRAMATTA RIVER CATCHMENT 7

2.1 Catchment Details 7
2.2 Available Data within the Upper Parramatta Catchment Area 9
2.3 Rainfall-Runoff Model 10

3. ALTERNATIVE RAINFALL MODELS 12

3.1 Thiessen Polygons 12
3.2 Inverse Distance Weights 14
3.3 Kriging 15
3.4 Trend Surfaces 18
3.5 Spline Surfaces 19

4. LITERATURE REVIEW OF RELATED WORKS 21

4.1 Spatial and Temporal Distribution of Rainfall on Storm Runoff 21
4.2 Estimation of Areal Mean Rainfall 23
4.3 Application of GIS in Water Management Modelling 25

5. ARC/INFO - AN OVERVIEW 27

5.1 General 27
5.2 Data Structure 27
5.3 Grid Map Structure 28
5.4 ARC/INFO Commands and ARC Macro Language (AML) 29

6. IMPLEMENTATION OF THE RAINFALL DISTRIBUTION MODELS 30

6.1 General 30
6.2 Naming Convention 30
6.3 Data Documentation 32
6.4 Database Development 32
6.4.1 Primary Coverages 33
6.4.2 Primary Grid Maps 34
6.5 AML Procedure 37
6.5.1 General 37
6.5.2 Logic and Flow Chart of Operations 37

7. COMPARISON OF ALTERNATIVE RAINFALL MODELS 41

7.1 General 41

7.2 Testing Data 42

7.2.1 Artificial Rainfall 42

7.2.2 Real Data 44

7.2.3 Hypothetical Case – Rain Gauge Malfunctioning 48

7.3 Results and Comparison 49

7.3.1 General 49

7.3.2 Artificial Storm Event 50

7.3.3 Real Storm Events 66

7.3.4 Summary of Comparison 83

8. CONCLUSION 86

9. REFERENCES 88

APPENDIX A – TECHNIQUES NOT AVAILABLE IN ARC/INFO A1

APPENDIX B – LIST OF DATA FILES, PROGRAMS AND MAPS B1

APPENDIX C – DATA DICTIONARY C1

APPENDIX D – QUALITY AND ACCURACY REPORT D1

APPENDIX E – ESTIMATION ON THE ARTIFICIAL STORM EVENTS E1

APPENDIX F – ESTIMATION ON THE REAL STORM EVENTS F1

LIST OF TABLES

1. Accuracy of Rainfall-Runoff Models (after Urbonas et al. 1992)
2. Descriptors for Maps
3. Primary Coverages
4. Comparison of Subcatchment Areas
5. Artificial Rainstorm Event
6. Two Real Rainstorm Events
7. Comparison of Subcatchment Rainfall Estimated by Alternative Rainfall Models
8. Predicted Peak Rainfall Intensities
9. Estimation of the Missing Values for Gauges 1 and 7
10. Estimation of Areal Mean Rainfall Before and After Omission of Two Gauges
11. Comparison of Rainfall Estimation for Two Real Storm Events
12. Insertion of Missing Values for the 5 Nov 92 Storm Event
13. Insertion of Missing Values for the 6 Nov 92 Storm Event
14. Estimation Before and After Omission of Two Gauges for the Event on 5 Nov 92
15. Estimation Before and After Omission of Two Gauges for the Event on 6 Nov 92
16 Summary of Comparison for the Artificial Rainstorm Event
17 Summary of Comparison for the Real Rainstorm Events

LIST OF FIGURES

1. Location of the Study Catchment
2. The Upper Parramatta River Catchment
3. Subcatchment Boundaries of the Upper Parramatta River Catchment
4. Thiessen Polygons for the Upper Parramatta River Catchment
5. A Typical Semivariogram
6. Naming Convention for a Map
7. Subcatchment Grid of the Upper Parramatta River Catchment
8. Comparison of Areas Approximated by Different Grid Sizes
9. Flowchart of Operations Needed to Create the Rainfall Model by Thiessen Polygon Method
10. Theoretical Distribution of an Artificial Rainstorm Centred at (302250, 6259250)
11. Track of Storm Centres of an Artificial Moving Storm
12. Daily Rainfall Depth of a Real Storm Event on 5 Nov 92
13. Daily Rainfall Depth of a Real Storm Event on 6 Nov 92
14. Rainfall Pattern of an Artificial Storm Event Estimated by the Thiessen Polygon Method
15. Rainfall Pattern of an Artificial Storm Event Estimated by the Inverse Distance Weighted Method
16. Rainfall Pattern of an Artificial Storm Event Estimated by the Kriging Method
17. Rainfall Pattern of an Artificial Storm Event Estimated by the Trend Method
18. Rainfall Pattern of an Artificial Storm Event Estimated by the Spline Method
19. Comparison of Predicted and Theoretical Rainfall Intensities for Time Steps 1
20. Comparison of Predicted and Theoretical Rainfall Intensities for Time Steps 2 and 3
21. Comparison of Predicted and Theoretical Rainfall Intensities for Time Step 4 and 5
22. Tracking the Storm Movement
23. Consistency of Rainfall Estimation Before and After Omission of Two Gauges
24. Rainfall Pattern Estimated by Kriging for the Storm Event on 5 Nov 92
25. Rainfall Pattern Estimated by Trend for the Storm Event on 5 Nov 92
26. Rainfall Pattern Estimated by Spline for the Storm Event on 5 Nov 92
27. Rainfall Pattern Estimated by Kriging for the Storm Event on 6 Nov 92
28. Rainfall Pattern Estimated by Trend for the Storm Event on 6 Nov 92

29. Rainfall Pattern Estimated by Spline for the Storm Event on 6 Nov 92
30. Comparison of Predicted and Mean Rainfall Intensities for Two Real Events
31. Consistency of Estimation of the Rainfall Models for the Event on 5 Nov 92
32. Consistency of Estimation of the Rainfall Models for the Event on 6 Nov 92

1. INTRODUCTION

1.1 General

Management of water quantity and quality in urban and rural drainage systems is a complex task which, over the last few years, has become increasingly important to the community. This community awareness has increased the need for managers of these systems to obtain information relevant to the response of the systems invested in their control. The upsurge of concerns has increased the demand for user friendly, informative systems that managers can use to evaluate the economic and environmental consequences of alternative management schemes.

The management of drainage systems requires the handling of various sorts of data of the catchment, and most of those data are geographically referenced, i.e. related to the position of the earth. For example, rainfall, land use, soil types, drainage network, and population, etc. Geographic Information Systems (GISs) have played an increasingly important role in the management of drainage systems due to the important fact that they have the capability to turn data from many different sources into a useful piece of information, such as a map, for decision making.

Geographic Information Systems are described by a leading GIS software developer – Environmental Systems Research Institute, Inc. (ESRI) as an organised collection of computer hardware, software, geographic data, and personnel designed to efficiently capture, store, update, manipulate, analyse, and display all forms of geographically referenced information (ESRI, 1995).

While accurate, comprehensive, and widely accepted, this definition does not mean much at first glance. In simpler terms, a GIS is a computer system used to handle geographical objects and non spatial attributes of those objects. Geographical objects include natural phenomena (such as rivers, lakes and forest), man-made structures (such as rain gauges, buildings and highways), and other convenient objects that may define the location and extent of a geographical phenomena (such as a particular soil type). Non spatial attributes

associated with those objects can be the length of a river, rainfall readings of a rain gauge, and the permeability of a particular type of soil.

Spatial objects and non spatial attributes are stored in the GIS database. The database allows the attributes to be queried and objects associated with those attributes to be displayed. Selective display of features is a major capability of a GIS that facilitates decision making. In addition, the GIS can correlate different layers of information into a single view, discovering relationships, patterns and trends that would otherwise go unnoticed. An example is the overlay of flood extent on households to determine the number and location of the people affected by flooding.

Because of their powerful capability in handling geographically referenced information, GISs have wide applications in many fields of science and technology, such as natural resources management, transportation planning, and emergency management, etc.

With respect to water management, the main application of GISs has been the linking of GISs with water management models. Within the context of water quantity, the primary function of water management models is the transformation of precipitation into runoff for a given catchment to assess the impact of flows on the catchment. However, few such models have a well developed capability to analyse and display spatial information. Because of this, the complex physical processes of a catchment have been simplified. For instance, a catchment is divided into smaller areas with an assumption that each area has uniform property. In addition, each area is assumed to receive the same amount of rainfall as that recorded at its closest rain gauge. The accuracy of the modelling results derived from such simplification is always questionable. On the other hand, the outputs of the models are hydrographs or numerical values at a few predefined locations within the catchment. These modelling outputs lack spatial dimension and decision makers can get only limited information from these results.

GISs can assist in this problem. Traditionally, the role played by GISs has been twofold: namely, (1) as pre-processors to extract hydrological parameters, such as the proportion of permeable area in a catchment, for inputting into the catchment response models; and (2) as

post-processors to provide graphical displays based on spatial interpolation/extrapolation of the results from the models.

With rapid development in GISs and computer technology, a further important role that GISs can play to enhance catchment modelling is identified. GISs can now be applied for the spatial analysis of time-varying variables of a catchment, notably rainfall. The application of GIS for the modelling of spatial distribution of rainfall is the main focus of the present study.

Rainfall is a dynamic process which varies both in space and time. Given the same amount of rainfall, the impact on a catchment depends very much on the spatial and temporal patterns of the rainfall. This variability must be considered. However, for most catchments, the rainfall is recorded by only a few rain gauges. The analysis of rainfall distribution based on a few point measurements is a difficult subject and has attracted significant research effort.

Various algorithms ranging from simple arithmetic mean to sophisticated regression analysis for determination of the rainfall distribution were investigated prior to the development of the GISs. The sophisticated techniques were found to give a more accurate representation of the real rainfall distribution. However, these sophisticated techniques have not gained wide-spread applications in water management modelling due to complexity of the techniques and the lack of powerful spatial analysis tools. The use of such sophisticated techniques has been limited therefore to a few research studies.

Within the last decade, GISs have undergone significant development. Some now include powerful spatial analysis tools in their package. For instance, a leading proprietary GIS software – ARC/INFO®[1], has included some sophisticated algorithms as built-in functions for modelling spatial variables. This study explored the powerful capability of ARC/INFO and showed that by building up some procedures in ARC/INFO, the sophisticated methods can be used as easily as the simple ones.

[1] ARC/INFO is registered trademarks of Environmental System Research Institute, Inc., Redlands, CA, USA.

ARC/INFO is one of the most popular and powerful GISs available in the market. Users are found all around the world and include government agencies, universities and private companies. These users form a huge database employing the same data format, enabling the exchange of information among different organisation and disciplines. The popularity of ARC/INFO enables third party developments that benefit many users. Another distinctive advantage of ARC/INFO is its programmability. The ARC/INFO provides a macro programming language called Arc Macro Language (AML), which permits sequencing of ARC/INFO commands. Consequently, all operations can be programmed as an automatic procedure which can save a lot of time and effort in development. Moreover, novice users can invoke the procedure by just typing a single command or pointing-and-clicking on the menu, without knowing the underlying complexity of the procedure.

The popularity, power and programmability were the main reasons for selection of ARC/INFO as the GIS for this study. To explore and promote the application of the powerful spatial analysis tools in this generic GIS system for water management modelling is the primary aim of this study. It is hoped that the procedure developed in this study can unleash the advanced techniques for spatial modelling to a wide range of users.

1.2 Outline of the Study

This study investigated the application of the ARC/INFO GIS for the estimation of the spatial distribution of rainfall over a catchment based on point measurements. The determination of areal mean rainfall for subcatchment and the total catchment was investigated also.

Five spatial interpolation techniques were implemented in ARC/INFO for comparison; these techniques were:

(a) Thiessen Polygon Method;
(b) Inverse Distance-Weighted Method;
(c) Kriging Method;
(d) Trend Method (polynomial); and
(e) Spline Method.

All five techniques were applied to one hypothetical and two real storm events on the study catchment. Results obtained for these events were analysed to ascertain the applicability of the alternative techniques.

This study developed a series of programs (procedure) written in the ARC/INFO Arc Macro Language to automate the modelling process. That is to say, once the rainfall data was input to the system, the five techniques would be executed in turn to estimate the distribution of rainfall. At the end of each computer run, results were tabulated for comparison.

The Upper Parramatta River Catchment of Western Sydney is used as a case study. The catchment characteristics and the hydrometric network are described in detail in Chapter 2 of this report.

The background theories of the five techniques are outlined in Chapter 3. The merits and drawbacks of each method are discussed there.

Following the background to the techniques is a literature review of related studies. As presented in Chapter 4, three aspects are reviewed; these are: (1) the importance of the spatial and temporal distribution of rainfall in water management modelling; (2) the review of previous works on comparison of different techniques for estimation of spatial rainfall distribution; and (3) the application of GISs in water management modelling.

An overview of ARC/INFO GIS is given in Chapter 5. Discussions are made on GIS data structures, the ARC/INFO command interface and the ARC macro language (AML).

Chapter 6 describes the implementation of this study under ARC/INFO, including the general procedure, flowchart of operation, etc. The importance of maintaining a consistent naming convention for maps and keeping good documentation are stressed.

Test data and results are presented in Chapter 7. The test data included both hypothetical and real rainstorm events. In comparing the alternative algorithms, both visual and arithmetic comparisons are established.

Concluding remarks are given in Chapter 8, which is the final chapter of this report. Following that are six appendices providing supplementary information for this report.

2. THE UPPER PARRAMATTA RIVER CATCHMENT

2.1 Catchment Details

As shown in Figure 1, The Upper Parramatta River Catchment is located in the western suburbs of Sydney, New South Wales. The study catchment is 112 km^2 in area and is defined by the catchment area draining to the Charles Street weir.

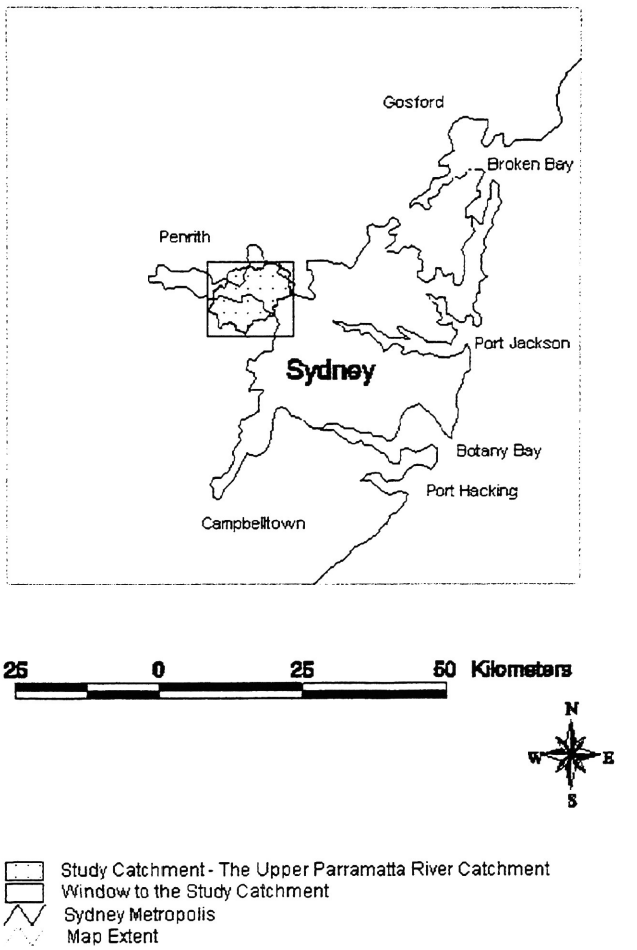

Figure 1 - Location of the Study Catchment

The Parramatta River drains into Sydney Harbour and is tidal to the Charles Street Weir in Parramatta. The section of the Parramatta River immediately upstream of the Charles Street Weir passes through part of the Parramatta central business district. There are two main tributaries, namely Toongabbie Creek and Darling Mills Creek. They join about 2.5km upstream of the Charles Street weir, as shown in Figure 2.

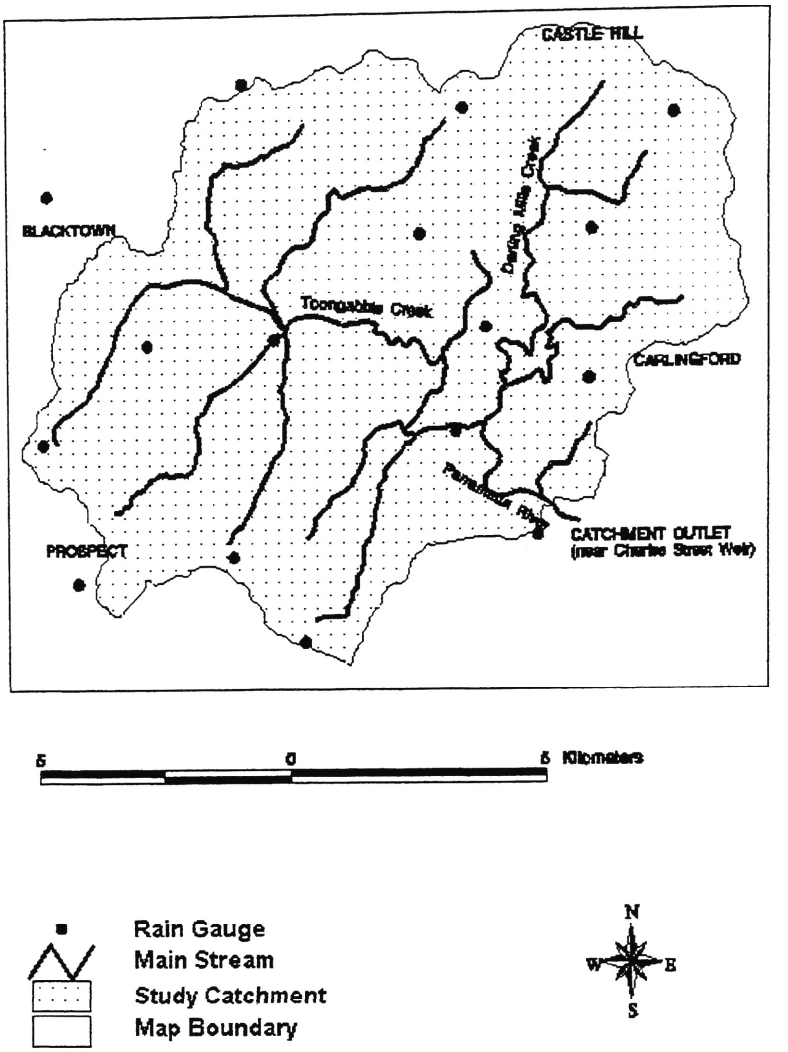

Figure 2 - The Upper Paramatta River Catchment

The catchment is rather steep with the confining ridges being 180 metres Australian Height Datum (AHD) at Thompsons Corner, Castle Hill, and 100 metres AHD at Prospect. The average slope of the catchment is about 1.2%. The dominant land use is typical of urban environment with a mix of residential, industrial, commercial and open space (parkland) areas.

Considerable development has occurred within the catchment over the past two decades and this has resulted in an increase in the frequency of recorded flood levels. To mitigate the social and economic losses associated with flood events in this catchment, the Upper Parramatta River Catchment Trust (UPRCT) was instituted in 1989 with the role of managing flood mitigation measures within the catchment area.

2.2 Available Data within the Upper Parramatta Catchment Area

There are sixteen (16) continuous rain gauges within or in close proximity to the catchment; locations of these gauges are shown in Figure 2. The majority of these gauges have been installed by the UPRCT since its formation. Consequently, long-term records are not available from these gauges.

The rationale for installation of these gauges was for improving the flood forecasting for the catchment area. On average, one point rainfall sample is being obtained for every seven (7) km^2 of catchment. While this is a high density of rain gauge information for most catchments, Urbonas et al. (1992) suggested that an even higher density of spatial information is required if accurate predictions of catchment response are to be obtained for convective storm events. Presented in Table 1 are the accuracies obtained for peak flow estimation by Urbonas et al. (1992) with different gauge network. A gauge density of $1.6\,km^2$/gauge was used as a basis for comparison. It is important to note that, while the mean error over a number of events may be within reasonable limits, the range of errors for individual events can be significant.

TABLE 1
ACCURACY OF RAINFALL-RUNOFF MODELS
(after Urbonas et al. 1992)

Gauge Density (km^2/gauge)	Range (%)	Mean Deviation (%)
8.0	−100.0 to 150.0	−24.2
4.0	−75.3 to 94.5	0.5
2.7	−32.2 to 63.6	15.8
2.0	−32.2 to 18.8	−0.9
1.6	0.0 to 0.0	0.0

2.3 Rainfall-Runoff Model

For catchment management purposes and, particularly, the flood management aspects of the catchment, the UPRCT has been implementing a rainfall-runoff model of the catchment. This model uses the RAFTS software (WP Software, 1995) which is based on the nonlinear reservoir model of Laurenson (1964).

For the present study, the catchment was divided into twenty four (24) subcatchments; the delineation was generally based on the RAFTS model established by the UPRCT. It should be noted that the original delineation in the RAFTS model consisted of more subcatchments than the present study. The reason for reducing the number of subcatchments for the present study was to lump the small and uneven areas together to reduce computational effort. These 24 subcatchments were used in the analysis of the predicted spatial distribution of rainfall obtained from the alternative techniques considered in this study.

Shown in Figure 3 are the subcatchment boundaries. As expected, the area of each of these subcatchments was not constant but rather differed according to the catchment characteristics. The largest subcatchment was approximately 9 km^2 while the smallest was approximately 1 km^2. The remaining subcatchment areas were evenly distributed between these limits.

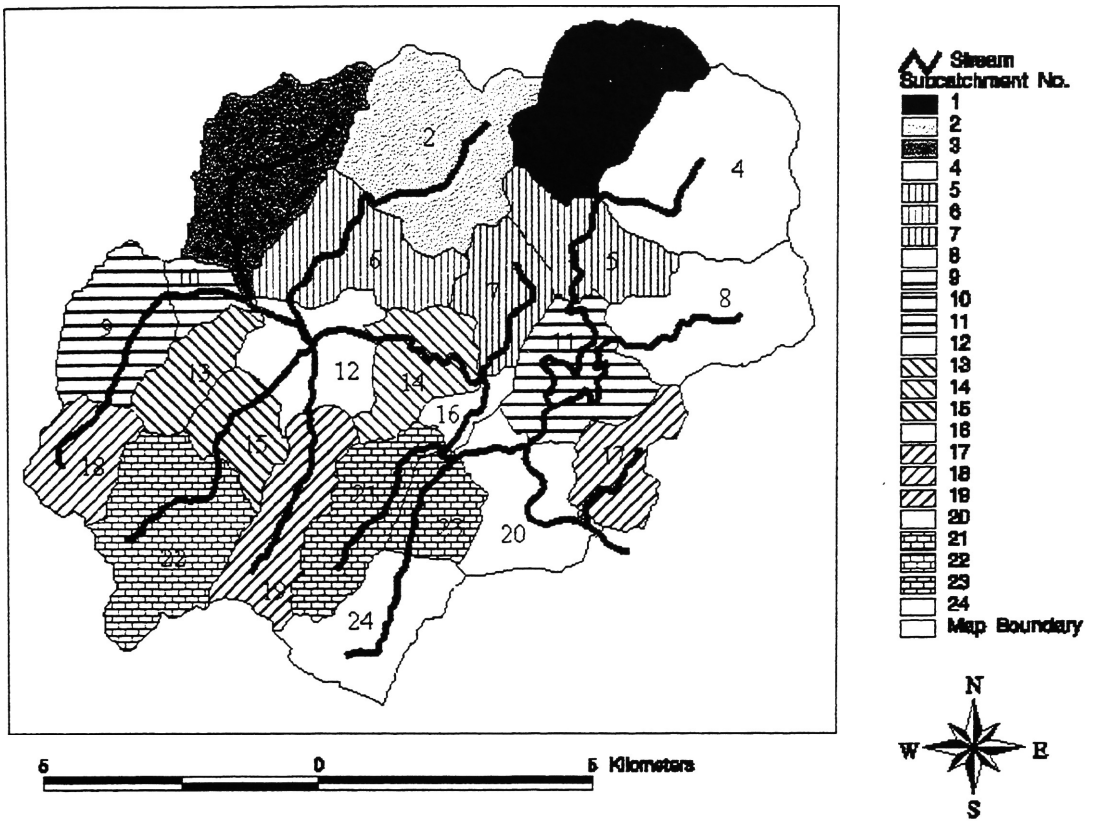

Subcatchment No.	Area (km^2)	Subcatchment No.	Area (km^2)	Subcatchment No.	Area (km^2)
1	6.70	9	4.48	17	3.06
2	8.64	10	1.41	18	3.09
3	7.47	11	4.83	19	4.49
4	8.96	12	4.38	20	5.06
5	4.05	13	2.54	21	4.32
6	5.34	14	3.58	22	7.21
7	3.34	15	2.67	23	2.46
8	6.04	16	1.20	24	4.64

Figure 3 - Subcatchment Boundaries of the Upper Parramatta River Catchment

3. ALTERNATIVE RAINFALL MODELS

The measurement of rainfall during a storm event consists of determining the time over which an increment of rainfall depth occurs at a defined location; the rainfall intensity is defined then by the gradient of the rainfall mass curve. Consequently, the measurement of rainfall is a point measurement of a spatially varying parameter. Information, such as the rainfall depth or intensity, at locations other than the measurement location are not defined by the measurement process and must be inferred from other known information.

Many alternative techniques have been developed for the inference of the spatial distribution of rainfall from the measured rainfall at a specific location; these alternative techniques are in effect alternative models of the spatial distribution of rainfall. The following sections give a brief theoretical background to the five techniques implemented as part of this investigation. More detailed descriptions of the techniques can be found in Burrough (1986).

3.1 Thiessen Polygons

Thiessen polygons are probably the most common approach for modelling the spatial distribution of rainfall. As presented by Thiessen (1911), the approach defines the zone of influence of each rain gauge by determining the area closer to a particular gauge than any other gauges. It is then assumed that the rainfall records at the gauge are representative of rainfall over the zone of influence. Shown in Figure 4 are the sixteen (16) Thiessen polygons constructed for the study catchment.

It should be noted that the Thiessen polygons divide an area in a way that is totally determined by the configuration of the rain gauges, without taking the rainfall values into account. An impact of the use of Thiessen polygons is the development of discontinuous functions defining the rainfall depth over the catchment. This effect is very evident at the boundaries of the polygons where a discrete change in rainfall depth, or intensity, occurs.

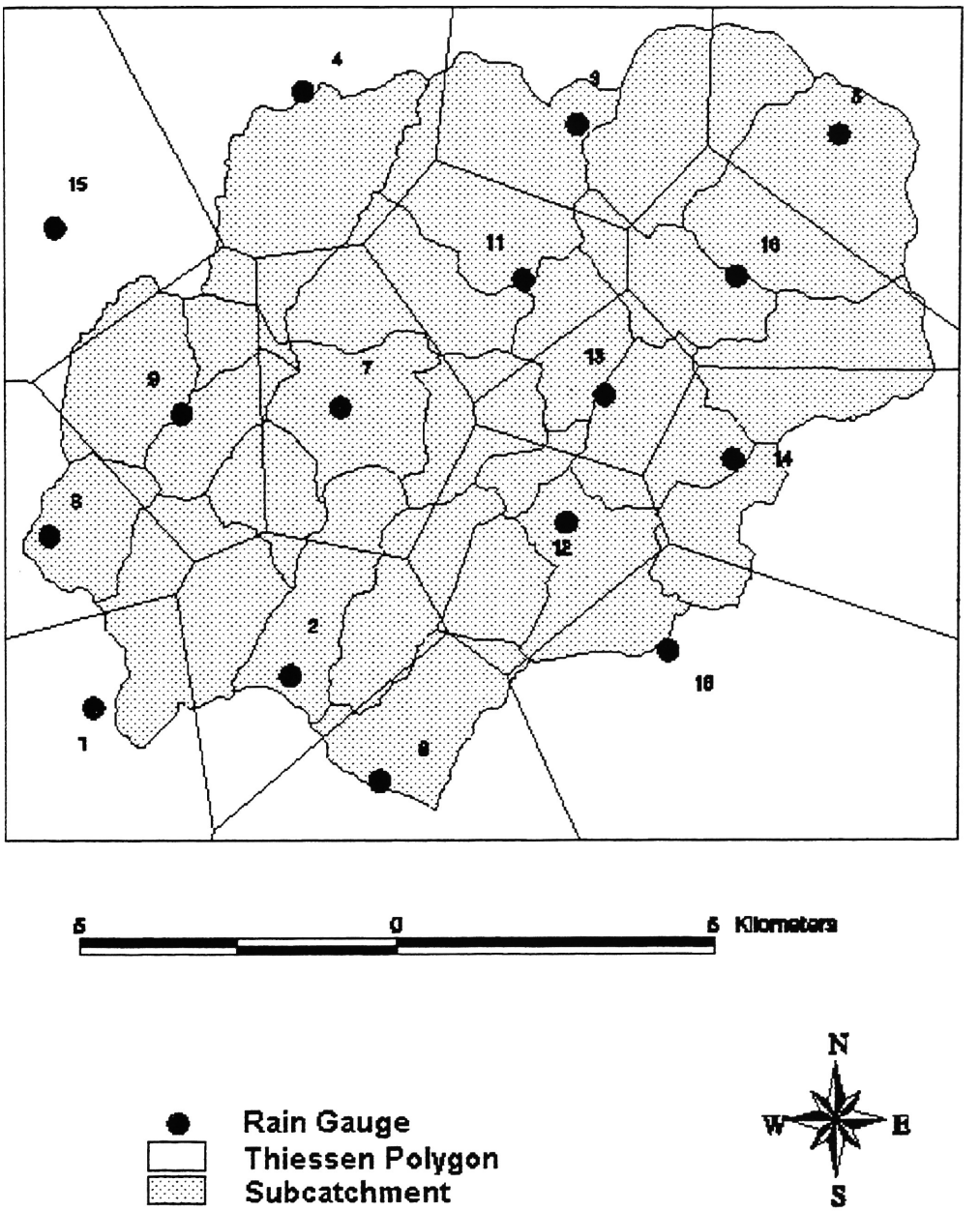

Figure 4 - Thiessen Polygons for the Upper Parramatta River Catchment

3.2 Inverse Distance Weights

The inverse distance-weighted method as presented by Watson and Philip (1985) estimates the rainfall at a point by a weighted interpolation based on the distance of each rainfall gauge to the point under consideration. Interpolation weights (w_{ij}) for each gauge are determined from

$$w_{ij} = \frac{d_{ij}^{-r}}{\sum_{i=1}^{n} d_{ij}^{-r}} \qquad (1)$$

where d_{ij} is the distance from point j to gauge i ;

n is the total number of gauges in the catchment; and

r is the exponent applied to distance. A higher value results in less influence from distant points. It can be any real number greater than zero but the normal value ranges from 0.5 to 3. A value of 2 was used throughout this project.

The rainfall (P_j) at the desired location, therefore, is given by

$$P_j = \sum_{i=1}^{n} w_{ij} P_i \qquad (2)$$

where P_i is the rainfall value at gauge i.

Similar to the Thiessen polygons, the inverse distance weights are based on the geometry of the catchment. In contrast to the Thiessen polygon method, however, this approach results in a smooth transition of values between rain gauge locations.

It should be pointed out that with this interpolation algorithm the maxima and minima in the interpolated surface can occur only at gauge points. Furthermore, the values estimated by this method are susceptible to clustering in the gauge points.

3.3 Kriging

The Kriging method is based on the "theory of regionalized variables" developed by Matheron (1963, 1971). In the context of rainfall modelling, the theory assumes that the spatial variation in rainfall values is statistically homogeneous throughout the rainfall surface (i.e. the same pattern of variation can be observed at all locations on the rainfall surface).

The Kriging method uses autocorrelation between the rain gauge readings and estimates values at ungauged points or regions without bias and with minimum estimation variance.

Similar to autocorrelation analysis of time series data, but with the replacement of the time domain with the space domain, the method assumes that the spatial variation of any rainfall can be expressed as the sum of three major components. These are:

(a) a structural component, associated with a constant mean value or a constant trend;
(b) a random, spatially correlated component; and
(c) a random noise or residual error term.

If x is a position in the catchment, then the rainfall P(x) at x is given by

$$P(x) = m(x) + \varepsilon'(x) + \varepsilon'' \qquad (3)$$

where m(x) is a deterministic function describing the "structural" component of P at x, $\varepsilon'(x)$ is the term denoting the stochastic, locally varying, spatially dependent residuals from m(x), and ε'' is a residual, spatially independent Gaussian noise term having zero mean and variance σ^2.

It is assumed that the variance of differences depends only on the distance between sites, h, so that

$$E[\{P(x) - P(x+h)\}^2] = E[\{\varepsilon'(x) - \varepsilon'(x+h)\}^2]$$
$$= 2\gamma(h) \quad (4)$$

where $\gamma(h)$ is a function known as the semi-variance.

The semivariance can be estimated from observed rainfall using the relationship

$$\gamma^*(h) = \frac{1}{2n}\sum_{i=1}^{n}\{P(X_i) - P(X_i + h)\}^2 \quad (5)$$

where n is the number of pairs of rain gauges separated by distance h. A plot of $\gamma^*(h)$ against h is known as the sample semi-variogram.

Figure 5 shows the semi-variogram obtained for the artificial rainfall event applied to the study catchment. Details of the rainfall data for this event are presented in Chapter 7 of this report.

There are several important features worth noting in the plot of the sample semi-variogram. At relatively short lag distances of h, the semi-variance is small, but increases with the distance between the pairs of sample points. At a distance referred to as the range, the semi-variance levels off to a relatively constant value referred to as the sill. This implies that beyond this range distance, the variation in P values is no longer spatially correlated. Within the range, the P value variation is smaller when the pairs of gauge sites are closer together.

The cogent point Kriging is the fitting of the semi-variogram by a mathematical function. Once it is fitted, rainfall at any point within the study area can be estimated by interpolation from known sites using Equation (3).

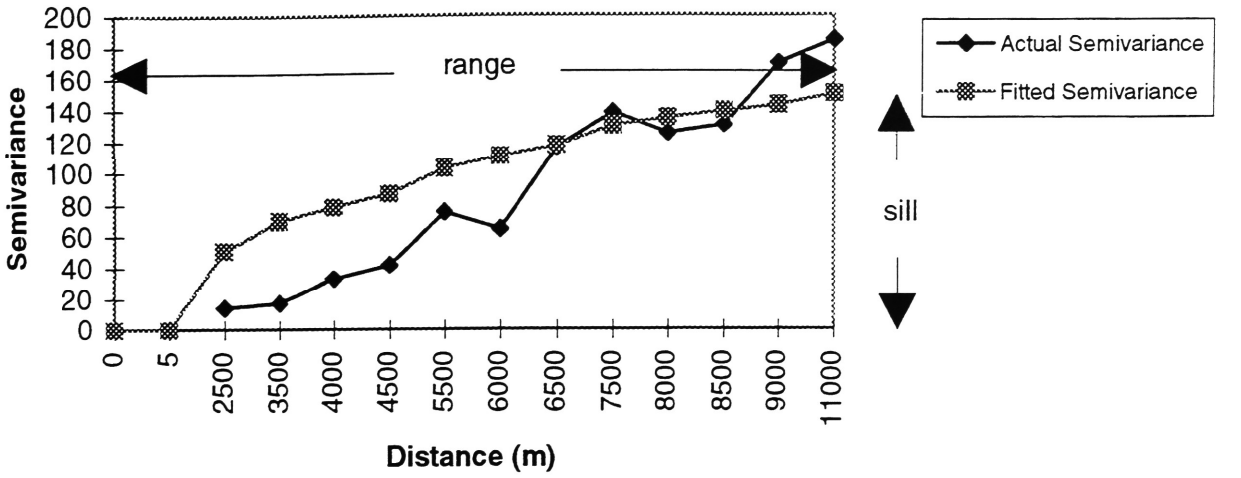

Figure 5 - A Typical Semivariogram

ARC/INFO offers five (5) mathematical functions which can be used as possible candidates for fitting a semivariogram of a given data set. These functions are spherical, circular, exponential, Gaussian, and linear. The choice of the appropriate function involves interpretation and judgement. This often requires a large number of "trial and error" computations. The task of function selection is best performed by an expert. Alternatively, it can be implemented with an aid of an expert system. For the purpose of this study, however, only the spherical function is used; this is the default option within ARC/INFO.

Kriging is considered as an optimal interpolator in the sense that the estimates are unbiased and have known minimum variances. Since the estimation variances can be determined, we can determine the confidence we can place in the estimates.

Unlike Thiessen polygons and inverse distance weights, the rainfall surface estimated by Kriging depends heavily on rainfall readings at gauges as well as the configuration of the gauge network.

3.4 Trend Surfaces

As discussed by Burrough (1986), the trend method uses a polynomial equation to construct a surface to fit the input points with minimisation of least-square errors.

In two dimensions, the surface polynomials are of the form

$$f(x,y) = \sum_{r+s} b_{rs} x^r y^s \tag{6}$$

where the order of the surface is p which is given by $p \geq r + s$.

In equation (6), the coefficients (b_{rs}) are chosen to minimise

$$\sum_{i=1}^{n} \{Z(x_i,y_i) - f(x_i,y_i)\}^2 \tag{7}$$

where $Z(x_i, y_i)$ are measured data

n is the number of data points

The Trend method creates smooth surfaces. Since the fitting of the polynomial function is based on a best fit for the complete catchment, the generated function seldom passes through the original data points.

The higher order of a polynomial will result in a surface closer to the data points, but it tends to create a wavy surface. In general, the order of a polynomial should be less than the number of data points. In this study, an order of 3 was adopted to avoid wavy surfaces and reduce computational efforts.

3.5 Spline Surfaces

Like the Trend method, the Spline method is a surface fitting technique. However, the Spline involves interpolation between the given data points by attaching together several low order polynomials, while maintaining the values and gradients at the connection points. This avoids laborious computation of a high order polynomial and also prevents undesirable maxima and minima between the given data points.

ARC/INFO adopts the minimum-curvature Spline interpolation method which has the following two conditions imposed:

1. The surface must pass exactly through the data points.
2. The surface must have minimum curvature - the cumulative sum of the squares of the second derivative terms of the surface, taken over each point on the surface, must be a minimum.

This minimum-curvature technique is also referred to as thin plate spline interpolation. It ensures a smooth (continuous and differentiable) surface together with continuous first-derivative surfaces.

The Spline function uses the following formula for the surface interpolation:

$$f(x,y) = T(x,y) + \sum_{i=1}^{N} \lambda_i R(r_i) \qquad (8)$$

where N is the number of data points

λ_i are weighting coefficients

r_i is the distance from the point (x,y) to point i

while T(x,y) and R(r) are defined as follows:

$$T(x,y) = a_1 + a_2x + a_3y \tag{9}$$

$$R(r) = \frac{1}{2\pi}\{\frac{r^{\varphi}}{4}[\ln(\frac{r}{2\tau}) + c - 1] + \tau^{\varphi}[K_o(\frac{r}{\tau}) + c + \ln(\frac{r}{2\pi})]\} \tag{10}$$

where φ defines the weight attached to the first derivative terms during minimisation

τ defines the weight of the third derivatives terms during minimisation

r is the distance between the point and the sample,

K_o is the modified Bessel function,

c is a constant equal to 0.577215,

a_i are coefficients found by the solution of a system of linear equations.

Spline functions are mathematical equivalents of a flexible ruler. They are piecewise functions, which is to say they are fitted to a small number of data points exactly, while at the same time ensuring that the joins between one part of the curve and another are continuous.

Because splines are piecewise functions using few points at a time, the interpolation can be quickly calculated. In contrast to trend surfaces and inverse distance weights, splines retain small-scale features.

Spline surfaces have been found to be a robust spatial interpolation for many meteorological problems; for example, Hutchinson (1991) applied spline surfaces to long term monthly mean values of daily maximum and minimum temperature across Tasmania, Australia.

4. LITERATURE REVIEW OF RELATED WORKS

Implementation of the five (5) techniques described previously in a generic GIS for the estimation of spatially distributed rainfall is a new approach to the problem of estimating the spatial variability of rainfall. It is appropriate therefore to review previous research on related subjects to provide a perspective for the present study.

This literature review was broadly divided into three parts. The first part of the review highlighted the significance of estimation of spatial and temporal distribution of rainfall, and its influence on the modelling of the hydrological process in the catchment; the second part provided a brief account on the previous works on using different algorithms for estimating the spatial distribution of rainfall; and the final part discussed the application of GIS in water management modelling.

4.1 Spatial and Temporal Distribution of Rainfall on Storm Runoff

As discussed by Ball (1992), the modelling of the catchment response to a storm event could be arbitrarily divided into four conceptual components; namely, generation, collection, transportation and disposal. Within the context of water quantity modelling, these conceptual components are illustrated as follows:

(1) Generation - the prediction of the spatial and temporal distribution of rainfall over the catchment, and the estimation of spatial variation of the physical properties of the catchment.

(2) Collection - the prediction of the amount of water entering the physical drainage system.

(3) Transport - the prediction of the motion of water within the physical drainage system.

(4) Disposal - the prediction of the impact of the discharge of the water into the floodplain and receiving waters.

An important aspect of the first conceptual component is the accurate prediction of both spatial and temporal distribution of rainfall over a catchment. Without satisfactory results from the rainfall model, accurate predictions from other components in the total catchment model will not be achievable.

Rainfall data are usually measured as point values (from rain gauges). However, rainfall rarely occurs uniformly over an area. Variations in intensity and total depth of rainfall occur from the centres to the peripheries of storms. The estimation of the spatial extent and intensity of rainfall from a few rain gauges is difficult and attracts much attention for research. In an investigation of likely errors arising from poor predictions of the spatial and temporal distribution of rainfall, Urbanas et al. (1993) found that using low density rain gauge data as input to runoff models could result in enormous deviations from field measurements.

Fontaine (1991) investigated the magnitude of error in measurement of areal mean rainfall using historic rainfalls and a set of hypothetical catchments and gauge networks representing typical conditions encountered in practice. The results for one of the storms used indicated that there was a 25% chance of overestimating areal mean rainfall by 11% or more and a 25% chance of underestimating the areal mean rainfall by 26% or more. It was concluded that gauge density, gauge arrangement and catchment area were significant in getting reliable estimation.

Wilson et al. (1979) investigated the influence of the rainfall spatial distribution on the catchment discharge by comparing the differences between predictions using 1 gauge and 20 gauges for a catchment of 70 km^2 in Puerto Rico. They found that even in cases when the total depth of rainfall was not in serious error, the spatial distribution of the input might lead to large discrepancies in the volume of the runoff output. Beven and Hornberger (1982) reached a similar conclusion from an independent study on a catchment of 400 km^2 in central Illinois.

It was also demonstrated by Hamlin (1983) that, for drainage basins with areas less than about 3000 km^2, the spatial and temporal rainfall pattern was important for the determination of runoff.

Apart from the spatial distribution of rainfall, the temporal pattern of rainfall has significant influence on the modelling of storm runoff. Ball (1994) analysed the influence of storm temporal pattern by a kinematic wave model which consisted of an artificial infinitely wide catchment surface. Several simplified and design patterns of rainfall were input to the model for testing. It was concluded that the time of concentration and time of occurrence of peak flow were influenced by the temporal pattern of rainfall excess.

4.2 Estimation of Areal Mean Rainfall

Granted that the catchment response is significantly influenced by the rainfall input, the development of accurate algorithms for estimating the spatial rainfall patterns and areal mean rainfall from gauge data is an important task. Available algorithms range from the simple arithmetic mean to sophisticated Kriging interpolation techniques, as discussed previously in Chapter 3 of this report.

Creutin and Obled (1982) compared various methods for point rainfall estimation using rain gauge data. The comparison was done for a mountainous area and it was in terms of total rainfall depth at a point. The methods compared were: Thiessen polygons, arithmetic means, spline surfaces, Kriging, Gandin's (1965) method[2] and a method based on an expansion of the random rainfall field to orthogonal functions. They concluded that none of the methods examined was able to fully account for the statistical properties of the observed rainfall fields. They recommended Gandin's method as an efficient method of interpolation and they cautioned against the use of the Thiessen polygon method as being clearly unsatisfactory.

Tabios III and Salas (1985) made a similar comparison. The techniques considered were: Thiessen polygons, polynomial, inverse distance weights, multiquadric, Gandin's, and Kriging. The test area was 52,000 km^2 with a network of 29 rain gauges. There were 30 years of monthly rainfall data. Based on bias and quadratic performance criteria the authors

[2] The interpolation methods not available in ARC/INFO are discussed in Appendix A.

concluded that the traditionally used Thiessen polygon method was significantly inferior to others with Gandin's method and Kriging being the better methods.

Patrick and Stephenson (1991) compared four (4) surface fitting methods, namely; inverse distance squared, multi-quadratic, polynomial surfaces and distance-weighted least-squares. The comparison was made on artificially generated data sets of 100 data points on a regular 10 by 10 grid. Of the four methods compared, they found that the inverse distance squared method was the most consistent, especially for minimal source of data points.

All the above works reached a similar conclusion, namely, the simple methods, such as arithmetic mean and Thiessen polygons were not satisfactory in modelling the rainfall distribution and that the sophisticated methods gave better estimation of real rainstorm patterns.

This fact has been recognised for many years, yet the simple methods are still the most commonly used tools in most water management studies. The reason for this may be partly due to the underlying principles that the sophisticated algorithms are difficult to understand and, more importantly, the sophisticated algorithms are difficult to apply in a generalised manner for a catchment, i.e. any catchment, irrespective of its size and location. Also, until recently, high speed computers were not commonly available. The use of sophisticated algorithms has therefore been limited to a few academics and specialists in a research environment.

With the rapid development in computer technology, speed of computation is no longer a constraint and computers with sufficient computational power are available at an affordable price. In addition, GIS software, such as ARC/INFO provides a generic platform for spatial modelling. Most of the sophisticated algorithms are built-in functions of GIS software. This report shows that within ARC/INFO, sophisticated methods can be implemented as easily as the simpler methods.

The benefit of the present study over the previous works is that the rainfall models are built upon an "off-the-shelf" generic GIS. The more accurate but sophisticated algorithms are

readily available for engineers and managers with some basic knowledge of GISs. Other advantages of using a GIS for rainfall modelling include:

- rainfall distribution can be colour-coded and displayed on screen for visual analysis;
- database can be easily updated or modified to cope with future changes or development, for example, the installation of additional gauges;
- output of rainfall estimation can readily be linked to water management models for subsequent analysis;
- the rainfall model can be fully automated and applied in real time; and
- loss of data during an event due to equipment failure can be accommodated.

4.3 Application of GIS in Water Management Modelling

The application of GIS in water management studies has been expanding over the past decade. There are numerous publications in this field with new applications continually being explored. The following are just a few examples of current areas of application. They include:

- displaying and mapping of the results of water management models;
- modelling changes in catchment characteristics; and
- automating the modelling of hydrological process.

A case described by Paudyal and Syme (1994) was the integration of a GIS (ARC/INFO) with the one-dimensional hydrodynamic model known as MIKE-11 to produce an integrated spatial decision support system for floodplain management in Bangladesh. The MIKE-11 software provided powerful hydrodynamic analytic tools to model flood flows along the river network, whereas the ARC/INFO software provided various spatial analysis tools and display functions to couple the flow data with spatial data on agriculture, fisheries and properties to assess the impact of flooding.

GISs are particularly powerful in assessing change in catchments. Muzik (1993) applied a GIS-Unit Hydrograph model to simulate runoff on catchments undergoing urban development, with a view to assessing the change of frequencies of peak flows due to urbanisation. The author compared his model with the conventional regression method. It was shown that once the GIS database was created the time required for hydrologic simulation was up to 100 times shorter than would be needed for simulation not support by the GIS. More importantly, the GIS database could be easily updated or modified to study the impact of catchment changes, such as urbanisation, on runoff. This was proved to be useful in planning studies exploring impacts of various stages of urban development on flood flows.

Stuebe and Johnston (1990) used a raster GIS (GRASS) for all phases of the US Soil Conservation Service (SCS) modelling process, including catchment delineation and routing of runoff to estimate the outlet runoff volume. They compared the GIS approach with the manual method on six catchments and concluded that the GIS approach was a satisfactory alternative to the manual method for a catchment lacking relatively flat terrain. They also inferred that the GIS-based method of estimating runoff would tend to be advantageous if study areas were large or numerous, runoff was modelled repetitively, alternative landuse or landcover scenarios were explored, or if the data already comprised part of an existing database. However, they cautioned that the manual method might be preferred for flatter catchments because of potential problems with catchment delineation.

It can be observed that GISs are playing an increasingly important role in water management. With the rapid development of GISs and computer technology, there are many potential areas of application, notably the linking of remote sensing information and artificial intelligence with GISs. This study is in line with such development. An important aspect of this study is to promote and explore the application of GIS, and provide a framework for future development.

5. ARC/INFO – AN OVERVIEW

5.1 General

ARC/INFO was developed by the Environmental System Research Institute (ESRI), Inc., Redlands, California. Since its development in the late 1980s, it has become the most successful commercial geographic information system (GIS).

As described by Peuquet et al. (1990), the main characteristics of ARC/INFO are its data model, the GIS functions it performs, its modular design, its ability to integrate many types of data, its utility for developing application specific user interfaces with screen menus, its fourth generation macro language, its open architecture which allows for integration with numerous relational database management systems (DBMS), and its ability to operate on many types of computers with a variety of graphics hardware.

ARC/INFO is a hybrid data model; spatial data are represented by a vector or grid data structure (data structure will be explained in the following Section), while attribute data are represented by a relational DBMS. In the name ARC/INFO, ARC refers to the spatial data component developed by ESRI, while INFO, the attribute data component, is a relational DBMS developed by Henco Corporation. Such a hybrid data model greatly facilitates efficient and simultaneous handling of the two generic classes of GIS data.

5.2 Data Structure

In ARC/INFO, there are two main data structures, namely the vector data structure and raster data structure. Vector data consists of points, lines and polygons to represent the features on the Earth's surface. Raster data, on the other hand, considers an entity as divided into a rectangular grid or matrix of cells. The grid is organised as a set of rows and columns. Each row or column contains a group of cells. Cells have values representing a geographic phenomenon; for example, rainfall depth, soil type, elevation, land use class, slope, and so on. Cell values are numbers. The numbers can represent nominal data such as land use classes or can be measures such as rainfall depth in millimetres.

There are relative merits and demerits of the two data structures. However, the two data structures are complementary and in many cases convertible. The spatial rainfall distribution model of this project is primarily constructed upon a raster data structure because the raster structure is suitable to represent high spatial variations and compatible with remote sensing images. Further development of the model will benefit from a large source of information such as from radar sensing of rainfall. In ARC/INFO, raster data are exclusively handled by a separate module called GRID, which provides a large suite of modelling functions for performing spatial analysis.

5.3 Grid Map Structure

Due to the fact that grid maps are extensively used in this project, a detailed description of the grid map structure is given here.

A grid map has a cell-based structure. Each cell is a square, has the same size as other cells in the grid and contains a numeric value. The cell values represent the theme or layer values. Cell values can be integer or real numbers.

An integer grid has a value attribute table (VAT) which stores attribute information for the set of cell values in a grid. Two items are always created by default: VALUE and COUNT. The VALUE refers to the value of a cell and the COUNT is the number of cells in the map having such a value. Additional items can be added to the VAT and used to relate attribute information stored in other tables to cell values. Interpretation of a grid map is mainly through the analysis of the VAT.

5.4 ARC/INFO Commands and ARC Macro Language (AML)

All ARC/INFO functions can be executed under a command interface environment. The command syntax is simple, and a job is executed simply by typing the name of the function followed by a list of mandatory and optional arguments. For example, overlaying 2 maps A and B, and saving the result to a separate map C, is executed simply by typing **intersect** ***A B C*** at the command prompt. Such commands can be executed one by one through a terminal, or collectively as a batch job using the ARC Macro Language (AML).

The AML is a very powerful programming language with facilities to use named variables, perform logical branching and loops, manipulate character strings and text, perform arithmetic, trigonometric, and spatial modelling operations, make calls and pass variables to other AML programs, and perform GIS operations. Commands can be grouped under an AML program for efficient execution. Complex and repetitive GIS operations can be automated by the AML.

The rainfall distribution models of this project were mainly implemented by AML programs to take advantage of the powerful features of the AML. A list of the AML programs is shown in Appendix B.

6. IMPLEMENTATION OF THE RAINFALL DISTRIBUTION MODELS

6.1 General

The rainfall distribution models of this project involved the following stages of development:

- data capture
- data conversion
- automation of operation by Arc Macro Language (AML) programs

The first stage of development involved capturing features on paper maps to a digital format on the computer. This was mainly done by manual digitisation. The maps created were in vector format. A vector map is referred to as a coverage in ARC/INFO terminology. Due to the fact that the spatial modelling functions of ARC/INFO required the execution be carried out on grid maps, the second stage of work was, therefore, the conversion of coverages into grid maps. Finally, the lengthy and repeated operations for rainfall modelling were automated by a series of programs written in AML.

6.2 Naming Convention

In building up the rainfall models, a considerable number of maps were created. It was essential, therefore, to maintain a consistent naming convention for ease of reference. Moreover, using a consistent map index was extremely useful in implementing the AML for automating the repeated operations. The same program could be reused for different events by changing only the map index.

Each map was named by a character string comprising three descriptors:

(1) a map type identifier distinguishing coverages and grid maps (one character long);

(2) a feature identifier indicating what geographic features the map was representing (three characters long);

(3) (optional) an additional descriptor giving more information on the map (flexible length). A map index could be placed here.

Figure 6 illustrates the way by which a map was named.

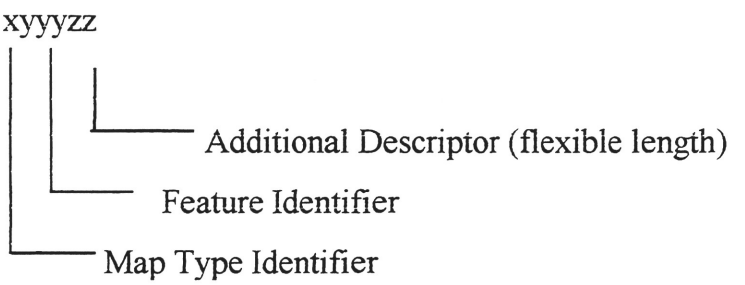

Figure 6-Naming Convention for a Map

The map type identifiers and feature identifiers used in this project are shown in Table 2 below.

TABLE 2
DESCRIPTORS FOR MAPS

	Notation	Description
Map Type Identifier	c	Coverage (vector map)
	g	Grid
Feature Identifier	syd	Sydney metropolis
	cbn	Catchment boundary
	scb	Subcatchment boundary
	str	Stream
	rga	Rain gauge
	act	Artificial / Actual Rainfall data
	tpg	Thiessen polygons
	idw	Inverse distant weights
	kri	Kriging
	tre	Trend
	spl	Spline

6.3 Data Documentation

The contents of the GIS database and the procedures involved in developing the database were documented to assure less redundancy of data and, most importantly, standardisation of data content and format.

A Data Dictionary (see Appendix C for a sample) was used to register definitions of feature attribute tables and their associated data. It was a list maintaining, for each coverage or grid, a description of all feature attributes. The data dictionary was used as a useful reference during the course of developing the database. For example, relational operations involving two maps required the presence of common items of exactly the same identification (ID) and format. Making a quick reference to the data dictionary was required to ensure that an operation requirement was satisfied. The data dictionary was referred to when the database was updated or transferred.

A Quality and Accuracy Report (see Appendix D for a sample) was used to provide an overview and a detailed description of the map layers. Specific information related to data sources reliability, automation methodologies and data quality were also incorporated into the report.

6.4 Database Development

The database was developed using ARC/INFO version 7.0.3. Maps were digitised at the Water Research Laboratory of the University of New South Wales. The digitised maps were in ASCII format and converted to ARC/INFO format using ARC/INFO conversion commands.

Maps were classified into Primary and Derived maps. The Primary maps constituted the core of the system and, usually, only changed in a long time scale. Derived maps were created through appropriate GIS operations performed upon the Primary maps, for example, grids for areal mean rainfall were Derived maps.

The purpose of the classification was to ensure that the primary maps were maintained in the computer, while the derived maps could be erased after use in order to save on computer storage. This was considered good practice for management of computer resources and enhancing efficiency. Consequently, it was considered to be extremely important for real-time applications.

6.4.1 Primary Coverages

Five primary coverages, as summarised in Table 3, were obtained by digitising paper maps, or by entering the coordinates of a feature from the keyboard, such as the positions of rain gauges.

TABLE 3
PRIMARY COVERAGES

Coverage Name	Description	Feature Class	Feature Attribute	Remarks
csyd	Sydney metropolis	lines	Sydney ID (identity)	2 arcs; one for coast line; the other for boundary of Sydney
ccbn	Catchment boundary	polygons	Catchment ID	1 polygon
cscb	Subcatchment boundaries	polygons	Subcatchment ID	24 polygons
crga	Rain gauges	point	Rain gauge ID	16 points, each defining a rain gauge station
cstr	Streams	arc	Streams ID	9 arcs, each defining a section of water course. Nodes of the arcs define positions of confluence

These primary coverages formed the core of the rainfall models. All other maps were derived from one or other of these coverages.

6.4.2 Primary Grid Maps

The following three grid maps were converted from the primary coverages:

gcbn	grid for total catchment
gscb	grid for subcatchment
grga	grid for rain gauges

As an illustration, Figure 7 shows the grid map **gscb** for subcatchments, which was converted from the coverage **cscb**.

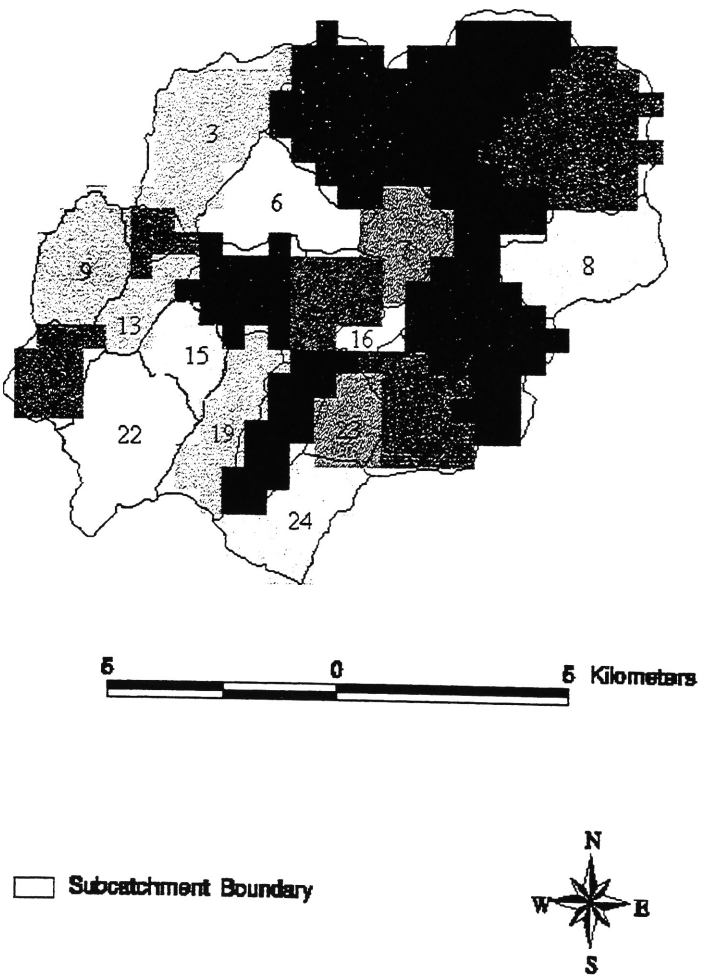

Figure 7 - Subcatchment Grid of Upper Parramatta River Catchment

For the study catchment with a total area of 110 km^2, a grid size of 500m × 500m was adopted. This resulted in a total of 440 cells (c.f. 11,000 cells of a 100m × 100m grid size). The choice was based on a balance of computational efficiency and errors in the approximation. A comparison of the areas of the original coverage and the converted grid maps in the two different grid scales is given in Table 4.

TABLE 4
COMPARISON OF SUBCATCHMENT AREAS

Sub-catchment no.	Area in Coverage (km^2)	Area in 500m×500m Grid (km^2)	Difference (km^2)	Difference (%)	Area in 100m×100m Grid (km^2)	Difference (km^2)	Difference (%)
1	6.70	6.75	+0.05	+0.75	6.68	–0.02	–0.30
2	8.64	8.75	+0.11	+1.27	8.66	+0.02	+0.23
3	7.47	7.00	–0.47	–6.29	7.42	–0.05	–0.67
4	8.96	9.00	+0.04	+0.45	8.98	+0.02	+0.22
5	4.05	3.50	–0.55	–13.58	4.05	0.00	0.00
6	5.34	5.75	+0.41	+7.68	5.35	+0.01	+0.19
7	3.34	3.25	–0.09	–2.69	3.35	+0.01	+0.30
8	6.04	5.75	–0.29	–4.80	6.05	+0.01	+0.17
9	4.48	4.75	+0.27	+6.03	4.44	–0.04	–0.89
10	1.41	1.50	+0.09	+6.38	1.43	+0.02	+1.42
11	4.83	5.75	+0.92	+19.05	4.80	–0.03	–0.62
12	4.38	4.25	–0.13	–2.97	4.38	0.00	0.00
13	2.54	2.00	–0.54	–21.26	2.56	+0.02	+0.79
14	3.58	3.50	–0.08	–2.23	3.59	+0.01	+0.28
15	2.67	2.50	–0.17	–6.37	2.65	–0.02	–0.75
16	1.20	1.00	–0.20	–16.67	1.21	+0.01	+0.83
17	3.06	3.00	–0.06	–1.96	3.09	+0.03	+0.98
18	3.09	3.00	–0.09	–2.91	3.10	+0.01	+0.32
19	4.49	4.25	–0.24	–5.35	4.48	–0.01	–0.22
20	5.06	4.50	–0.56	–11.07	5.06	+0.00	0.00
21	4.32	4.50	+0.18	+4.17	4.35	+0.03	+0.69
22	7.21	7.75	+0.54	+7.49	7.22	+0.01	+0.14
23	2.46	2.75	+0.29	+11.79	2.45	–0.01	–0.41
24	4.64	4.75	+0.11	+2.37	4.59	–0.05	–1.08
Total	109.96	109.5	–0.46	–0.42	109.94	–0.02	–0.02
Root Mean Sq. Error			+0.35			+0.02	

It can be seen that the two grid maps approximate closely to the actual areas of the subcatchments. The percentage errors of the 500m × 500m grid map range from –21.26% to +19.05%; whereas those for the 100m × 100m grid map ranges from –1.08% to +1.42%.

Presented in Figure 8 are the errors resulting from the two alternative grid maps as a function of the size of subcatchment.

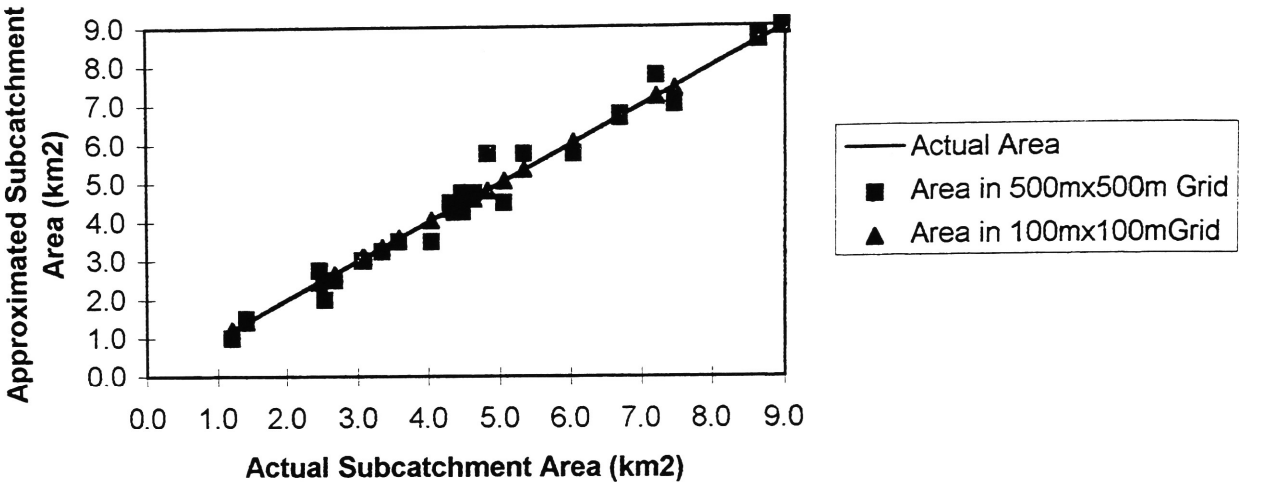

Figure 8 - Comparison of Areas Approximated by Different Grid Sizes

As shown in the above figure, both grid maps made good approximation to the actual sizes of the subcatchments. Although the 100m × 100m grid map resulted in less errors, it required 25 times more cells than the 500m × 500m grid map and, consequently, substantially greater computational effort.

It must be pointed out that the grid map was only used for modelling rainfall distribution. The actual catchment areas given in the coverage would be used to determine the volume of rainfall and subsequently used in water management models. For the purpose of making a comparison of different rainfall modelling techniques, a 500m × 500m grid was considered adequate.

6.5 AML Procedure

6.5.1 General

The AML was used to combine a series of ARC/INFO commands that were required to model the distribution of rainfall. Using the AML procedure was a great convenience and timesaver because the same sequence of commands was performed for different rainfall estimation techniques and for different rainfall events.

Each rainfall model was implemented by a single AML program. They could be run separately or joined together as a batch job. The only input to the models was rainfall at gauges and the output was a table summarising the areal mean rainfall for each subcatchment estimated by the five alternative techniques.

6.5.2 Logic and Flow Chart of Operations

Before writing the AML programs, the logic of operations had to be clearly identified. First of all, the basic maps (data) required were identified. The next step was to determine using clear logic how these base maps were to be processed to produce the required information. This was accomplished by drawing a flowchart similar to that shown as Figure 9. After this, the processing steps were translated into appropriate ARC/INFO commands. Finally, the sequence of commands were written in a text file which was then executed at the ARC/INFO command prompt to obtain the results.

The above procedure was illustrated through an example on modelling the rainfall distribution by Thiessen Polygon method as follows.

STEP 1 – Identify the base maps

The first map needed was a coverage of rain gauge locations, i.e. **cgra**. This coverage was used to create the Thiessens polygons. The second map was a map containing the rainfall values on each rain gauge. Since more than one rainstorm event was required to be

analysed, the rainfall map was indexed as **gact%i%rgs**, where **%i%** was a variable in AML's convention which could be substituted by an integer to reference to a rainstorm event. In order to obtain the areal mean rainfall for each subcatchment, a map containing the subcatchment areas, i.e. **gscb** was needed. Summing up, the following three maps were required:

(a)	**cgra**	(rain gauge coverage)
(b)	**gact%i%rgs**	(rainfall value grid)
(c)	**gscb**	(subcatchment grid)

STEP 2 – Logic and flowchart of Operations

The operations required the following ARC/INFO commands:

thiessen – to create Thiessen polygons from a point coverage.

polygrid – to convert a coverage to a grid map.

Zonalmax – to determine the rainfall values from the map gact%i%rgs and assign the values to the corresponding areas bounded by the Thiessen polygons.

Zonalmean – to determine the mean rainfall for each subcatchment from the values given in the Thiessen polygons.

An **if** conditional statement is required to select the rainfall values of each subcatchment.

The logic of the operations of the above commands is shown in Figure 9.

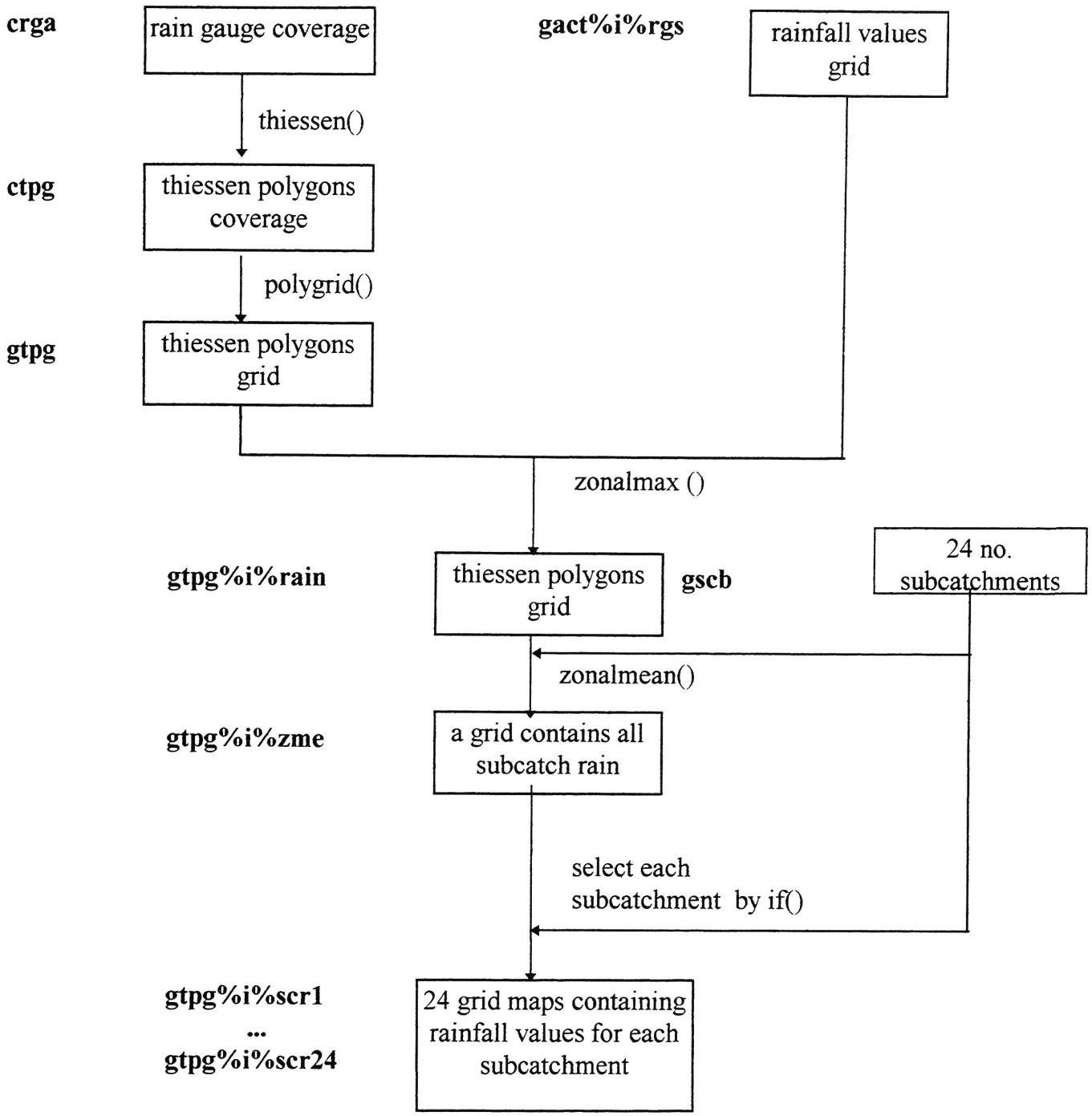

Key to flowchart:

(a) Map names are in bold.

(b) Descriptions of a map are given inside the box.

(c) ARC/INFO commands are shown in the text next to the link between boxes.

(d) %i% is an index to refer to different rainstorm incidents.

Figure 9 - Flowchart of Operations Needed to Create the Rainfall Model by Thiessen Polygon Method

STEP 3 – Automate the procedure by AML

AML programs are text files with a name ending in .aml. AML programs can be run interactively from the ARC/INFO command line, or as an executable line in another AML program, or as the result of an AML menu selection. (Note: a menu-driven user interface can be developed in ARC/INFO.)

The above command sequence was simply written in a text file as an AML program for execution. Using a loop conditional statement in the AML program, different rainfall events were analysed.

By executing the AML program in successive time steps, the temporal distribution of rainfall was automatically accounted for. With the AML, realtime operation of the rainfall distribution model was considered feasible.

7. COMPARISON OF ALTERNATIVE RAINFALL MODELS

7.1 General

This investigation of the spatial and temporal variability of rainfall over a catchment is aimed at improving the modelling of rainfall and hence the modelling of runoff hydrographs for a catchment. It was considered that investigation of the spatial variability of the alternative rainfall models would result in development of guidelines for use of the alternative models. Temporal variability can be considered then by interpolation over the time increments used for the catchment simulation.

In the comparisons of the predicted spatial variation in rainfall over the catchment obtained from each of the alternative rainfall models, the rainfall intensity for each individual grid cell was obtained from the rainfall model. These grid cell values were then converted to mean rainfall depths for an individual subcatchment. (The flowchart of operation was shown in Figure 9 of Chapter 6.)

In comparing the alternative rainfall models, both real and artificial storm events were considered. The artificial storms were used to ascertain the accuracy of rainfall estimated by the alternative models under ideal conditions, while the real events were used to assess the accuracy of rainfall estimated by the alternative models under conditions more likely to be found during real events. In addition, tests were undertaken with the assumption that some of the gauges were malfunctioning and, hence, were not recording during a storm event.

7.2 Testing Data

7.2.1 Artificial Rainfall

The artificial storm event was a five (5) hour storm event which moved from east to west over the catchment at a speed of 3km/h. At all times during this event, the spatial distribution of rainfall had a Gaussian pattern which was defined by:

$$p(x,y) = p_{max} e^{-az^2} \tag{11}$$

where p_{max} is rainfall intensity at centre of storm (mm/hr), Table 5 shows the location and intensity of rainfall at different point in time.

a is a coefficient which controls the spread of the rainfall, a value of 2.25×10^{-8} was adopted in this study.

Z is a position variable defined as $(x^2 + y^2)^{0.5}$

TABLE 5
ARTIFICIAL RAINSTORM EVENT

Time Step (hour)	Coordinates of Centre of Storm	Intensity at centre , P_{max} (mm/hr)
1	(308250, 6259250)	20
2	(305250, 6259250)	50
3	(302250, 6259250)	30
4	(299250, 6259250)	20
5	(296250, 6259250)	10

With the above equation, the rainfall intensity was generated at the centre of every grid cell of the catchment. As an illustration, Figure 10 shows the rainfall distribution at time step 3.

In addition, Figure 11 shows the track of the storm moving across the catchment during its 5-hour life span.

Generation of the spatial rainfall distribution for this artificial storm event was based on the rainfall information at the sixteen gauge locations; this information was extracted to input into the rainfall models as if recorded during an actual event.

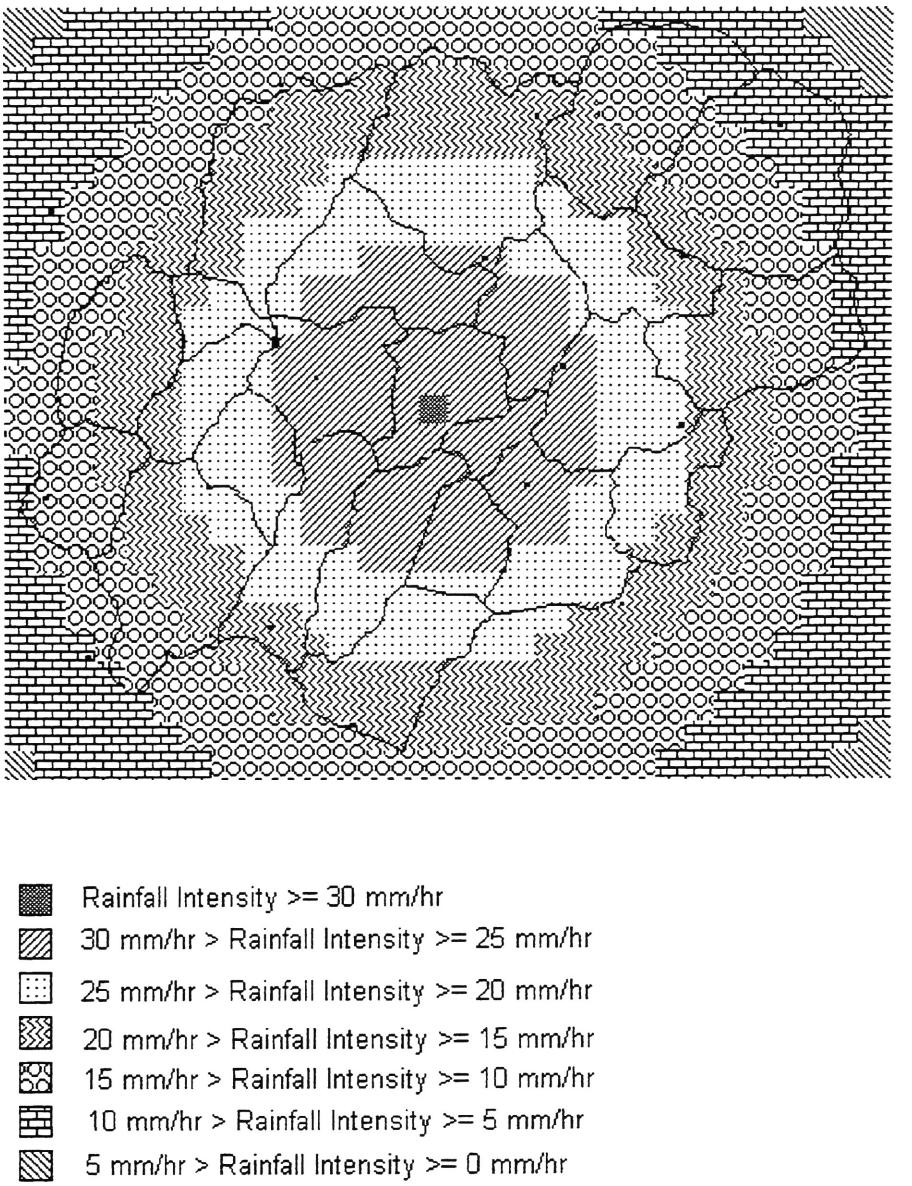

Figure 10 - Theoretical Distribution of an Artificial Rainstorm Centred at (302250, 6259250)

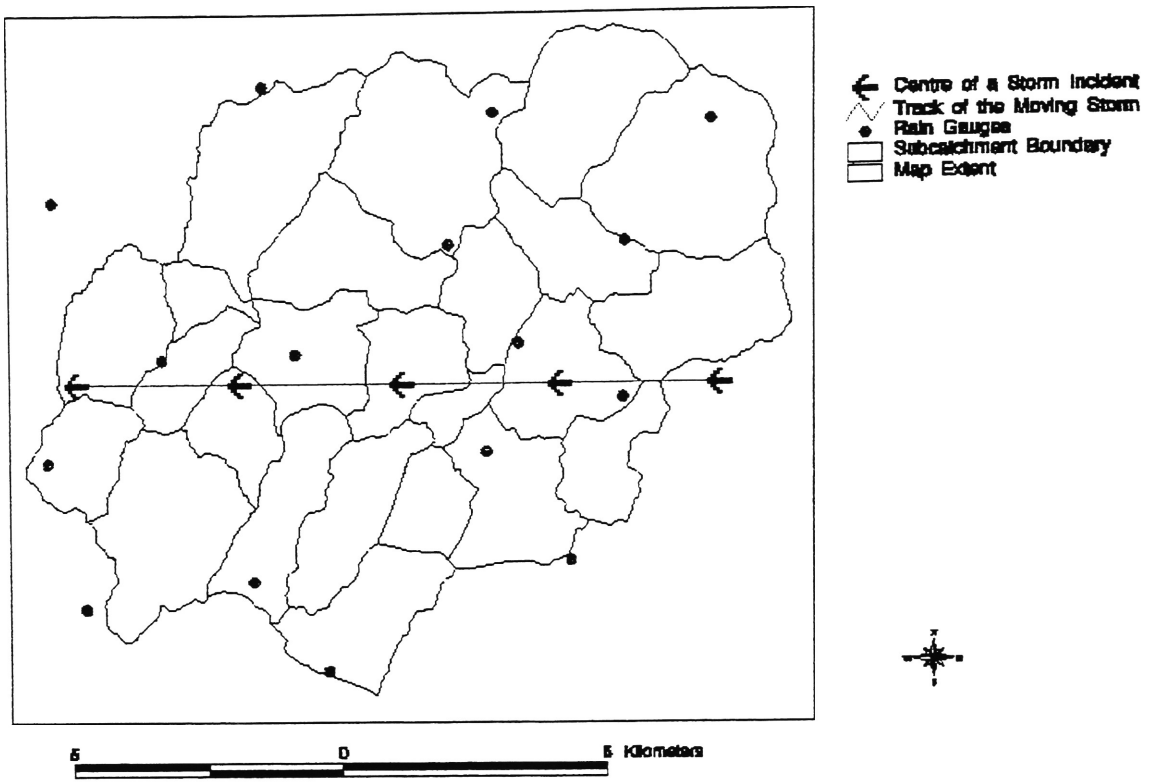

Figure 11 - Track of Storm Centres of an Artificial Moving Storm

7.2.2 Real Data

Two real rainstorm events used in the comparison were extracted from the Upper Parramatta River Catchment Trust's database. They were:

(a) daily rainfall on 5 Nov 92, and

(b) daily rainfall on 6 Nov 92.

Rainfall over these two days was of different magnitudes and variability in terms of their range and standard deviation; this enabled an assessment of the alternative models for different magnitudes and variability of rainfall.

The gauge readings of the two events are shown in Figure 12 and Figure 13 respectively. The readings are also given in Table 6 for ease of reference.

TABLE 6
TWO REAL RAINSTORM EVENTS

Gauge No.	UPRCT Ref. No.	Rainfall Depth on 5 Nov 92 (mm/day)	Rainfall Depth on 6 Nov 92 (mm/day)
1	7209	9	15
2	7251	12	26
3	7253	8.5	41.5
4	7255	25.5	38
5	7257	10.5	57.5
6	7259	13.5	22
7	7261	9	43
8	7263	13	28.5
9	7265	15.5	29
10	7267	7	47.5
11	7269	13	36.5
12	7281	16	64
13	7283	18.5	85
14	7285	9.5	35
15	7287	18	31.5
16	7299	8	27
Average value		12.9	39.2
Range		18.5	70
Standard Deviation		4.9	17.6

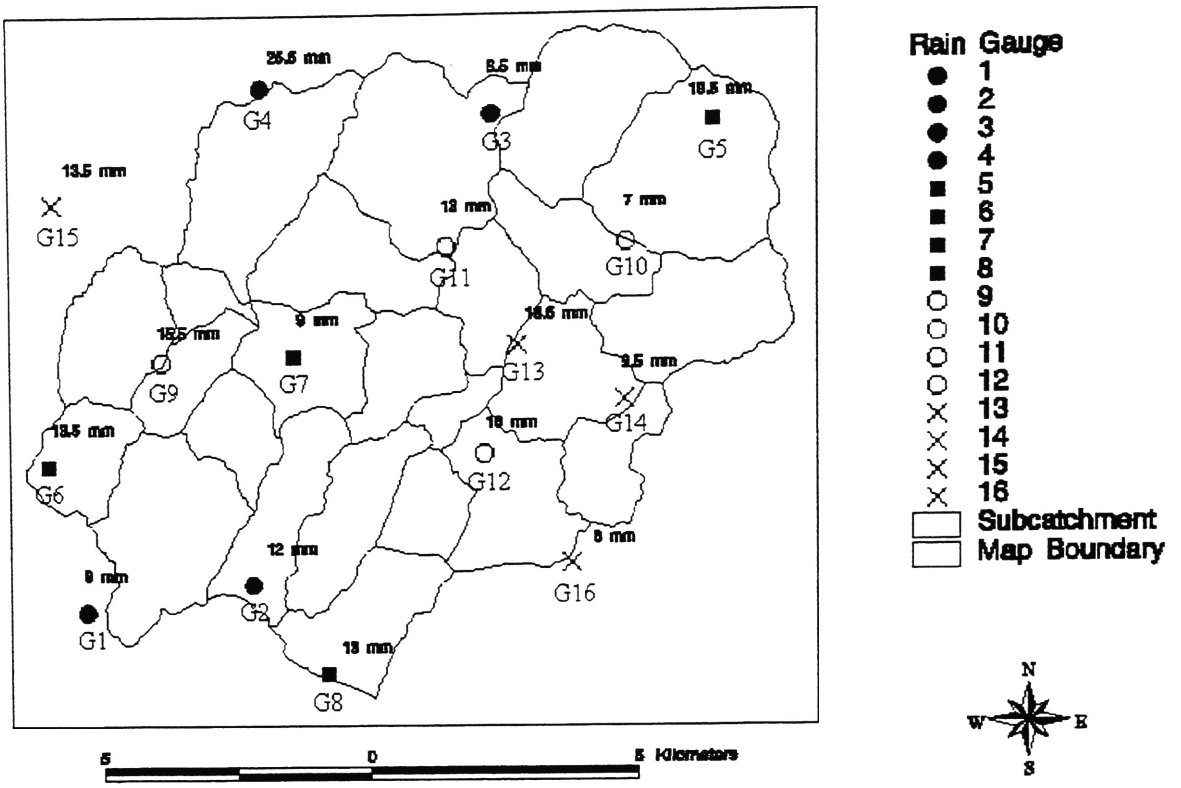

Gauge No.	Rainfall Intensity (mm/day)	Gauge No.	Rainfall Intensity (mm/day)
1	9	9	15.5
2	12	10	7
3	8.5	11	13
4	25.5	12	16
5	10.5	13	18.5
6	13.5	14	9.5
7	9	15	18
8	13	16	8

Figure 12 - Daily Rainfall Depth of a Real Storm Event on 5 Nov 92

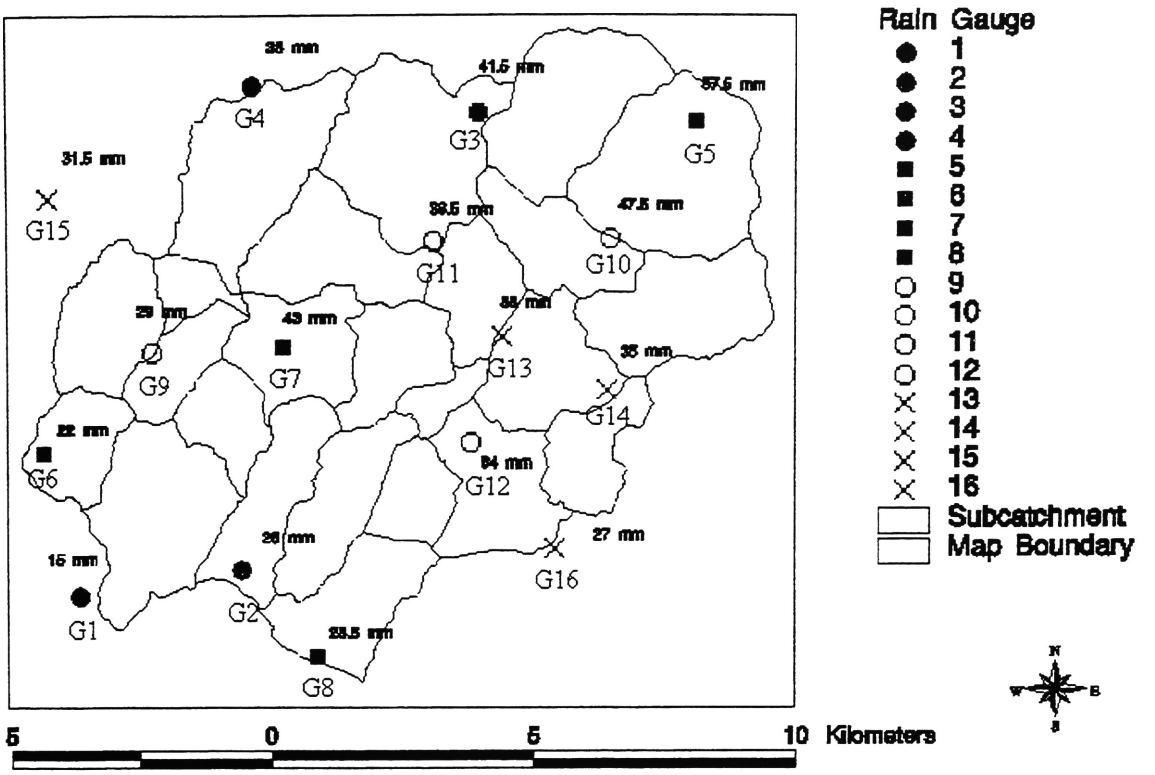

Gauge No.	Rainfall Intensity (mm/day)	Gauge No.	Rainfall Intensity (mm/day)
1	15	9	29
2	26	10	47.5
3	41.5	11	36.5
4	38	12	64
5	57.5	13	85
6	22	14	35
7	43	15	31.5
8	28.5	16	27

Figure 13 - Daily Rainfall Depth of a Real Storm Event on 6 Nov 92

7.2.3 Hypothetical Case - Rain Gauge Malfunctioning

Further tests were carried out to check the performance of the model when some gauges were assumed to be malfunctioning. The rainfall models were required to use the rainfall readings from the remaining gauges to estimate the missing values. In addition, the models' results were compared with their predictions before the omission of the gauges. This could test the models' sensitivity on missing values.

In this testing case, Gauges 1 and 7 were arbitrarily selected as malfunctioning during the following incidents:

(1) in the artificial event when the storm centred at (302250, 6259250); and

(2) in the two real events.

7.3 Results and Comparison

7.3.1 General

In comparing the predicted spatial rainfall distributions obtained from the alternative models, both visual and arithmetic comparisons were established. The arithmetic comparisons were based on the predicted rainfall occurring on each of the twenty four subcatchments into which the Upper Parramatta River Catchment had been divided for modelling purposes. In addition, for the artificial storm event, the comparisons were undertaken on hourly rainfall totals to consider motion of the storm centre. The various comparisons are summarised below.

(A) For the artificial events, the following comparisons were made:

(1) replicating the real rainfall patterns (by visual inspection);

(2) estimating areal mean rainfall at subcatchments;

(3) detecting peak values of the storm;

(4) tracking the movement of storm centres;

(5) estimating the rainfall values for two malfunctioned gauges;

(6) consistency in estimating areal mean rainfall for subcatchments before and after the omission of two gauge readings.

(B) For the real events, the following comparison were made:

(1) constructing reasonable rainfall patterns (by visual inspection);

(2) estimating areal mean rainfall for subcatchments;

(3) estimating the rainfall values for two malfunctioned gauges;

(4) consistency in estimating areal mean rainfall for subcatchments before and after the omission of two gauge readings.

7.3.2 Artificial Storm Event

(1) Rainfall Patterns (visual inspection)

Figures 14 to 18 present the rainfall distribution on the catchment estimated by the 5 methods at the incident when the storm was centred at (302250, 6259250). Similar maps can be obtained for other incidents.

By comparing these maps with Figure 10 of Section 7.2.1, the following general characteristics of the alternative rainfall models were noted.

- As expected, the Thiessen Polygon Method produced constant rainfall within the polygons, which did not represent the actual pattern of rainfall.
- The Inverse Distance Weighted method produced isolated peaks and troughs at the gauge locations. Additionally, the pattern of rainfall produced tended to differ significantly from the theoretical pattern.
- Kriging was able to identify the centre of the storm, but it failed to recognise the storm extent and, consequently, overestimated the rainfall intensity at the South-East corner of the catchment.
- The Trend surface was able to reproduce the Gaussian pattern of rainfall when used to interpolate data. However, when extrapolation of data beyond the available information was required, the Trend surface tended to predict negative rainfall depths.
- The model based on the spline surface resulted in the best fit to the theoretical rainfall pattern and, also, gave reasonable estimates of rainfall depth when extrapolation was required.

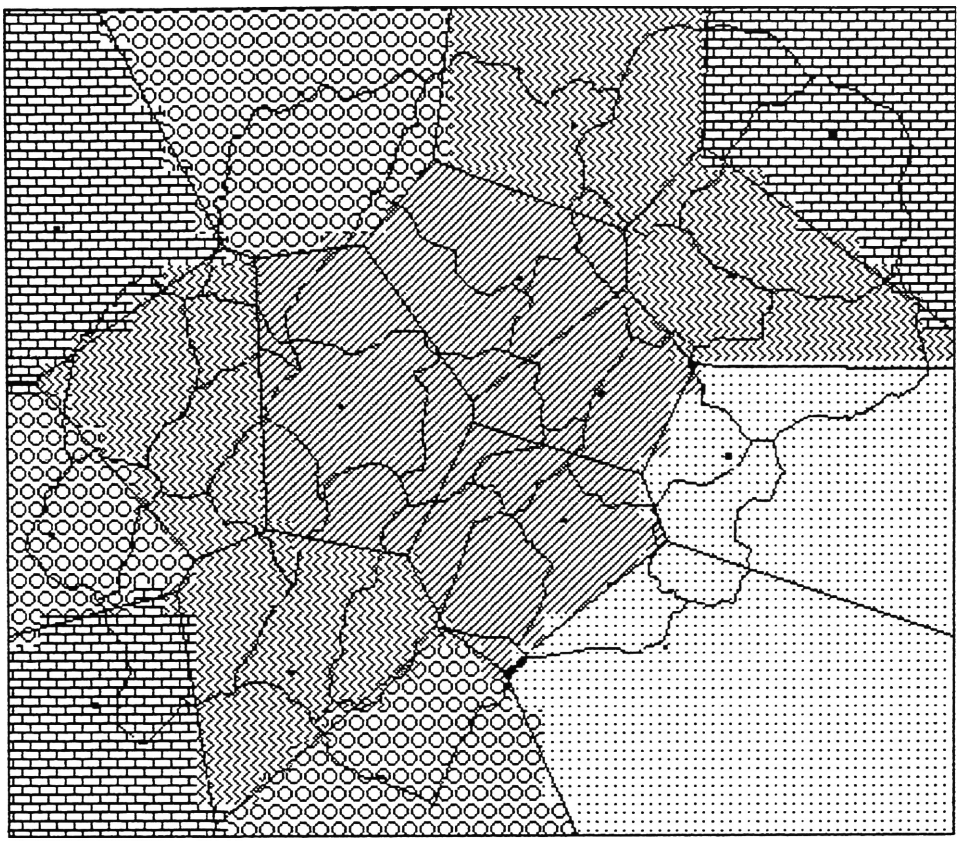

Figure 14 - Rainfall Pattern of An Artificial Rainstorm Event Estimated by the Thiessen Polygon Method

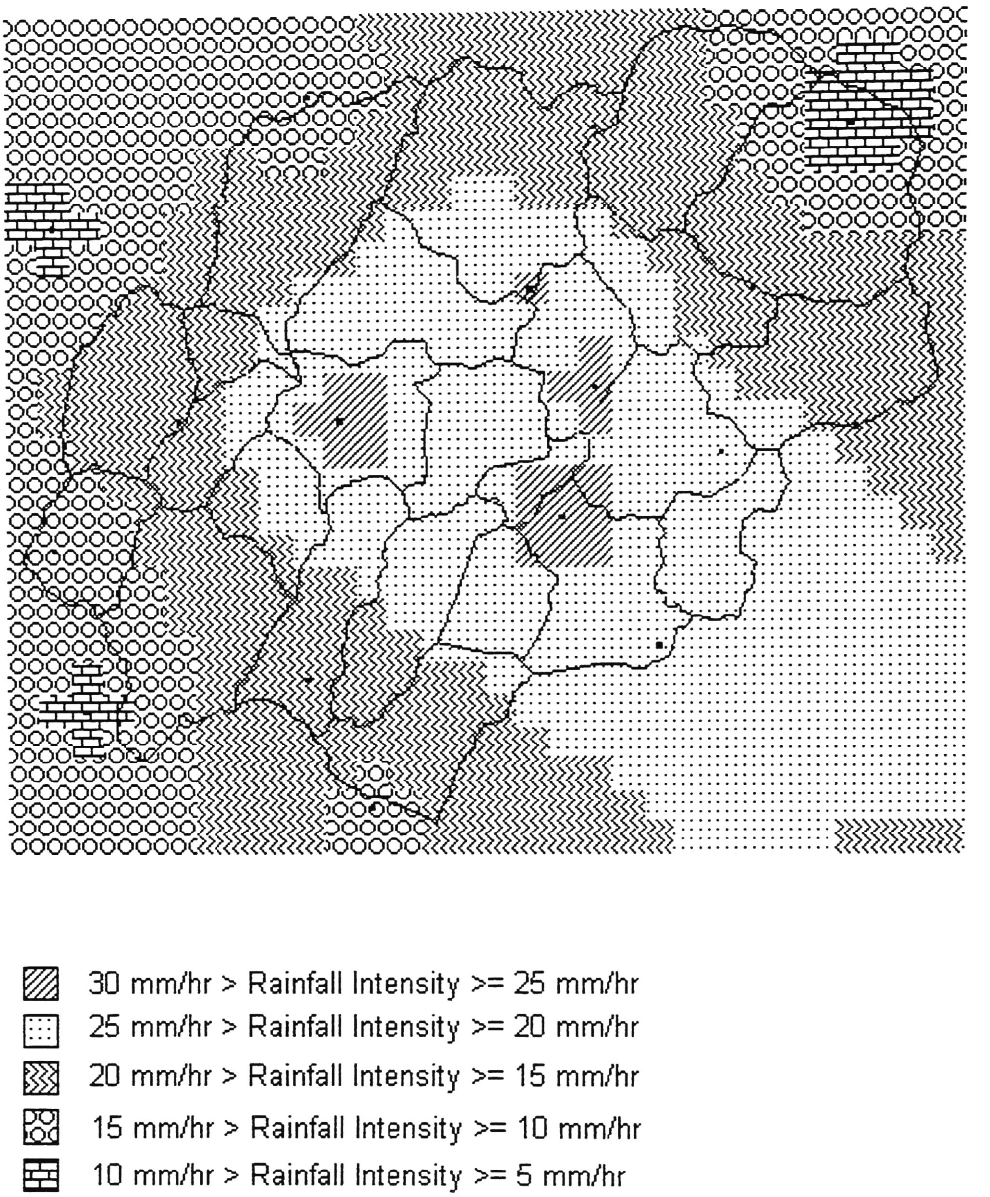

Figure 15 - Rainfall Pattern of An Artificial Rainstorm Event Estimated by the Inverse Distance Weighted Method

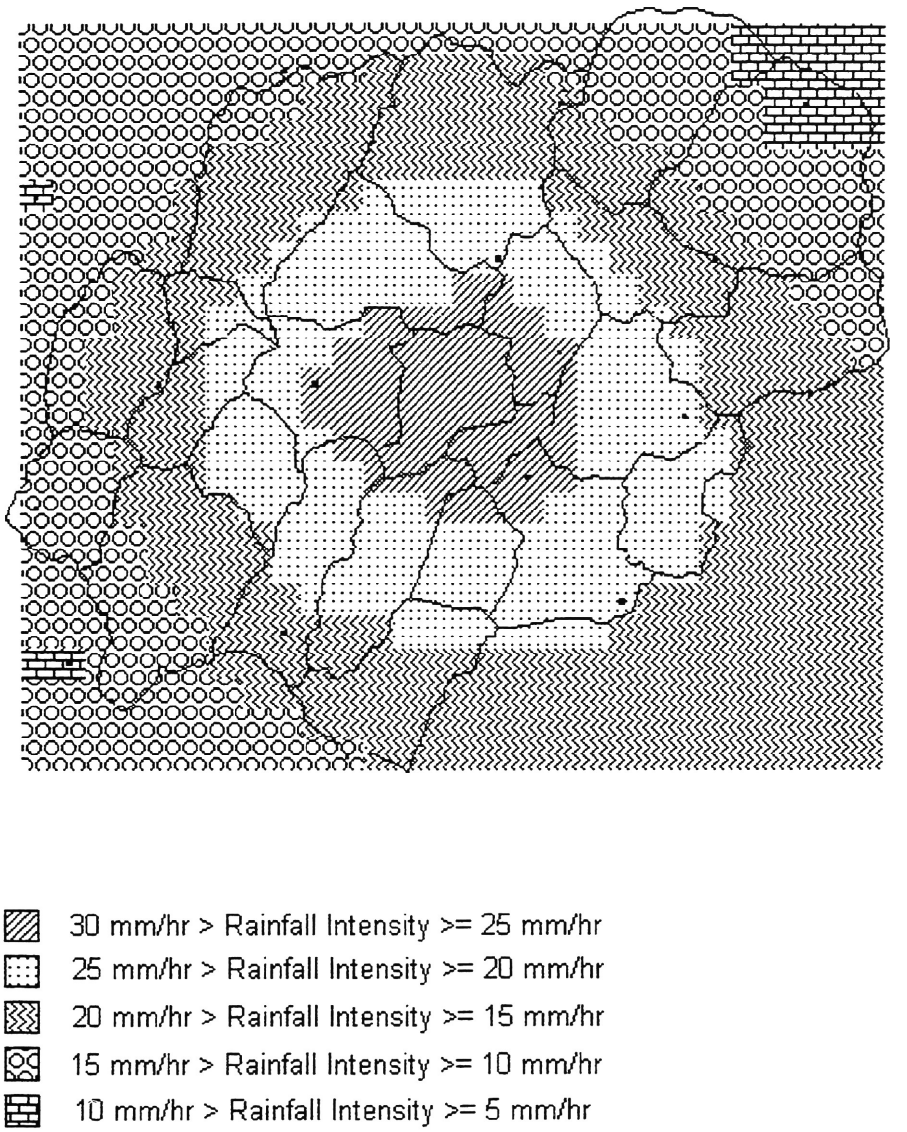

Figure 16 - Rainfall Pattern of An Artificial Rainstorm Event Estimated by the Kriging Method

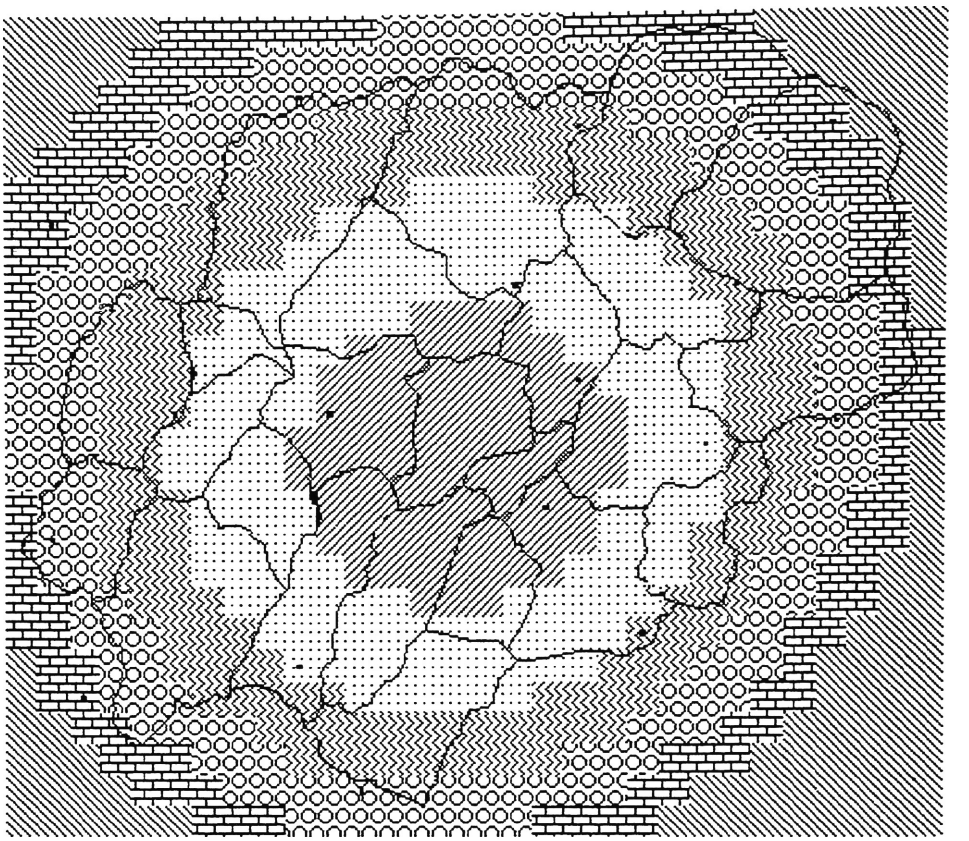

Figure 17 - Rainfall Pattern of An Artificial Rainstorm Event Estimated by the Trend Method

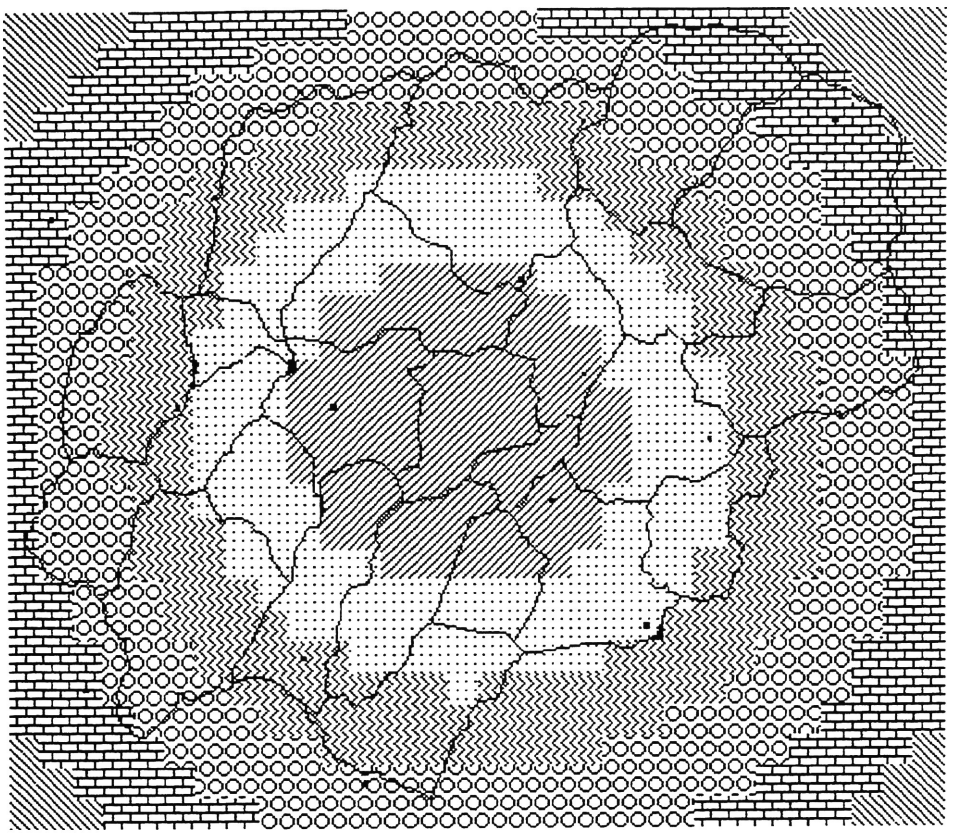

Figure 18 - Rainfall Pattern of An Artificial Rainstorm Event Estimated by the Spline Method

(2) Mean Rainfall at Subcatchments

The subcatchment mean rainfall estimated by the alternative rainfall models are detailed in Tables E1 to E5 in Appendix E. The salient points are summarised in Table 7 below.

TABLE 7
COMPARISON OF SUBCATCHMENT RAINFALL ESTIMATED BY THE ALTERNATIVE RAINFALL MODELS

	Total Volume of Rainfall during the five hours ($mm\text{-}km^2$)	Average of Root Mean Square Error	Number of Closest Estimation
Theoretical	7840	—	—
Thiessen	7710 (error −1.66%)	1.38	18
Kriging	7658 (error −2.32%)	1.11	18
Trend	7897 (error +0.73%)	0.53	29
Inverse Distance Weighted	7768 (error −0.92%)	1.68	7
Spline	7843 (error +0.04%)	0.32	51

In general, all five models were able to give reasonable estimation of the volume of rainfall. The largest percentage error was −2.32%, produced by Kriging. The closest estimation was produced by Spline, having an error of only +0.04%.

The average of root mean square errors was obtained by averaging the root mean square of errors estimated for each of the five time steps. Again, all five methods produced good results, with Spline being the best.

The number of closest estimation was obtained in the following manner: If a model gave the closest estimation to the theoretical values, it would receive a count. The total number of counts was the number of closest estimation. In this rainfall event, Spline scored the highest number of counts.

Shown in Figures 19 to 21 are the prediction errors for each model plotted as a function of the rainfall intensity. The following points were observed based on those figures.

- The Thiessen polygon method did not make accurate estimation in all five time increments. There were some significant deviations from the theoretical values as shown in the figures.
- Kriging performed well in first, second and last time steps of the rainstorm event. However, for the third and fourth time steps, Kriging over predicted at low rainfall intensity and under predicted at high rainfall intensity.
- Trend gave good estimation of the rainfall values for all five time increments of the storm event.
- Inverse distant weighted method in general over estimated the rainfall at low rainfall intensity and under estimated at high rainfall intensity.
- Spline provided excellent estimation of the rainfall values for all five time increments of the storm event.

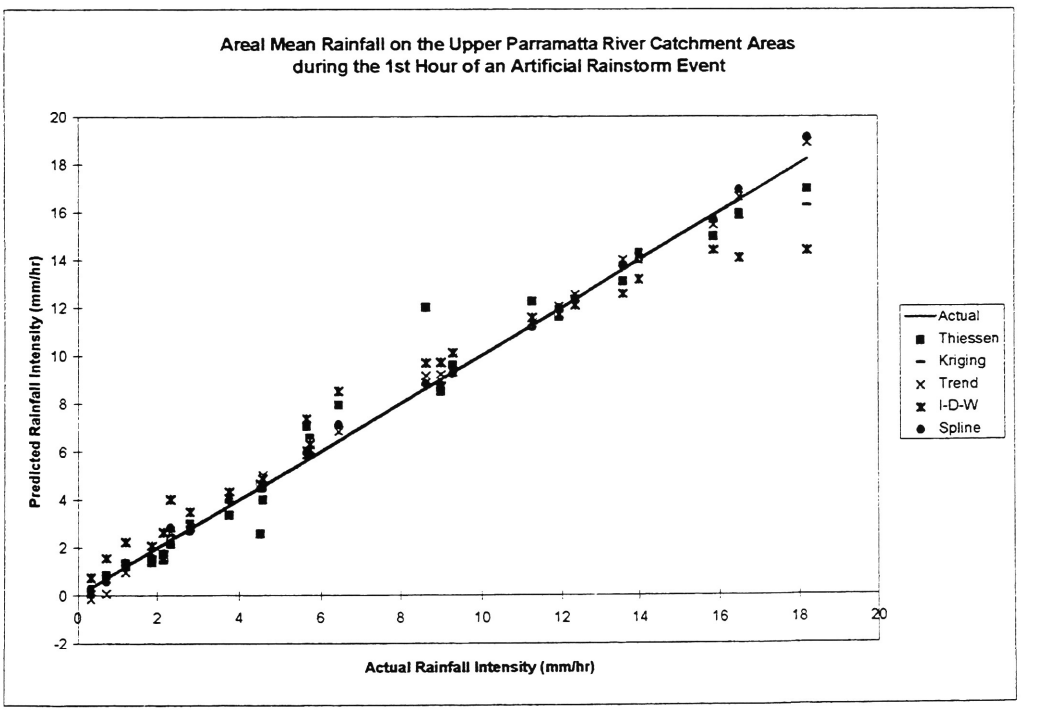

Figure 19 - Comparison of Predicted and Theoretical Rainfall Intensities for Time Step 1

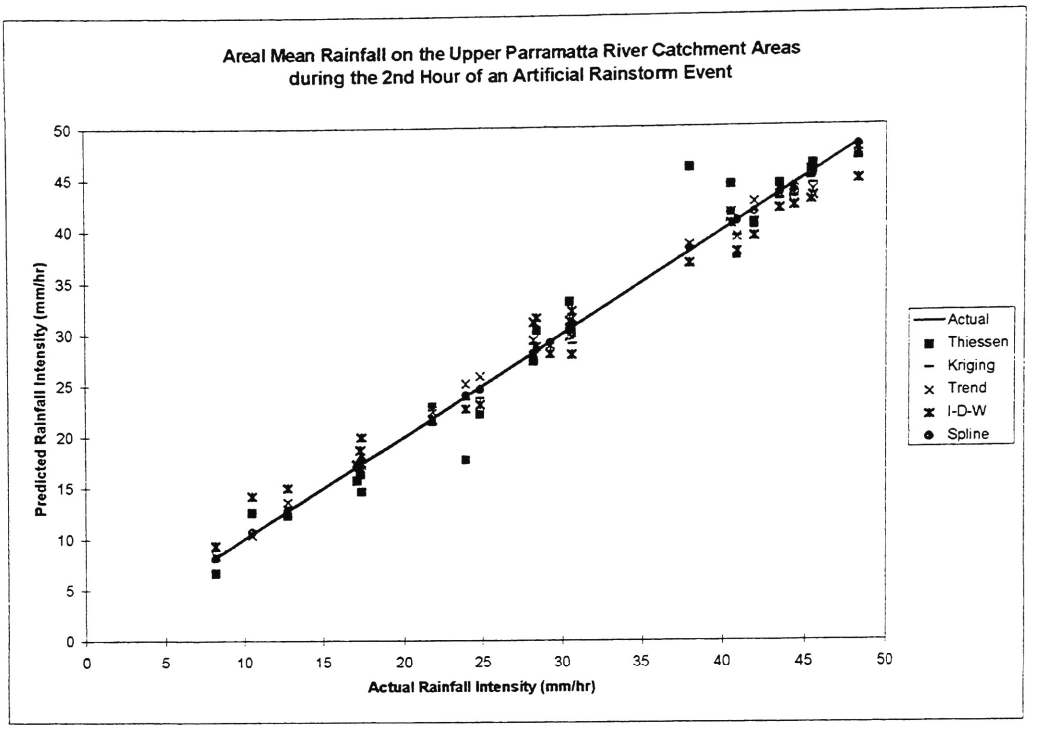

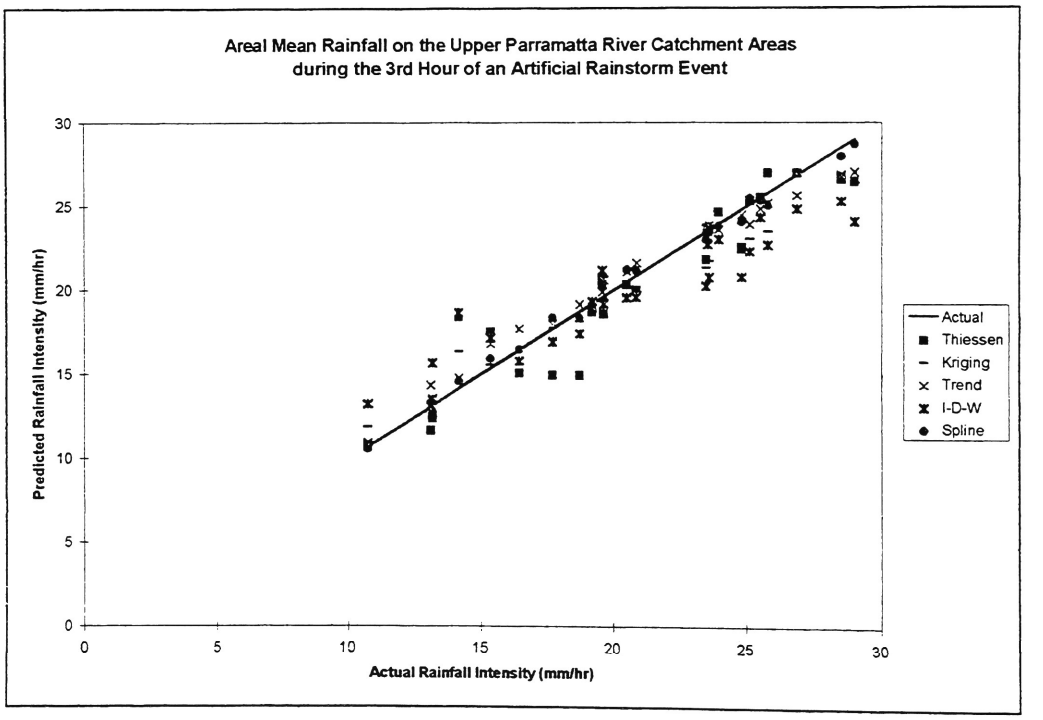

Figure 20 - Comparison of Predicted and Theoretical Rainfall Intensities for Time Steps 2 and 3

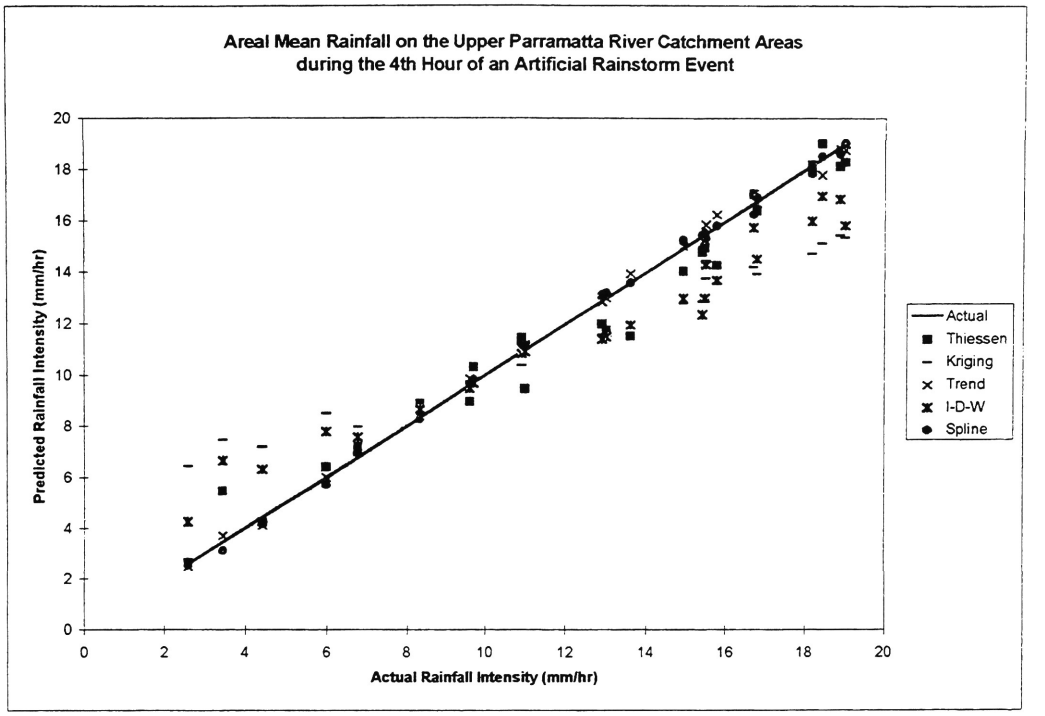

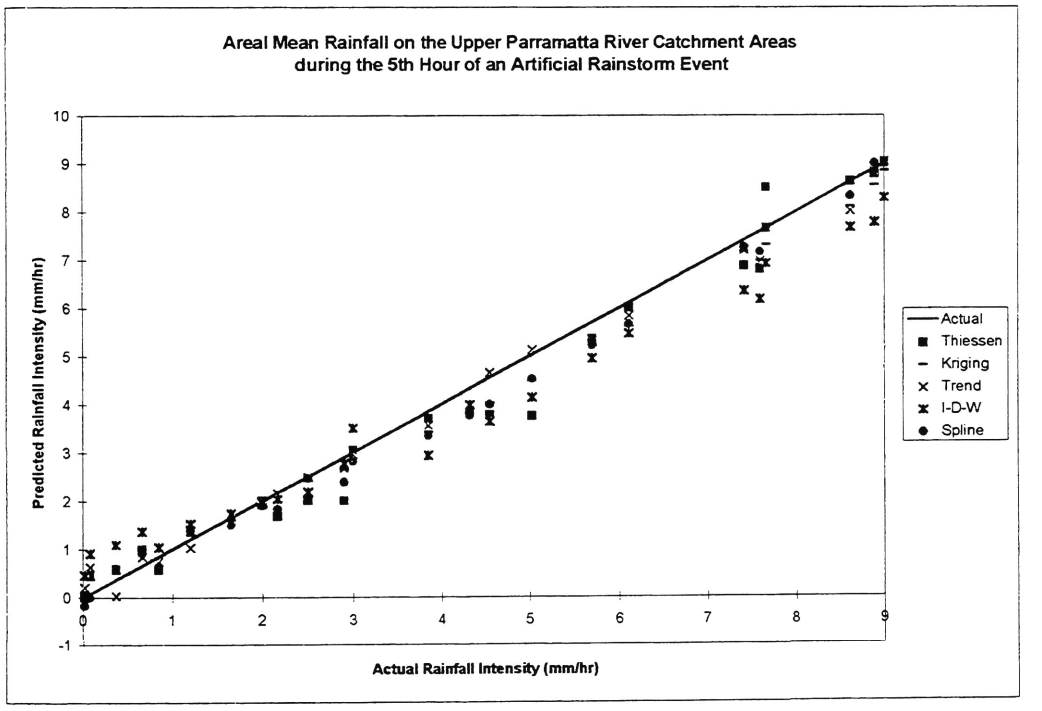

Figure 21 - Comparison of Predicted and Theoretical Rainfall Intensities for Time Steps 4 and 5

(3) Detection of Peak of Storm

Throughout the artificial storm event, the storm centre did not occur over any of the rain gauges. Of the five methods, only the Kriging, Trend and Spline can predict peak rainfall intensities at locations remote from the gauges.

Table 8 compares Kriging, Trend and Spline on their ability in finding the peak values of rainfall during the storm event.

TABLE 8
PREDICTED PEAK RAINFALL INTENSITIES

Time Step (Incident) (hr)	Actual Peak (mm/hr)	Max. Rainfall Recorded by Rain Gauge (mm/hr)	Peak estimated by Kriging (mm/hr)	Peak estimated by Trend (mm/hr)	Peak estimated by Spline (mm/hr)
1	20	18	18.00	21.65	22.44
2	50	48	48.35	48.67	48.98
3	30	27	27.00	27.44	29.12
4	20	19	19.00	19.07	19.37
5	10	9	9.08	9.61	9.61

The Kriging method was only able to predict peak rainfall intensity of slightly higher values than those recorded at gauges.

Both Trend and Spline provided reasonable estimates of the peak rainfall intensities with both tending to slightly over estimate the peak at the first time step, but under estimate thereafter.

(4) Tracking the Storm Movement

Figure 22 shows the track of peak of rainstorm predicted by the three models. It was noted that the Spline method provided the best estimation in tracking the storm movement, while Kriging and Trend had considerable deviation from the theoretical path.

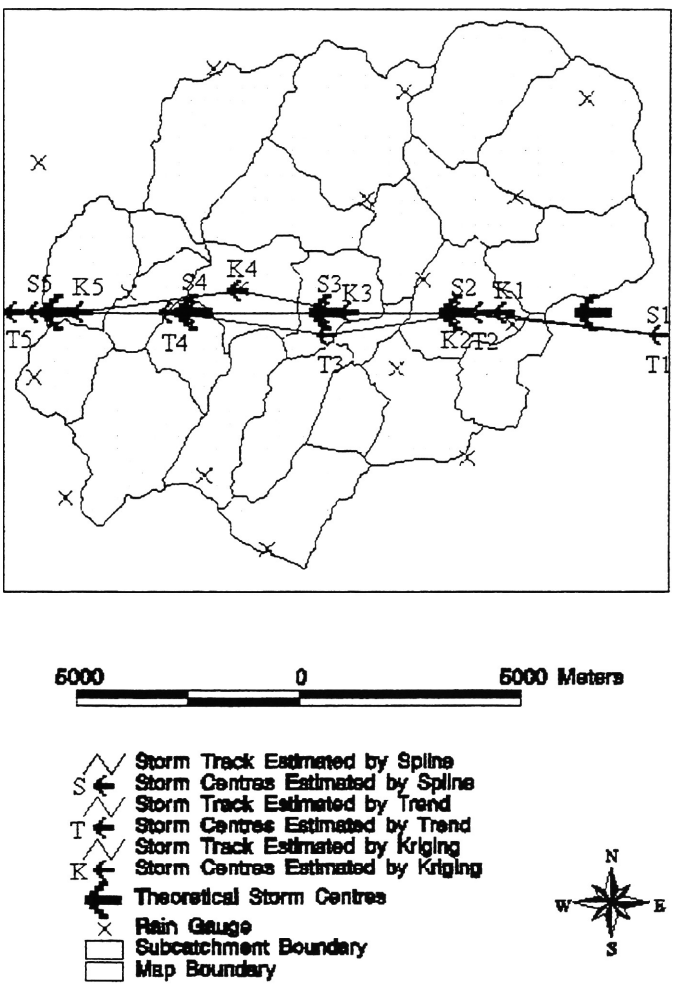

Figure 22 - Tracking the Storm Movement

(5) Hypothetical Case of Rain Gauges Malfunctioning

In this hypothetical case, rain gauges 1 and 7 were arbitrarily omitted. Gauge 1 is located at the south-west boundary of the catchment, while Gauge 7 is located near the centre of the catchment (see Figure 12 for the location of gauges). Kriging, Trend and Spline were allowed to use the remaining 14 gauges to estimate the distribution of rainfall. The estimated rainfall values at gauges 1 and 7 were extracted to compare with the known values.

TABLE 9
ESTIMATION OF THE MISSING VALUES FOR GAUGES 1 AND 7

Gauge no.	Actual value (mm/hr)	Estimated by Kriging (mm/hr)	Estimated by Trend (mm/hr)	Estimated by Spline (mm/hr)
1	9	14	5	8
7	27	22	25	26

Spline made an excellent estimation of the missing values for both gauges. Kriging and Trend were also able to produce reasonable estimation: Kriging tended to over estimate the value at gauge 1 and under estimate the value at gauge 7, while Trend under estimated for both gauges.

(6) Consistency of Estimation Before and After Omission of Two Gauge Readings

Quite often during a storm event some gauges were not able to record rainfall for a variety of reasons. In such cases, rainfall distribution must be determined using the information at the remaining gauges. It is considered that a good rainfall model should not be unduly influenced by missing values, unless the missing values are critical. For this artificial rainfall event, the Gaussian surface is smoothly distributed over the catchment, so the missing information in gauges 1 and 7 should not cause significant change in the estimation.

The estimation of areal mean rainfall with and without gauges 1 and 7 is presented in Table 10 while shown in Figure 23 are the comparisons of estimations produced by the three models as a function of the rainfall intensity.

It was noted that Trend and Spline gave consistent estimation regardless of the omission of two gauges. Kriging tended to under estimate the rainfall values after the omission of the two gauges.

TABLE 10
ESTIMATION OF AREAL MEAN RAINFALL
BEFORE AND AFTER OMISSION OF TWO GAUGES

Sub-Catchment No.	No. of Cell (no.)	Area (km^2)	Actual (mm/hr)	Kriging (mm/hr)	Kriging (gauges 1&7not working) (mm/hr)	Difference of Kriging (mm/hr)	Trend (mm/hr)	Trend (gauges 1&7not working) (mm/hr)	Difference of Trend (mm/hr)	Spline (mm/hr)	Spline (gauges 1&7not working) (mm/hr)	Difference of Spline (mm/hr)
1	27	6.75	13.14	13.64	13.97	0.33	13.56	13.95	0.39	12.75	12.75	0.00
2	35	8.75	19.20	18.71	18.44	-0.27	19.04	18.94	-0.10	19.12	19.12	0.00
3	28	7.00	17.71	16.98	15.50	-1.48	17.97	17.65	-0.32	18.36	18.24	-0.12
4	36	9.00	10.72	11.86	11.59	-0.27	10.93	10.62	-0.31	10.56	10.54	-0.02
5	14	3.50	19.64	18.99	19.20	0.21	20.60	20.33	-0.27	19.42	19.49	0.07
6	23	5.75	25.13	23.05	21.39	-1.66	23.94	23.74	-0.20	25.46	25.12	-0.34
7	13	3.25	25.53	24.44	24.98	0.54	24.86	24.74	-0.12	25.36	25.36	0.00
8	23	5.75	14.17	16.34	17.30	0.96	14.78	13.59	-1.19	14.58	14.46	-0.12
9	19	4.75	15.36	15.55	15.58	0.03	16.81	16.6	-0.21	15.91	16.04	0.13
10	6	1.50	20.50	19.59	18.05	-1.54	21.09	20.84	-0.25	21.22	20.98	-0.24
11	23	5.75	23.52	22.99	23.30	0.31	23.51	23.32	-0.19	23.45	23.48	0.03
12	17	4.25	26.88	25.02	22.35	-2.67	25.65	25.47	-0.18	26.98	26.34	-0.64
13	8	2.00	20.87	19.91	19.10	-0.81	21.62	21.24	-0.38	21.13	20.92	-0.21
14	14	3.50	29.00	26.43	25.47	-0.96	27.07	27.05	-0.02	28.72	28.34	-0.38
15	10	2.50	23.60	21.75	20.24	-1.51	23.84	23.47	-0.37	23.50	23.11	-0.39
16	4	1.00	28.50	26.43	26.49	0.06	26.91	27	0.09	27.99	27.87	-0.12
17	12	3.00	19.58	20.83	20.37	-0.46	19.88	19.77	-0.11	20.27	20.25	-0.02
18	12	3.00	13.08	13.23	13.48	0.25	14.36	13.37	-0.99	13.30	13.34	0.04
19	17	4.25	23.47	21.34	20.35	-0.99	23.68	23.31	-0.37	23.02	22.77	-0.25
20	18	4.50	23.94	23.17	22.97	-0.20	23.62	24.01	0.39	23.82	23.86	0.04
21	18	4.50	24.83	22.26	21.05	-1.21	24.52	24.5	-0.02	24.09	23.96	-0.13
22	31	7.75	16.45	15.58	16.76	1.18	17.71	16.48	-1.23	16.47	16.39	-0.08
23	11	2.75	25.81	23.50	22.29	-1.21	25.19	25.55	0.36	25.06	25.05	-0.01
24	19	4.75	18.73	18.14	16.92	-1.22	19.15	19.28	0.13	18.33	18.38	0.05
Volume of Rainfall ($mm\text{-}km^2/hr$)			2143.39	2077.52	2031.47	-46.05	2155.48	2126.85	-28.63	2141.73	2131.36	-10.37
Root Mean Square of Difference						1.06			0.47			0.21

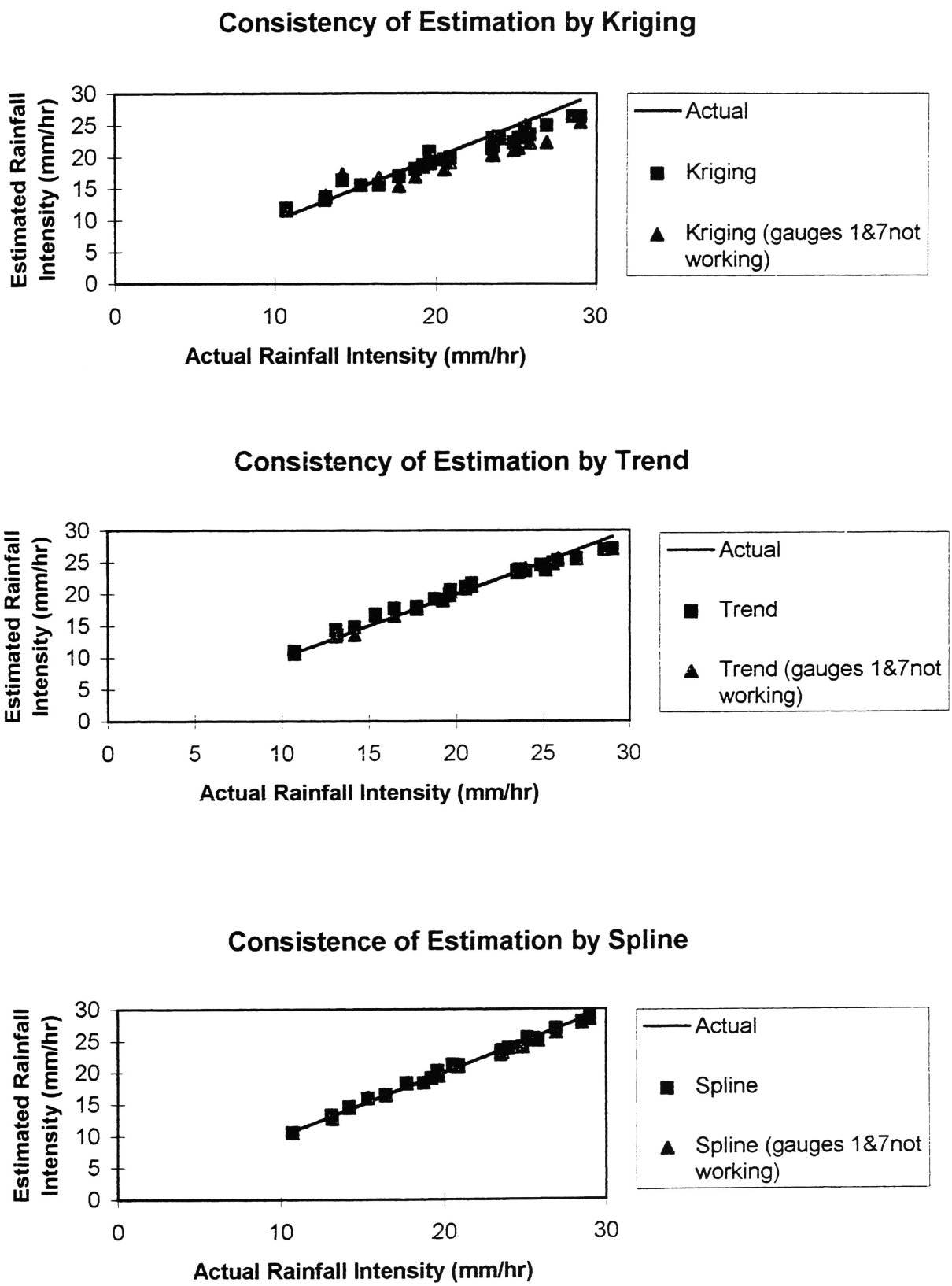

Figure 23 - Consistency of Rainfall Estimation Before and After Omission of Two Gauges

7.3.3 Real Storm Events

(1) Rainfall Distribution (visual inspection)

The rainfall distribution of the two real events estimated by Kringing, Trend and Spline are shown in Figures 24 to 29 inclusive. From these figures, the following general characteristics of the three rainfall models were noted.

- Kriging could not produce any clear pattern of rainfall for both events. It only averaged the rainfall from the gauge values for both the 5 and 6 Nov 92 events.
- For the 5 Nov 92 event, Trend was able to identify two storm centres, one at the north-west corner of the catchment, the other at south end of the catchment. Spline also detected two storm centres. By comparing rainfall values at the gauges, it was considered that Spline gave more accurate estimation of the location of the storm centres.
- For the 6 Nov 92 event, Spline and Trend produced a similar overall rainfall pattern. However, Spline predicted a sharper peak at the centre of the catchment because there was a very high value (85 mm) recorded by gauge no. 13. It was considered that Spline gave a better rainfall pattern.

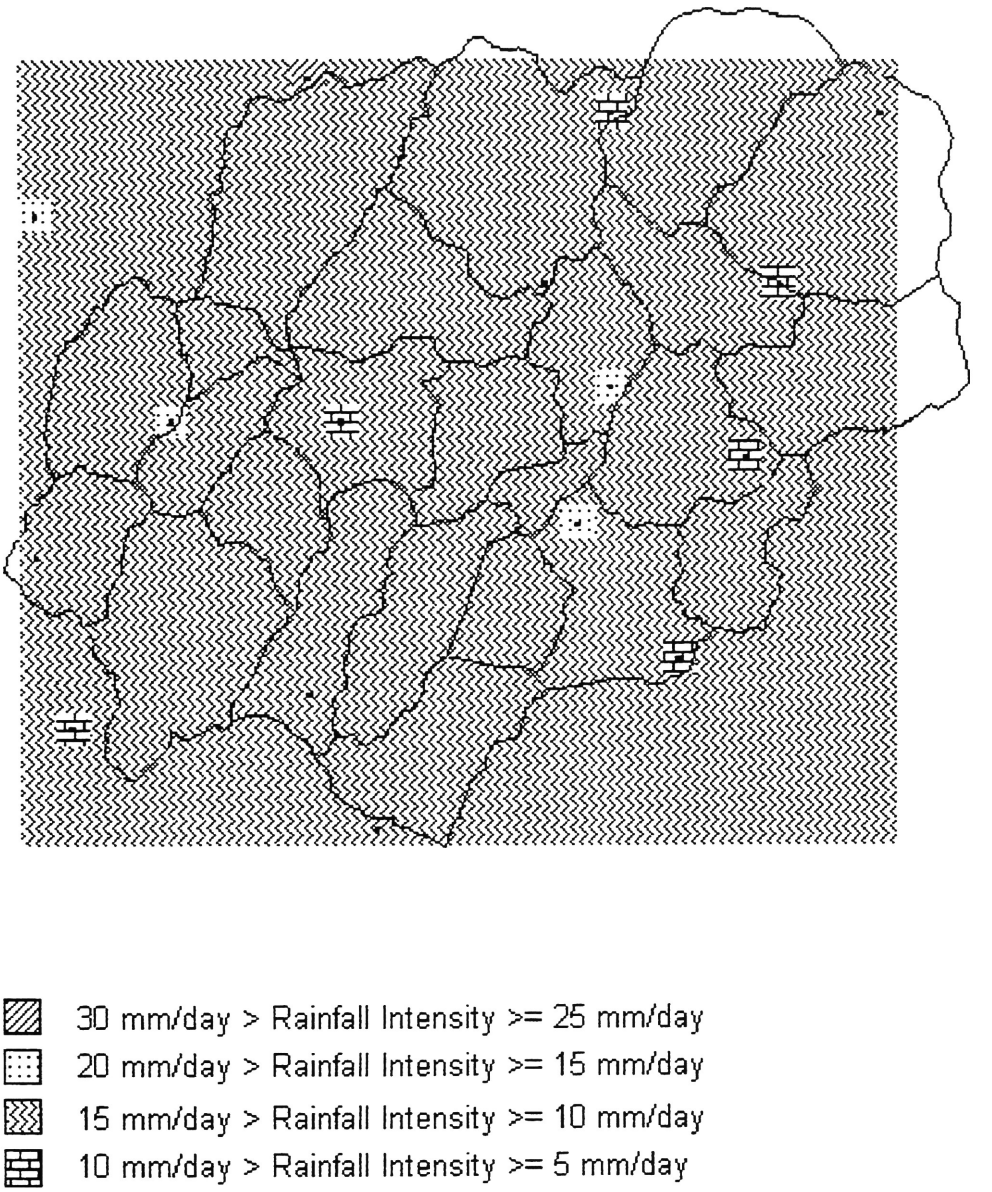

Figure 24 - Rainfall Pattern Estimated by Kriging for the Storm Event on 5 Nov 92

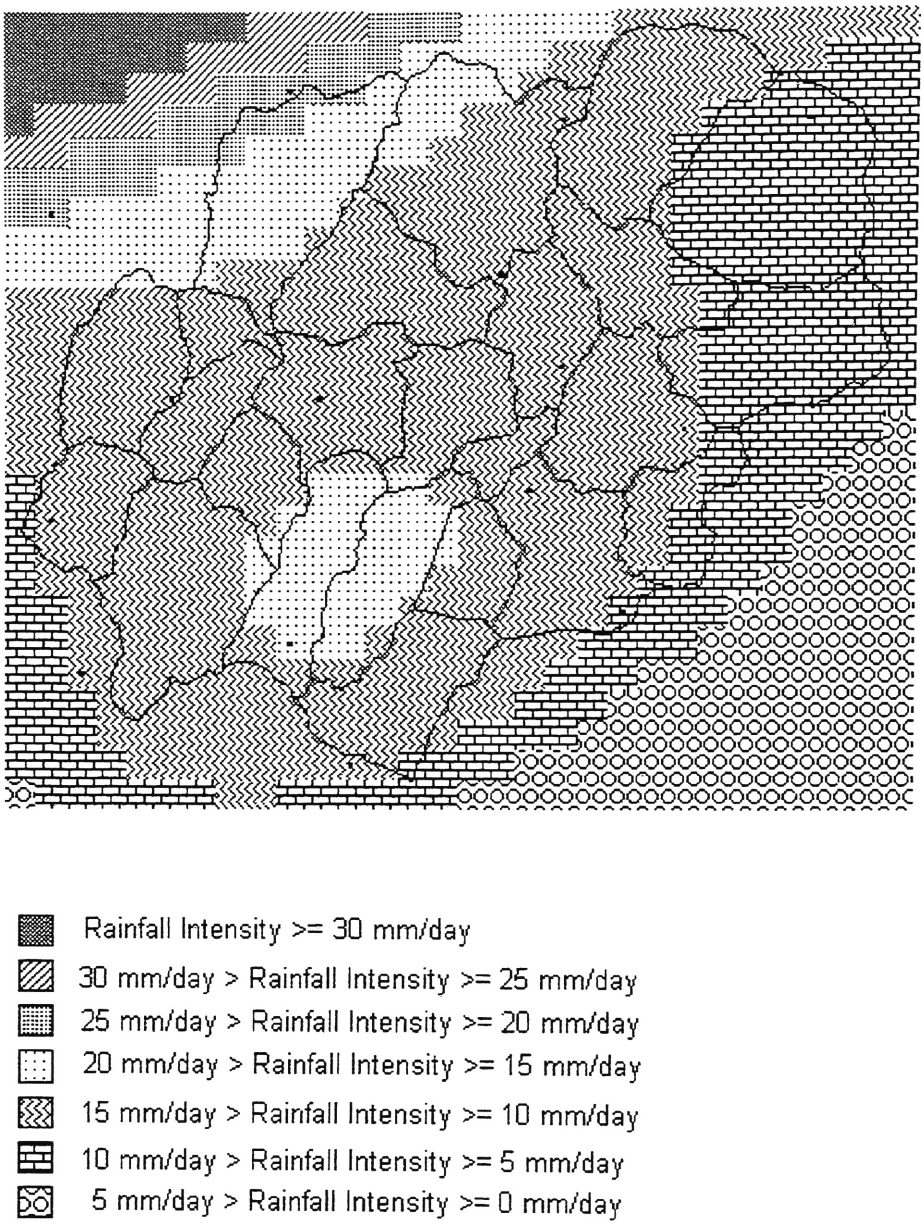

Figure 25 - Rainfall Pattern Estimated by Trend for the Storm Event on 5 Nov 92

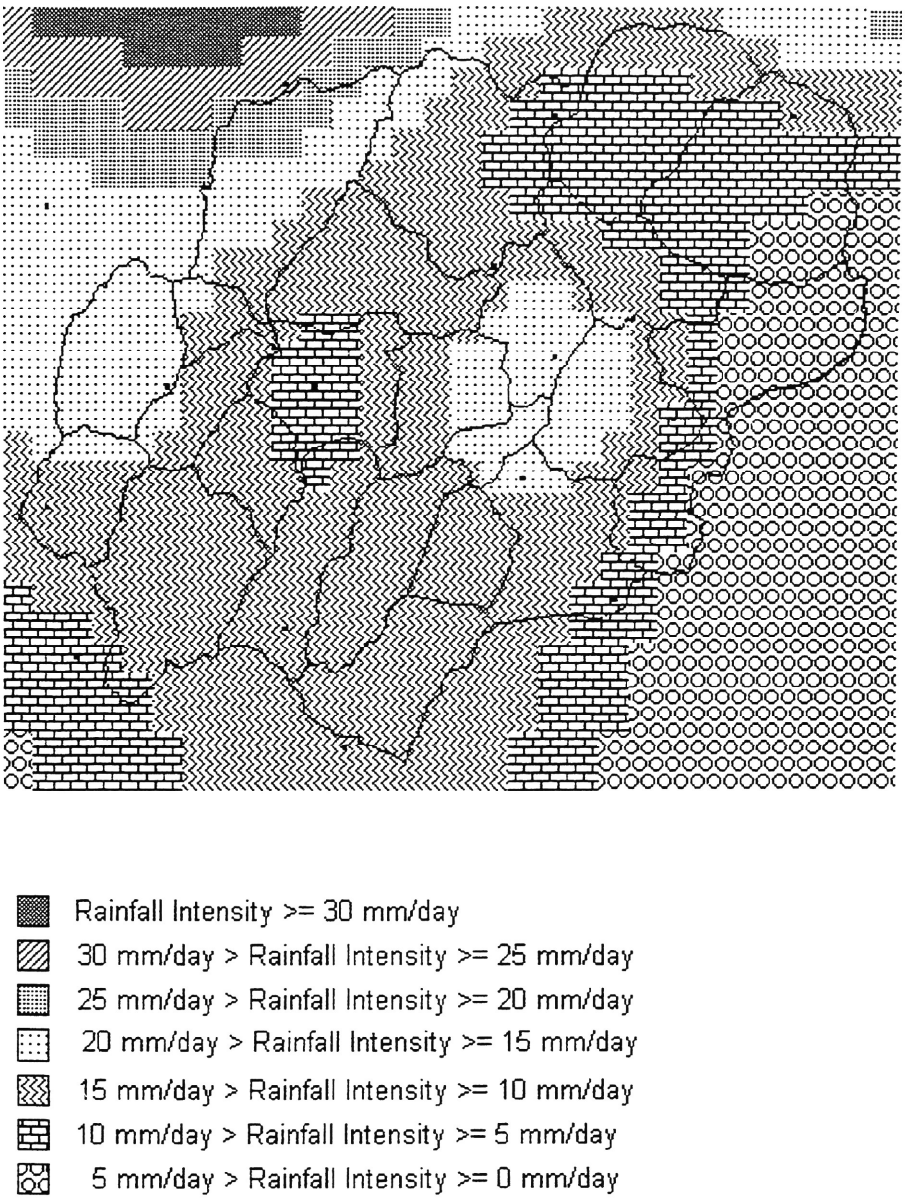

Figure 26 - Rainfall Pattern Estimated by Spline for the Storm Event on 5 Nov 92

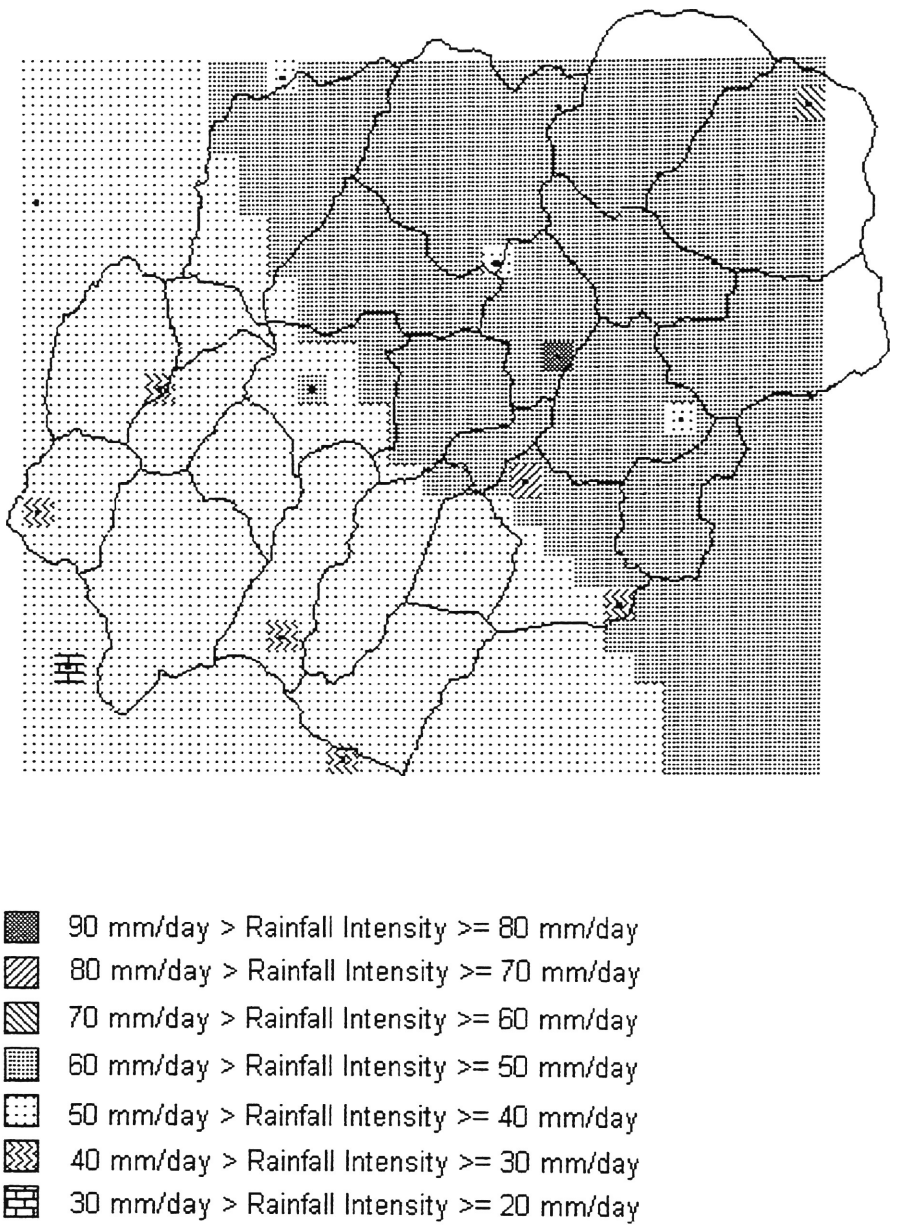

Figure 27 - Rainfall Pattern Estimated by Kriging for the Storm Event on 6 Nov 92

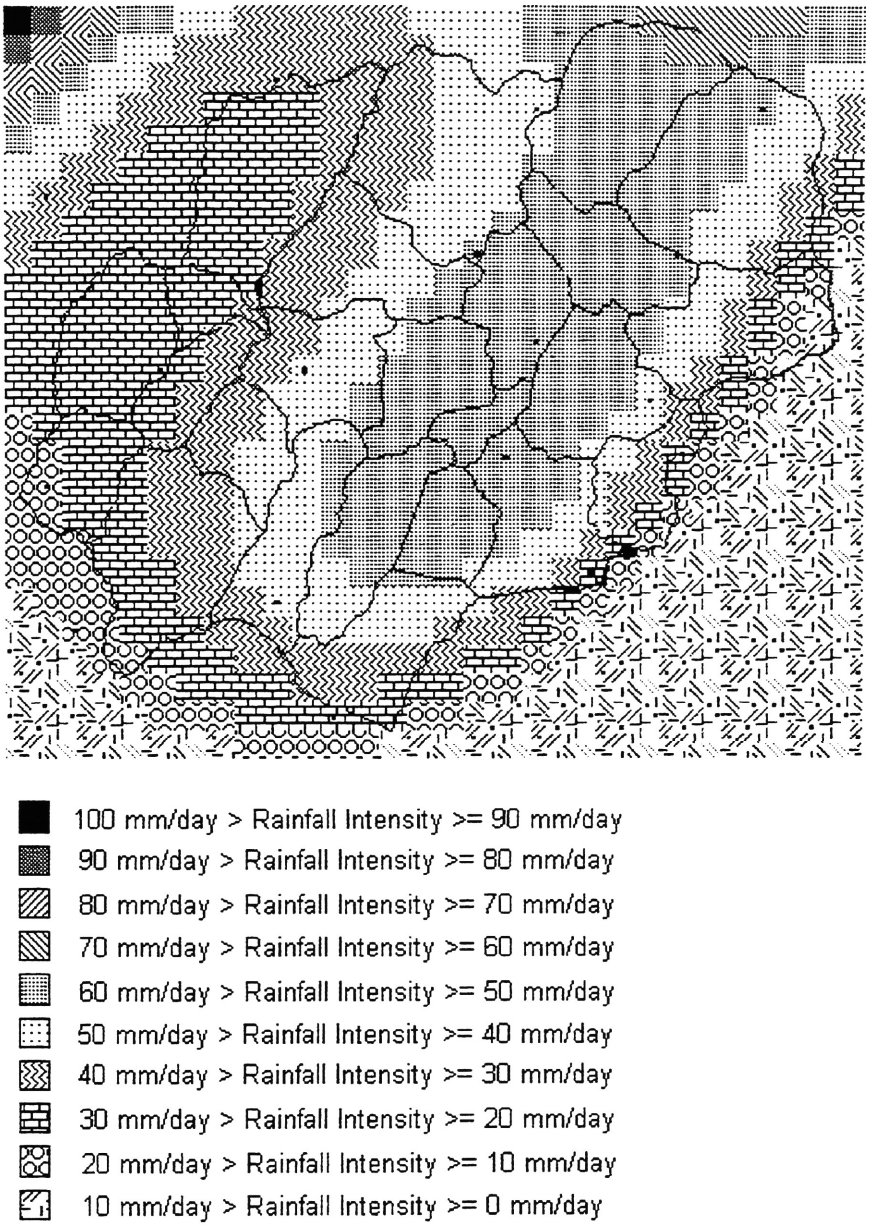

Figure 28 - Rainfall Pattern Estimated by Trend for the Storm Event on 6 Nov 92

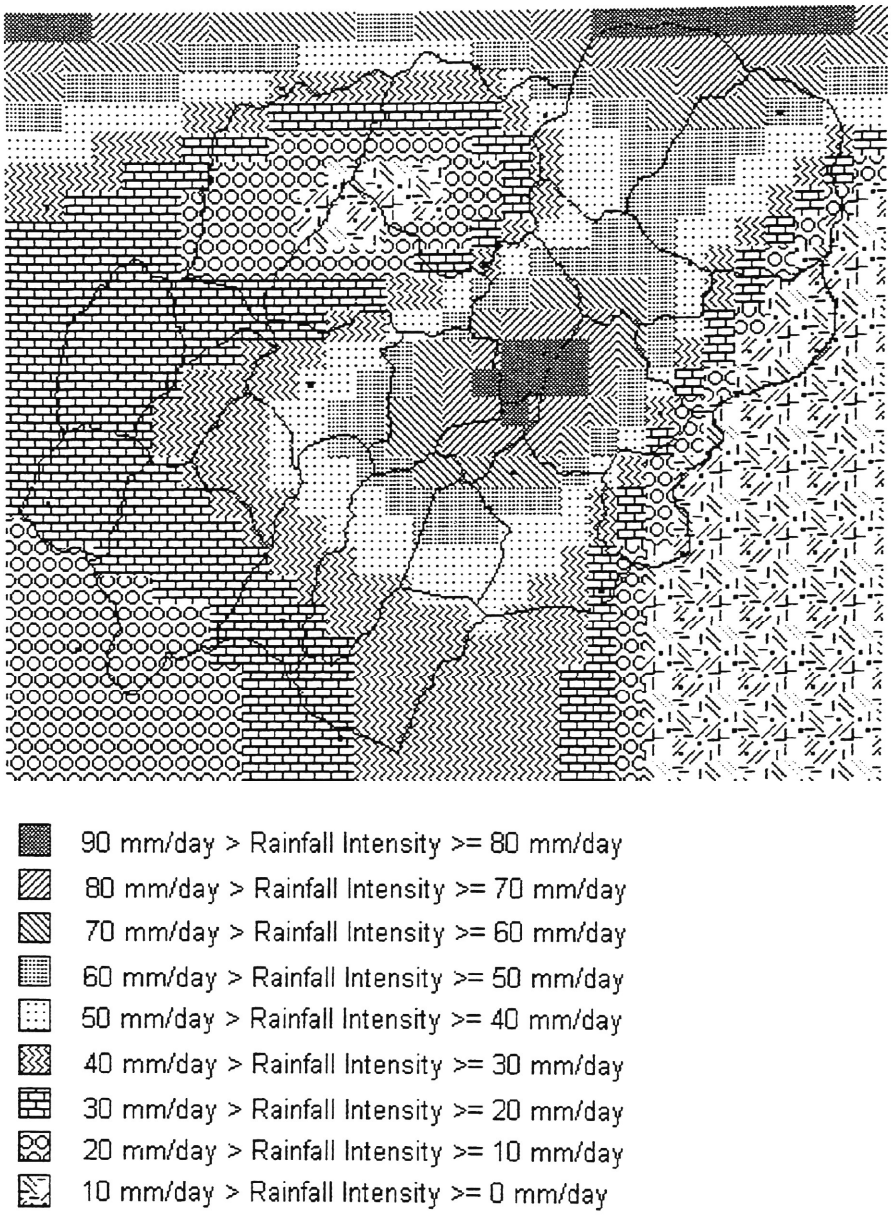

Figure 29 - Rainfall Pattern Estimated by Spline for the Storm Event on 6 Nov 92

(2) Mean Rainfall at Subcatchments

For the real events, the predicted could not be compared with theoretical values. Nonetheless, some valuable comparisons could still be made. The estimated subcatchment rainfall on 5 and 6 November 92 was detailed in Tables F1 and F2 in Appendix F. Presented in Table 11 below are the volumes of rainfall over the catchment predicted by the alternative rainfall models. As indicated by the volumes shown in this table, all five models predicted rainfall volumes that were within 10 % of the mean volumes; this mean volume of rainfall was determined from the average of the volumes predicted by each of the five alternative models. These variations in the predicted rainfall volume are less than the current accuracy with which lumped loss models, such as models of infiltration and interception, can be evaluated. Also shown in this table are the relative variations from the mean volume of rainfall. Due to these variations being obtained from the average of the predictions, the sum of the variations must be and is equal to zero.

TABLE 11
COMPARISON OF RAINFALL ESTIMATION FOR TWO REAL STORM EVENTS

	Rainfall Volume (mm-km^2)	
	5 Nov 1992	6 Nov 1992
Thiessen	1381 (0.6% diff. From mean)	4582 (2.6% diff. from mean)
Kriging	1425 (3.8% diff. From mean)	4523 (1.3% diff. from mean)
Trend	1398 (1.8% diff. From mean)	4597 (3.0% diff. from mean)
Inverse Distance Weighted	1381 (0.6% diff. from mean)	4602 (3.1% diff. from mean)
Spline	1280 (–6.8% diff. from mean)	4016 (–10.0% diff. from mean)
Mean of the 5 Estimations	1373	4464

Shown in Figure 30 is the variation in predicted rainfall depth on individual subcatchments compared to the mean predicted rainfall depth for that subcatchment. From an inspection of the spatial distribution of rainfall predicted by the alternative models, the following trends were noted.

- Predicted rainfall depths obtained from the Spline surface model tended to show the greatest variation from the average of all the models. Associated with this was a tendency for the Spline model to produce a high estimate for situations where the average rainfall depth was high and to produce a low estimate when the average rainfall depth was low. This trend is shown in Figure 30.

- The model based on Kriging produced the smoothest rainfall surface.

- The model using Thiessen polygons had the most abrupt changes in subcatchment rainfall.

- For individual subcatchments, the predicted rainfall depth obtained from each of the models displayed substantial variation; relative variations of 50% from the mean prediction (average of all predictions) were obtained.

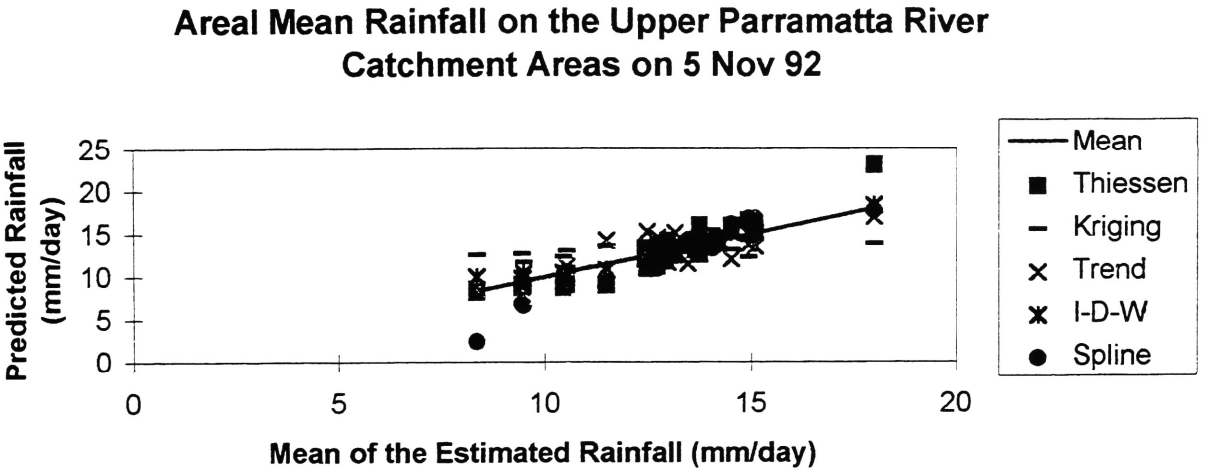

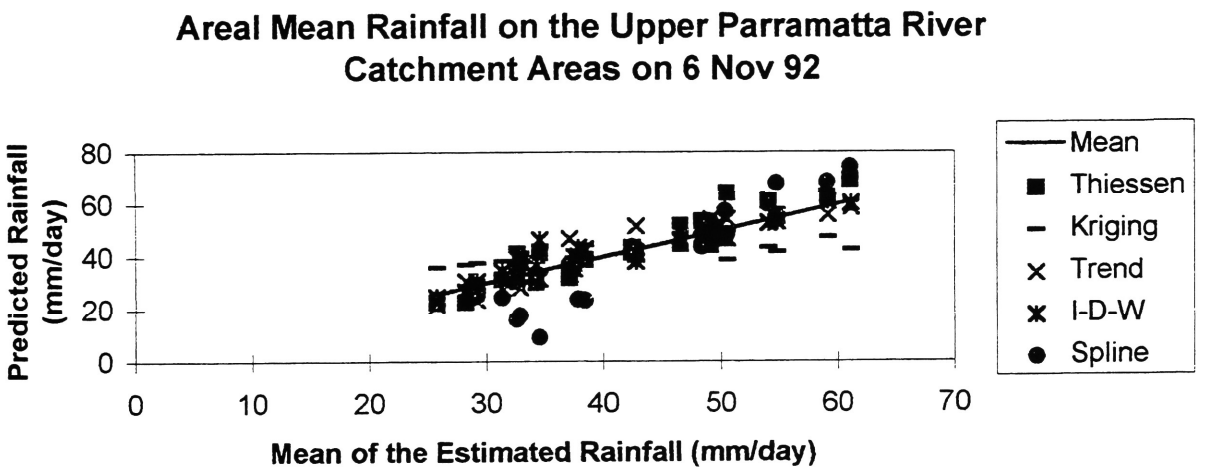

Figure 30 - Comparison of Predicted and Mean Rainfall Intensities for Two Real Events

(3) Insertion of Missing Values

The missing values of gauges 1 and 7 were estimated by the three rainfall models, namely Kriging, Trend and Spline using the information from the remaining gauges. The results are presented in Table 12 and Table 13 for the events on 5 and 6 November 92 respectively.

The 5 Nov 92 Event

TABLE 12
INSERTION OF MISSING VALUES FOR 5 NOV 92 STORM EVENT

Gauge no.	Actual value (mm/hr)	Estimated by Kriging (mm/hr)	Estimated by Trend (mm/hr)	Estimated by Spline (mm/hr)
1	9	13.9 (error +54.4%)	11.9 (error +32.2%)	13.0 (+44.4%)
7	9	14.6 (error +62.2%)	16.9 (error +87.8%)	16.9 (+87.8%)
Average error		58.3%	60.0%	66.1%

All the three methods could not accurately re-provide the missing values. They tended to over predict the rainfall. Among the three, Kriging produced the closest estimates, but still having an average percentage error of 58%.

The 6 Nov 92 Event

TABLE 13
INSERTION OF MISSING VALUES FOR 6 NOV 92 STORM EVENT

Gauge no.	Actual value (mm/hr)	Estimated by Kriging (mm/hr)	Estimated by Trend (mm/hr)	Estimated by Spline (mm/hr)
1	15	27.4 (error +82.7%)	6.9 (error –54%)	11.2 (error –25.3%)
7	43	39.1 (error –9.1%)	43.1 (error +0.2%)	37.3 (error –13.3%)
Average error		45.9%	27.1%	19.3%

It was noted from Table 13 that the three methods made reasonable estimates of the missing values. Among the three rainfall models, Spline had the least average percentage errors while Trend gave an extremely good estimate for gauge 7.

(4) Estimates Before and After Omission of Two Gauge Readings

The 5 Nov 92 Event

Presented in Tables 14 is a comparison of the areal mean rainfall estimations with and without gauges 1 and 7, while shown in Figure 31 is a plot of the rainfall intensity estimated by 14 gauges against those estimated by 16 gauges. The following general characteristics were observed.

- All 3 models produced less than 10% difference in volume of rainfall before and after the omission of two gauges.
- Kriging had a random deviation between the two estimations.
- Trend tended to make higher estimation after the omission of the two gauges.
- Spline also made higher estimation after the omission of the two gauges, but the high values tended to concentrate on higher intensity of rainfall.

One possible explanation of the higher estimation of rainfall values after the omission of the two gauges was that both gauges 1 and 7 had a value of 9 mm/day which was below the average value of the 16 gauges, i.e. 12.9 mm/day. The omission of the two gauges, therefore, increased the average rainfall intensity.

TABLE 14
ESTIMATION BEFORE AND AFTER OMISSION OF TWO GAUGES FOR THE EVENT ON 5 NOVEMBER 92

Sub-Catchment No.	No. of Cell (no.)	Area (km^2)	Kriging (mm/day)	Kriging (gauges 1&7not working) (mm/day)	Difference of Kriging (mm/day)	Trend (mm/day)	Trend (gauges 1&7not working) (mm/day)	Difference of Trend (mm/day)	Spline (mm/day)	Spline (gauges 1&7not working) (mm/day)	Difference of Spline (mm/day)
1	27	6.75	13.07	9.63	-3.44	11.19	10.13	-1.06	9.09	9.05	-0.04
2	35	8.75	13.12	12.80	-0.32	13.98	14.71	0.73	12.06	12.07	0.01
3	28	7.00	13.84	19.09	5.25	16.99	19.14	2.15	17.71	19.16	1.45
4	36	9.00	12.67	9.25	-3.42	8.77	9.2	0.43	6.87	7.13	0.26
5	14	3.50	12.34	10.03	-2.31	10.50	10.91	0.41	10.23	9.53	-0.70
6	23	5.75	13.56	14.83	1.27	13.68	16.02	2.34	11.90	15.71	3.81
7	13	3.25	13.19	15.62	2.43	12.13	12.97	0.84	16.14	16.12	-0.02
8	23	5.75	12.59	9.30	-3.29	8.56	10.24	1.68	2.41	3.72	1.31
9	19	4.75	14.35	15.60	1.25	13.55	15.77	2.22	16.77	15.37	-1.40
10	6	1.50	14.29	15.46	1.17	14.19	17.25	3.06	13.82	16.53	2.71
11	23	5.75	12.07	13.16	1.09	11.66	11.92	0.26	14.05	13.70	-0.35
12	17	4.25	13.55	14.59	1.04	14.24	16.84	2.60	9.86	16.96	7.10
13	8	2.00	14.27	14.96	0.69	13.75	16.74	2.99	13.33	15.64	2.31
14	14	3.50	12.88	16.32	3.44	13.87	15.32	1.45	14.51	18.66	4.15
15	10	2.50	14.12	14.31	0.19	14.58	17.28	2.70	10.93	15.16	4.23
16	4	1.00	12.33	16.93	4.60	13.82	14.47	0.65	16.81	18.17	1.36
17	12	3.00	11.71	9.80	-1.91	9.80	9.75	-0.05	6.63	6.91	0.28
18	12	3.00	14.19	13.92	-0.27	11.56	13.28	1.72	14.26	13.80	-0.46
19	17	4.25	12.92	13.26	0.34	15.23	17.02	1.79	11.12	13.72	2.60
20	18	4.50	11.77	11.87	0.10	12.36	11.98	-0.38	12.50	11.96	-0.54
21	18	4.50	12.15	13.51	1.36	15.10	16.1	1.00	12.46	13.79	1.33
22	31	7.75	13.78	13.54	-0.24	13.65	15.88	2.23	11.90	13.12	1.22
23	11	2.75	11.85	13.46	1.61	14.36	14.48	0.12	13.36	13.36	0.00
24	19	4.75	12.10	12.66	0.56	12.80	12.87	0.07	12.80	12.08	-0.72
Volume of Rainfall (mm-km^2/day)			1425.30	1437.02	11.73	1397.75	1522.67	124.92	1279.90	1395.89	115.99
Root Mean Square of Difference					2.26			1.68			2.35

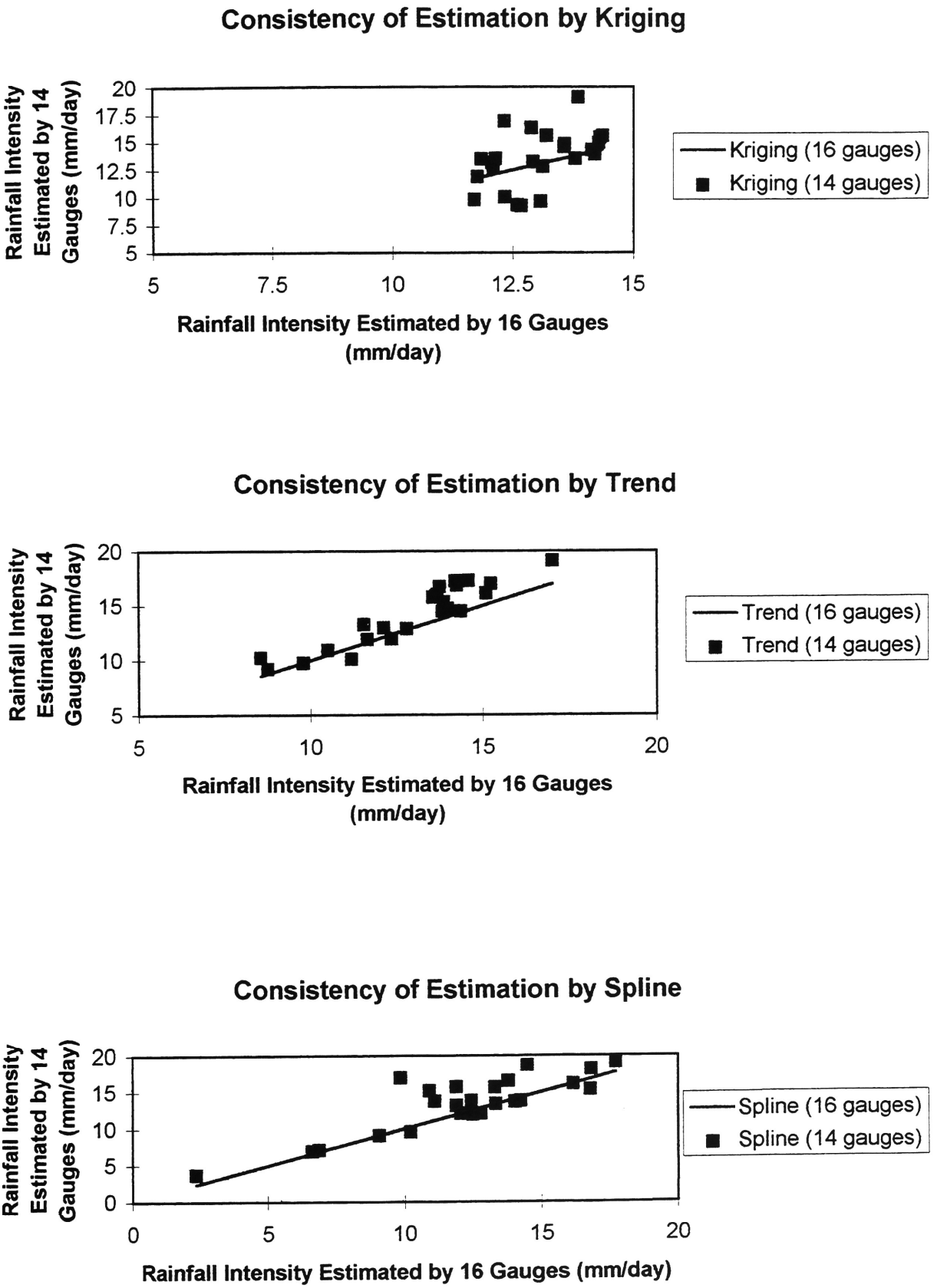

Figure 31 - Consistency of Estimation of the Rainfall Models for the Event on 5 Nov 92

The 6 Nov 92 Event

Presented in Table 15 is a comparison of the areal mean rainfall estimations with and without gauges 1 and 7, while shown in Figure 32 is a plot of the rainfall intensity estimated by 14 gauges against those estimated by 16 gauges. The following general characteristics were observed.

- All 3 models produced less than 5 % difference in volume of rainfall before and after the omission of two gauges. Trend had the least difference.
- Kriging had a random deviation between the two estimations.
- Trend and Spline made consistent estimation before and after the omission of the two gauges. They were less susceptible to missing values.

TABLE 15
ESTIMATION BEFORE AND AFTER OMISSION OF TWO GAUGES FOR THE EVENT ON 6 NOVEMBER 92

Sub-catchment No.	No. of Cell (no.)	Area (km^2)	Kriging (mm/day)	Kriging (gauges 1&7not working) (mm/day)	Difference of Kriging (mm/day)	Trend (mm/day)	Trend (gauges 1&7not working) (mm/day)	Difference of Trend (mm/day)	Spline (mm/day)	Spline (gauges 1&7not working) (mm/day)	Difference of Spline (mm/day)
1	27	6.75	44.46	46.52	2.06	55.24	55.64	0.40	57.47	57.50	0.03
2	35	8.75	44.24	35.37	-8.87	42.98	43.07	0.09	23.51	23.50	-0.01
3	28	7.00	41.41	32.91	-8.50	28.48	28.73	0.25	17.74	16.67	-1.07
4	36	9.00	44.64	50.39	5.75	48.31	47.8	-0.51	43.67	43.48	-0.19
5	14	3.50	44.40	50.53	6.13	54.14	53.69	-0.45	53.08	53.57	0.49
6	23	5.75	42.17	38.44	-3.73	40.32	40.95	0.63	23.86	21.15	-2.71
7	13	3.25	47.31	63.62	16.31	55.91	56.04	0.13	68.36	68.38	0.02
8	23	5.75	44.13	39.94	-4.19	31.67	29.67	-2.00	9.19	8.28	-0.91
9	19	4.75	37.71	29.34	-8.37	23.73	24.28	0.55	25.20	26.20	1.00
10	6	1.50	38.33	30.48	-7.85	27.88	28.75	0.87	24.49	22.52	-1.97
11	23	5.75	43.38	55.36	11.98	52.97	52.66	-0.31	59.80	60.03	0.23
12	17	4.25	39.16	40.54	1.38	43.47	44.29	0.82	43.62	38.63	-4.99
13	8	2.00	37.73	29.05	-8.68	30.79	31.31	0.52	31.36	29.73	-1.63
14	14	3.50	41.79	59.18	17.39	55.00	55.65	0.65	67.97	65.06	-2.91
15	10	2.50	37.10	31.67	-5.43	39.92	40.32	0.40	37.93	34.99	-2.94
16	4	1.00	42.56	67.07	24.51	58.81	59.34	0.53	74.30	73.35	-0.95
17	12	3.00	43.38	33.26	-10.12	32.27	31.97	-0.30	16.23	16.01	-0.22
18	12	3.00	35.86	23.99	-11.87	22.04	20.53	-1.51	23.91	24.26	0.35
19	17	4.25	36.41	34.20	-2.21	46.80	46.79	-0.01	37.16	35.38	-1.78
20	18	4.50	42.34	45.29	2.95	47.23	47.98	0.75	44.94	45.34	0.40
21	18	4.50	38.23	40.72	2.49	51.69	52.11	0.42	43.31	42.47	-0.84
22	31	7.75	37.04	25.99	-11.05	30.82	28.97	-1.85	23.83	22.80	-1.03
23	11	2.75	38.80	46.84	8.04	54.17	55.07	0.90	48.34	48.42	0.08
24	19	4.75	38.07	30.80	-7.27	37.35	37.69	0.34	33.41	34.05	0.64
Volume of Rainfall (mm-km^2/day)			4523.36	4409.54	-113.82	4596.99	4588.62	-8.37	4016.03	3934.20	-81.83
Root Mean Square of Difference					9.81			0.80			1.66

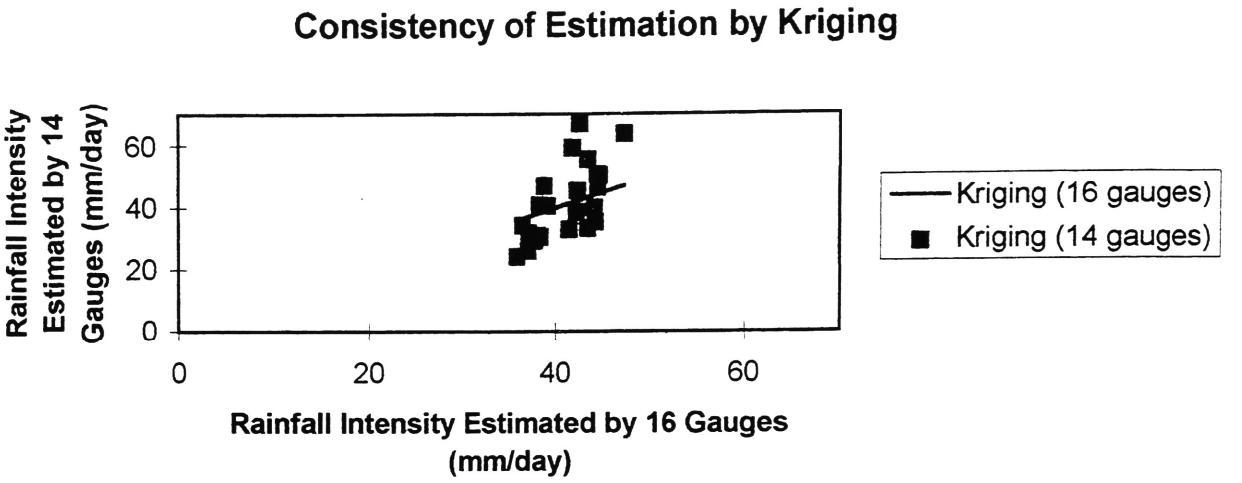

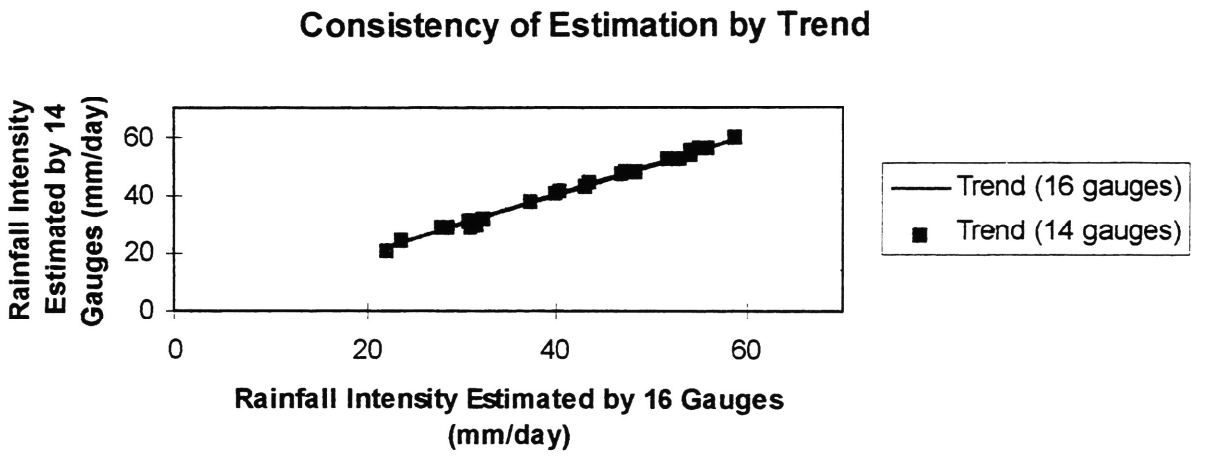

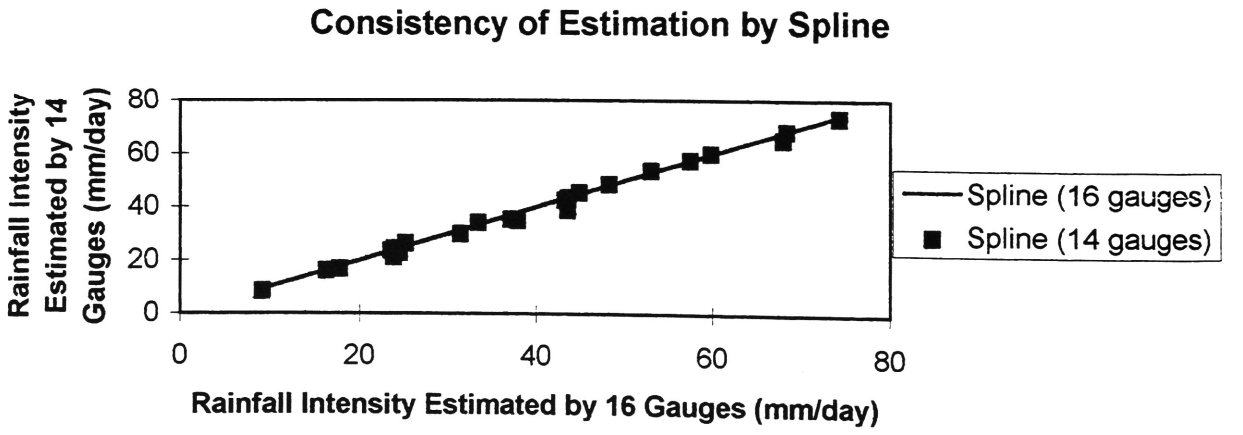

Figure 32 - Consistency of Estimation of the Rainfall Models for the Event on 6 Nov 92

7.3.4 Summary of Comparison

The five rainfall models were subjected to various tests to assess their strength and weakness. Presented in Tables 16 and 17 are summaries of the tests that were carried out in the previous sections. In these tables the results were ranked, with Rank 1 being considered as the best of all.

TABLE 16
SUMMARY OF COMPARISON FOR THE ARTIFICIAL RAINSTORM EVENT

Artificial Rainstorm Event					
	Thiessen Polygons	Inverse Distance Weighted	Kriging	Trend	Spline
Replicating the rainfall pattern	Rank 5. Not able to produce a real rainfall pattern.	Rank 4. Isolated peaks and troughs at gauge points.	Rank 3. Good in replicating the real rainfall pattern.	Rank 2. Excellent in replicating the real rainfall pattern.	Rank 1. Excellent in replicating the real rainfall pattern.
Estimating subcatchment rainfall (Based on sum or root mean square error)	Rank 4	Rank 5	Rank 3	Rank 2	Rank 1
Detecting peak values	N/A	N/A	Rank 3	Rank 2	Rank 1
Tracking storm movement	N/A	N/A	Rank 2	Rank 3	Rank 1
Estimating missing values	N/A	N/A	Rank 3	Rank 2	Rank 1
Consistency in estimation before and after omission of some gauges	N/A	N/A	Fair	Good	Good

TABLE 17
SUMMARY OF COMPARISON FOR THE REAL RAINSTORM EVENTS

The 5 and 6 Nov 92 Rainstorm Events					
	Thiessen Polygons	Inverse Distance Weighted	Kriging	Trend	Spline
Constructing rainfall pattern	Not tested.	Not tested.	Uniform rainfall over the whole catchment.	A reasonable rainfall pattern.	A reasonable rainfall pattern as if constructed by human.
Estimating subcatchment rainfall	All five rainfall models predicted rainfall volumes were within 10% of the mean volumes. Of the five models, Spline had the greatest variation from the average values while Kriging produced the smoothest rainfall surface.				
Estimating missing values	N/A	N/A	Rank 3	Rank 2	Rank 1
Consistency in estimation before and after omission of some gauges	N/A	N/A	Quite consistent. Kriging had a random deviation between the two estimation.	Very consistent.	Very consistent.

Before summarising the comparison, it must be pointed out that the tests in this study were by no means exhaustive; in the sense that not all the attributes of the alternative models were tested. For example, higher or lower order polynomials could be used in the Trend method; similarly, various methods could be used to fit the semivariogram in the Kriging method. In this study, only the most common option in each rainfall model was adopted for testing. This was due to the main focus of the study being the demonstration of the application of GIS for rainfall modelling and to make a general comparison of the available techniques within ARC/INFO. An extensive investigation into each rainfall model was beyond the scope of this study.

The Spline method provided the best overall performance in this study. It could closely replicate the theoretical rainfall patterns of the artificial event, and construct reasonable patterns of rainfall for the two real events. It also produced the closest estimation for the subcatchment rainfall values. In tracking the storm movement and storm peak values, the

Spline method was again the best. In addition, Spline's performance was not unduly influenced by missing values.

Based on the results of this study, the Spline method was considered to provide the best estimator for the rainfall distribution. The good performance of the Spline method is attributable to its ability to use the available data, while retaining small-scale features at the measurement points. This is achieved by the fact that Spline surfaces pass through all data points with minimum curvatures.

The Trend method was the second best. It was not as good as the Spline method because it made a global fitting of all data points while details at data points were lost. The use of higher order polynomials could get a closer fit to the data points, but would result in wavy surfaces and demanded greater computational efforts.

In theory, Kriging is an optimal interpolator and should be able to produce a good estimation of the rainfall field, with minimum variances. The performance of Kriging was satisfactory in the artificial event, but not so good in the real events, especially as it failed to recognise any rainfall patterns for the two real events. Kriging also was not good at coping with missing data, the estimation being unduly influenced by the missing values. The performance of Kriging could be improved by trying various methods to get a better fit of the semivariogram, but it is suspected that this would not change the overall conclusions of this study.

The Thiessen method failed to replicate the rainfall patterns, nor accurately estimate subcatchment rainfalls. The average percentage error in estimating subcatchment rainfall was around 10 % with a range from –43 % to +58 %. This would certainly produce unreliable inputs for a subsequent water management model.

The Inverse Distance Weighted method did not show any superiority to the Thiessen method, although the former used a more complicated formulae in estimating the rainfall distribution. This result suggests that the rainfall field is not a simple function of square of distance.

8. CONCLUSION

The powerful spatial analysis capabilities of a Geographic Information System such as the ARC/INFO software suite has been demonstrated in this project through the development of spatial rainfall distribution models for the Upper Parramatta River Catchment.

The rainfall models were built upon an automated procedure written in ARC/INFO's macro language. With minor modifications, the procedure can be easily applied to any catchments and operated by users with a basic understanding of ARC/INFO or any other Geographic Information Systems. The procedure developed in this study also can be adopted for real-time applications. For example, running the models during a rainstorm event to give a real-time estimation of the rainfall distribution in time and space. This information can be used as input for a water management model to assess the impact of the storm event on a catchment.

In this study, a general comparison was made of five rainfall distribution models. Each of them implemented a spatial analysis technique available in the ARC/INFO. The techniques used were: Thiessen Polygon, Inverse Distance Weighted, Kriging, Trend and Spline.

An artificial and two real rainstorm events were applied to the alternative rainfall models to assess their accuracy and reliability. Each model produced similar results on estimating total volume of rainfall over the catchement. However, there were marked differences in producing the rainfall patterns and, consequently, giving significantly different estimations of subcatchment rainfall values.

Among the five rainfall models, the Spline method showed the best estimation of the patterns of rainfall for both artificial and real events.

Tested in the artificial event with a Gaussian spatial distribution of rainfall, the Spline method was found to be the most accurate method in reproducing the theoretical rainfall distribution and estimating the subcatchment mean rainfall values. It was also the best method in tracking the peak values of the storm and their positions.

For the real storm events on 5 and 6 November 92, the Spline method was able to produce reasonable patterns of rainfall based on the available gauge readings. It was also shown that the Spline method produced consistent estimation regardless of missing data.

Based on the results of this study, the Spline method proved to be a robust and accurate estimator for spatially variable rainfall. In the past, the implementation of such a sophisticated technique required special programming effort and thus limited its application. Now, with the ARC/INFO GIS, this and other powerful techniques are readily available to all GIS users. With the enhancement in rainfall modelling, the catchment responses can be more accurately determined, thus improving our capability in management of water in a catchment.

9. REFERENCES

Ball, J. E. (1992), "A Review of Numerical Models for Prediction of Catchment Water Quantity and Quality, Water Research Laboratory, *Research Report* No 180/38.

Ball, J. E. (1994), "The Influence of Storm Temporal Patterns on Catchment Response", *Journal of Hydrology*, 158, p285-303.

Beven, K. J. and Hornberger, G. M. (1982), "Assessing the Effect of Spatial Pattern of Precipitation in Modelling Stream Flow Hydrographs", *Water Resources Bulletin*, Vol. 18, No. 5. p 823-829.

Burrough, P. A. (1986), *Principles of Geographical Information Systems for Land Resources Assessment*, Clarendon Press, Oxford.

Creutin, J. D. and Obled, C. (1982), "Objective Analyses and Mapping Techniques for Rainfall Fields: An Objective Comparison", *Water Resources Research*, Vol. 18, No. 2, p413-431.

Environmental Systems Research Institute, Inc. (ESRI) (1995), *Understanding GIS – The ARC/INFO Method*, 3rd edition.

Fontaine, T. A. (1991), "Predicting Measurement Error of Areal Mean Precipitation During Extreme Events", *Water Resources Bulletin*, Vol. 27, No. 3, p. 509-520.

Gandin, L. S. (1965), *Objective Analysis of Meteorological Fields*, Israel Program for Scientific Trainslations. Jeruslaem, 242 pp.

Hamlin, M. J. (1983), "The Significance of Rainfall in the Study of Hydrological Process at Basin Scale", *Journal of Hydrology*, 65, p73-94.

Hutchinson, M. F. (1991), "The Application of Thin Plate Smoothing Splines to Continent-Wide Data Assimilation", in Jasper, J. D. (editor), *Data Assimilation Systems*, Research Report No. 27, Bureau of Meteorology, Australia, pp 104-113.

Laurenson, E. M. (1964), "A Catchment Storage Model for Runoff Routing", *Journal of Hydrology*, 2:141-163.

Matheron, G. (1963), "Principles of Geostatics", *Economic Geology*, Vol. 58, pp. 1246-1266.

Matheron, G. (1971), "The Theory of Regionalized Variables and Its Application", *Les Cahrers du Centre de Morphologie Mathematique*, Fas. 5, C. G. Fontainebleau.

Muzik, I. (1993), "Application of a GIS to Assess Changes in Flood Hydrology of Urbanizing Watersheds", Chapter 20 in *New Techniques for Modelling the Management of Stormwater Quality Impacts.* Edited by William James. Published by Lewis Publishers.

Patrick, N. A. and Stephenson, D. (1990), "Spatial Variation of Rainfall Intensities for Short Duration Storms", *Hydrological Sciences Journal*, 35, 6, p667-680.

Pandyal, G. N. and Syme, M. J. (1994), "Bangladesh Flood Management Model - Towards a Spatial Decision Support System", *2nd International Conference on River Flood Hydraulics*. Edited by White, W. R. and Watts, J. p.167-176.

Peuquet, D., and Marble, D. F. (1990), Eds., *Introductory Readings in Geographic Information Systems*, Taylor & Francis, London.

Stuebe, M. M. and Johnston, D. M. (1990), "Runoff Volume Estimation Using GIS Techniques", *Water Resources Bulletin*, Vol. 26, No. 4. p.611-620.

Tabios III, G. Q. and Salas, J. D. (1986), "A Comparative Analysis of Techniques for Spatial Interpolation of Precipitation", *Water Resources Bulletin*, Vol. 21, No. 3, p365-380.

Thiessen, A. H. (1911), "Precipitation Averages for Large Areas", *Monthly Weather Review* 39(7):1082-1084.

Urbonas, B. R., Guo, J. C. Y. and Janesekok, M. P. (1992), "Hyetograph Density Effects on Urban Runoff Modelling", *Proc. International Conf. On Computer Applications in Water Resources*, Tamkang University, Tamsui, Taiwan, pp 32-37.

Watson, D. F. and Philip, G. M. (1985), "A Refinement of Inverse Distance Weighted Interpolation", *Geo-Processing*, 2: pp 315-327.

Wilson, C. B., et al. (1979), "On the Influence of the Spatial Distribution of Rainfall on Storm Runoff", *Water Resources Research*, Vol. 15, No. 2, p321-328

WP Software (1995), *RAFTS-XP: Runoff Analysis and Flow Training Simulation Incorporating the Expert User Environment – Version 5*, Unpublished Report, WP Software, Belconnen, ACT, Australia.

APPENDIX A

THEORY OF SOME INTERPOLATION METHODS DISCUSSED IN THE LITERATURE REVIEW BUT NOT AVAILABLE IN ARC/INFO

This appendix provides a brief introduction of some interpolation methods discussed in the literature review. As of the time of writing this report, these methods were not available in the ARC/INFO GIS, therefore they were not discussed in Chapter 3 and were not applied in this study.

The following discussion are mainly abstracted from Creutin, J. D. and Obled, C (1982).

1. Gandin's Optimal Interpolation

Gandin's method was developed by L. S. Gandin (1965). In this method, the value at the ungauged point j is estimated as a linear combination of n surrounding observed values:

$$z^*(t^0) = \sum_{i=1}^{n} \lambda_i z(t^i) \qquad \text{(A1)}$$

The weights λ_i are determined by minimising the estimation variance

$$E[(z(t^0) - z^*(t^0))^2] \qquad \text{(A2)}$$

which leads to Gandin's system:

$$\sum_{i=1}^{n} \lambda_i * C(t^i, t^j) = C(t^j, t^0) \qquad \text{(A3)}$$

where j = 1,...,n and

C(t,t') = E[z(t)z(t')] is a covariance.

If the estimator is to be unbiased, i.e., E[(z(t')] = E[z*(t')], either a constraint should be applied to the weights λ_i or the expectations E[(z(t)] must be equal to zero. In the Gandin method, the E(z(t)] term is assumed zero while the Kriging applies a constraint on the weights .

According to Cretin and Obled, the Gandin's method relies on three hypotheses.

a. The events considered are realisations of a unique random process or come from the same population. [This may be false if, for example, the rainfall patterns differ systematically according to weather types.]

b. Weak stationarity or homogeneity is usually assumed when choosing the correlation function.

c. The mean field m(t) = E[z(t)] and eventually the standard deviation field $\sigma(t)$ are available separately.

2. Orthogonal Functions (EOF)

This method used empirical orthogonal functions (EOF). It comes from the method known as Karhunen-Loeve expansion for unidimensional random processes over an interval (a, b). These expansions are orthogonal in that the functions used are orthogonal over (a, b). The EOF method is based on the 2-dimensional Karhunen-Loeve expansion.

Expressed in mathematical terms, the random process is expanded as a linear combination of eigenfunctions φ_i:

$$z(t) = \sum_{i=1}^{\infty} Y_i \varphi_i(t) \qquad \text{(A4)}$$

where Y_i are coefficients of the expansion.

In practice, the estimation of the eigenfunctions requires a numerical solution, and splitting the continuous surface into small surface elements.

Details of the numerical methods for solving equation (A4) are beyond the scope of this study. Nevertheless, this method offers some interesting advantages. Notably, no model needs to be fitted to the correlation function as in the Gandin's or Kriging's methods. This

method is thus less constraining than Gandin's or Kriging in terms of homogeneity and isotropy requirements.

Like the Trend (polynomial) method, this method is a smoothing method and is used globally, since the whole surface domain is considered.

APPENDIX B

LIST OF DATA FILES, PROGRAMS AND MAPS

TABLE B.1
DATA FILES

File Name	Type	Description
par_catch.txt	lines	ASCII file of catchment boundary created by digitizer at Manly Vale.
par_subcat.txt	lines	ASCII file of sub-catchment boundary created by digitizer at Manly Vale.
par_gauge.txt	points	ASCII file of rain gauges co-ordinates.
par_stream.txt	lines	ASCII file of main streams created by digitizer at Manly Vale.
boundary.txt	lines	ASCII file of map boundary.
Bpoint.txt	points	ASCII file contains coordinates of centre of every grid cell of the catchment. It is used to facilitate the creation of artificial rainfall data files.
Gau1rain.awk	program	Unix awk program for generating rainfall with Gaussian distribution, centred at (308250, 6259250) and peak intensity = 20 mm/hr.
act1rain.dat	points	An output ASCII file generated by the gau1rain.awk program. It contains rainfall values at centre of every grid cell of the catchment.
gau2rain.awk	program	Unix awk program for generating rainfall with Gaussian distribution, centred at (305250, 6259250) and peak intensity = 50 mm/hr.
act2rain.dat	points	An output ASCII file generated by the gau2rain.awk program. It contains rainfall values at centre of every grid cell of the catchment.
gau3rain.awk	program	Unix awk program for generating rainfall with Gaussian distribution, centred at (302250, 6259250) and peak intensity = 30 mm/hr.
act3rain.dat	points	An output ASCII file generated by the gau3rain.awk program. It contains rainfall values at centre of every grid cell of the catchment.
gau4rain.awk	program	Unix awk program for generating rainfall with Gaussian distribution, centred at (299250, 6259250) and peak intensity = 20 mm/hr.
act4rain.dat	points	An output ASCII file generated by the gau4rain.awk program. It contains rainfall values at centre of every grid cell of the catchment.
gau5rain.awk	program	Unix awk program for generating rainfall with Gaussian distribution, centred at (296250, 6259250) and peak intensity = 10 mm/hr.
act5rain.dat	points	An output ASCII file generated by the gau5rain.awk program. It contains rainfall values at centre of every grid cell of the catchment.
zerorain.awk	program	Unix awk program for generating zero rainfall for each grid cell of the catchment.
zerorain.dat	points	An output ASCII file generated by the zerorain.awk program. It contains zero rainfall value at centre of every grid cell of the catchment.
*.res	text	ASCII result files stored under the info sub-directory.
result*.awk	program	AWK programs to extract and tabulate results from the *.res files for comparison.

TABLE B.2
PROGRAM FILES (PART 1)

File Name	Type	Description
mainrain.aml	program	Main program to call all relevant sub-programs to determine subcatchment rainfall by the corresponding methods. The input rainfall data are artificial.
genrain.aml	program	Sub-program called by mainrain.aml to generate Gaussian distributed rainfall on every grid cell.
getrain.aml	program	Sub-program called by mainrain.aml to extract rainfall for the 16 gauge positions.
actraindist.aml	program	Sub-program called by mainrain.aml to determine actual mean rainfall for the 24 sub-catchments.
actrainres.aml	program	Sub-program called by mainrain.aml to output actual mean rainfall for the 24 sub-catchments to an ASCII file.
killactmap.aml	program	Sub-program called by mainrain.aml to remove unwanted maps created by actraindist.aml.
kriraindist.aml	program	Sub-program called by mainrain.aml to determine mean rainfall for the 24 sub-catchments by the Kriging method.
krirainres.aml	program	Sub-program called by mainrain.aml to output mean rainfall estimated by Kriging for the 24 sub-catchments to an ASCII file.
killkrimap.aml	program	Sub-program called by mainrain.aml to remove unwanted maps created by kriraindist.aml.
tpgraindist.aml	program	Sub-program called by mainrain.aml to determine mean rainfall for the 24 sub-catchments by the Thiessen Polygon method.
tpgrainres.aml	program	Sub-program called by mainrain.aml to output mean rainfall estimated by Thiessen Polygon Method for the 24 sub-catchments to an ASCII file.
killtpgmap.aml	program	Sub-program called by mainrain.aml to remove unwanted maps created by tpgraindist.aml.
treraindist.aml	program	Sub-program called by mainrain.aml to determine mean rainfall for the 24 sub-catchments by the Trend method.
trerainres.aml	program	Sub-program called by mainrain.aml to output mean rainfall estimated by the Trend method for the 24 sub-catchments to an ASCII file.
killtremap.aml	program	Sub-program called by mainrain.aml to remove unwanted maps created by treraindist.aml.
idwraindist.aml	program	Sub-program called by mainrain.aml to determine mean rainfall for the 24 sub-catchments by the Inverse Distance Weighted method.
idwrainres.aml	program	Sub-program called by mainrain.aml to output mean rainfall estimated by Inverse Distance Weighted Method for the 24 sub-catchments to an ASCII file.
killidwmap.aml	program	Sub-program called by mainrain.aml to remove unwanted maps created by idwraindist.aml.
splraindist.aml	program	Sub-program called by mainrain.aml to determine mean rainfall for the 24 sub-catchments by the Spline method.
Splrainres.aml	program	Sub-program called by mainrain.aml to output mean rainfall estimated by the Spline method for the 24 sub-catchments to an ASCII file.
killsplmap.aml	program	Sub-program called by mainrain.aml to remove unwanted maps created by splraindist.aml.

TABLE B.3
PROGRAM FILES (PART 2)

File Name	Type	Description
realrain.aml	program	Main program to call the relevant sub-programs to determine subcatchment rainfall by the corresponding methods. The input rainfall data are real.
Zerorain.aml	program	Standalone program to create 16 grid maps containing zero values for each gauge site.
actrain51.aml	program	Standalone program to create 16 grid maps containing the actual rainfall values on 5 Nov 92.
Mergegrid51.aml	program	Standalone program to merge the 16 grid maps of real rainfall on 5 Nov 92 to one grid map.
actrain52.aml	program	Standalone program to create a grid map containing the actual rainfall values on 6 Nov 92.
Mergegrid52.aml	program	Standalone program to merge the 16 grid maps of real rainfall on 6 Nov 92 to one grid map.
Krigaurain.aml	program	Main program to call the relevant sub-program to get rainfall values estimated by the Kriging Method from the 16 gauge sites.
Kriraingau.aml	program	Sub-program called by krigaurain.aml to extract values from the 16 gauge sites.
krirgres.aml	program	Sub-program called by krigaurain.aml to output the results to an ASCII file.
Killkrigmap.aml	program	Sub-program called by krigaurain.aml to remove unwanted maps created by kriraingau.aml.
tregaurain.aml	program	Main program to call the relevant sub-program to get rainfall values estimated by the Trend Method from the 16 gauge sites.
Treraingau.aml	program	Sub-program called by tregaurain.aml to extract values from the 16 gauge sites.
Trergres.aml	program	Sub-program called by tregaurain.aml to output the results to an ASCII file.
Killtregmap.aml	program	Sub-program called by tregaurain.aml to remove unwanted maps created by treraingau.aml.
splgaurain.aml	program	Main program to call the relevant sub-program to get rainfall values estimated by the Spline Method from the 16 gauge sites.
Splraingau.aml	program	Sub-program called by splgaurain.aml to extract values from the 16 gauge sites.
splrgres.aml	program	Sub-program called by splgaurain.aml to output the results to an ASCII file.
Killtregmap.aml	program	Sub-program called by splgaurain.aml to remove unwanted maps created by splraingau.aml.
testmisgau.aml	program	Main program to call relevant sub-programs to test the rainfall estimation when some gauges were malfunctioning. The rainfall inputs were from real events on 5 Nov 92 and 6 Nov 92.
Mergegrid53.aml	program	Sub-program called by testmisgau.aml to create a grid map containing real rainfall values on 5 Nov 92, but with missing values at gauges 1 and 7.
Mergegrid54.aml	program	Sub-program called by testmisgau.aml to create a grid map containing real rainfall values on 6 Nov 92, but with missing values at gauges 1 and 7.
Testmisart.aml	program	Main program to call relevant sub-programs to test the rainfall estimation when some gauges were malfunctioning. The rainfall input were from artificial events.

TABLE B.4
MAP FILES

File Name	Type	Description
ccbn	polygons	Catchment boundary.
cmpb	polygons	Map boundary.
cscb	polygons	Sub-catchment boundaries.
cstr	arcs	Streams.
crga	points	Rain gauges.
ctpg	polygons	Thiessen polygons.
gcbn	grid	Catchment grid.
Gscb	grid	Sub-catchment grid.
Grga	grid	Rain gauges.
cact%i%rain	points	Artificial rainfall on every pixel of the catchment. %i% = integer.
gact%i%rain	grid	Artificial rainfall on every grid of the catchment. %i% = integer.
gact%i%rgs	grid	Artificial/Actual rainfall at gauge locations. %i% = integer. %j% = 1, ..., 16.
gact%i%zme	grid	Artificial rainfall on 24 subcatchments. %i% = integer.
gact%i%scr%k%	grid	Artificial rainfall on each subcatchment. %i% = integer. %k% = 1, ..., 24.
cact%i%krir	points	Artificial/Actual rainfall at gauge locations. %i% = integer.
gkri%i%rain	grid	Rainfall distribution on all grid cells of the catchment estimated by Kriging. %i% = integer.
gkri%i%zme	grid	Mean rainfall on 24 subcatchments estimated by Kriging. %i% = integer.
gkri%i%scr%k%	grid	Mean rainfall on each subcatchment estimated by Kriging. %i% = integer. %k% = 1, ..., 24.
gtpg	grid	Thiessen polygons.
gtpg%i%rain	grid	Rainfall distribution on all grid cells determined by Thiessen Polygon Method. %i% = integer.
gtpg%i%zme	grid	Mean rainfall on sub-catchments determined by Thiessen Polygon Method. %i% = integer.
gtpg%i%scr%k%	grid	Mean rainfall on each sub-catchment determined by Thiessen Polygon Method. %i% = integer. %k% = 1, ..., 24.
cact%i%trer	points	Artificial/Actual rainfall at gauge locations. %i% = integer.
gtre%i%rain	grid	Rainfall distribution on all grid cells of the catchment estimated by the Trend method. %i% = integer.
gtre%i%zme	grid	Mean rainfall on 24 subcatchments estimated by the Trend method. %i% = integer.
gtre%i%scr%k%	grid	Mean rainfall on each subcatchment estimated by the Trend method. %i% = integer. %k% = 1, ..., 24.
cact%i%idwr	points	Artificial/Actual rainfall at gauge locations. %i% = integer.
gidw%i%rain	grid	Rainfall distribution on all grid cells of the catchment estimated by The Inverse Distance Weighted method. %i% = integer.
gidw%i%zme	grid	Mean rainfall on 24 subcatchments estimated by The Inverse Distance Weighted method. %i% = integer.
gidw%i%scr%k%	grid	Mean rainfall on each subcatchment estimated by The Inverse Distance Weighted method. %i% = integer. %k% = 1, ..., 24.
cact%i%splr	points	Artificial/Actual rainfall at gauge locations. %i% = integer.
gspl%i%rain	grid	Rainfall distribution on all grid cells of the catchment estimated by The Spline method. %i% = integer.
gspl%i%zme	grid	Mean rainfall on 24 subcatchments estimated by The Spline method. %I% = integer.
gspl%i%scr%k%	grid	Mean rainfall on each subcatchment estimated by The Spline method. %I% = integer. %k% = 1, ..., 24.

APPENDIX C

DATA DICTIONARY (SAMPLE)

Map Name : *cstr* _____ *1* of *1*

Description: *Mainstreams of the Catchment (arcs)*

I. DATA DICTIONARY

Attribute Name	Attribute Type and Details	Field width	Type	No of dec.	Unit	Attribute Value		
						Max	Min	Typical
FNODE#	*From node*	*4*	*B*	-	-			
TNODE#	*To node*	*4*	*B*	-	-			
LPOLY#	*Left polygon*	*4*	*B*	-	-			
RPOLY#	*Right polygon*	*4*	*B*	-	-			
LENGTH	*Length of stream*	*4*	*F*	*3*	*m*	*6450*	*296*	
CSTR#	*Internal-ID*	*4*	*B*	-	-	*22*	*1*	
CSTR#	*user-ID*	*4*	*B*	-	-	*22*	*1*	

APPENDIX D

QUALITY AND ACCURACY REPORT (SAMPLE)

I. GENERAL DETAILS

Coverage Descriptions : *cscb - subcatchment boundaries of the Upper Parramatta River Catchment*

Coverage Extent : _____

Hardware : *Sun SPARC II*

Operating System Platform: *Sun OS 4.1.3*

Software : *ARC INFO 7.0.3*

Data Structure : *X* Vector _____ Raster

II. SOURCE MATERIAL NO : *1*

Source : *Upper Parramatta River Catchment Trust*

Call Reference : _____

Date : _____/ *May* /*95*

Description : *RAFTS rainfall runoff model - Upper Parramatta River Sub-Catchment*

Scale : *1: 25000*

Datum : *Australian Height Datum*

Geographical Coordinates : *Australian Geodetic Datum 1966*

Map Projection : _____

Source Media : ___vellum _____mylar _____X_____paper map ___blueprint

___other _____

II. SOURCE MATERIAL NO : _____

Source : _____

Call Reference : _____

Date : _____/_____/_____

Description : _____

_____

Scale : _____ N/A

Datum : _____

Geographical Coordinates : _____

Map Projection : _____

Source Media : _____vellum _____mylar _____paper map _____blueprint

_____other _____

III. DATA AUTOMATION

Preautomation Compilation : _____

_____

Automation Equipment : *Digitizer*

Initial Automation : *Oct., 95*

Update Schedule : _____

Automation Algorithm : *ASCII format*

_____

IV. POSITIONAL ACCURACY

Completness : _____(%)

Positional Accuracy : _____

(relative to source materials)

Date of Check : _____/_____/_____

N/A

V. ATTRIBUTE ACCURACY

Completeness : _____(%)

Date of Check : _____/_____/_____

VI. LOGICAL CONSISTENCY

A. Cartographic Tests

Duplicated line eliminated :	*X* Yes	____No	____Unknown
Overshoots eliminated:	*X* Yes	____No	____Unknown
Undershoots eliminated:	*X* Yes	____No	____Unknown
Silvers eliminated :	*X* Yes	____No	____Unknown

B. Topology Tests

No. of polygons : *24*

Are polygon-id assigned to each polygon : *X* Yes __No___Unknown

Do polygons have more than one polygon-id : _____Yes *X* No __Unknown

Are the polygon-id unique : *X* Yes ____No ____Unknown

No. of lines : _____

Are the line-id unique : ___Yes ___No ___Unknown

No. of points : _____

Are the point-id unique : ___Yes ___No ___Unknown

APPENDIX E

TABLE E.1 — Artificial Event No. 1: Gaussian Distributed Rainfall, Centred at (308250, 6259250)

Sub-Catchment No. (no.)	No. of Cell (no.)	Area (km^2)	Actual (mm/hr)	Thiessen (mm/hr)	% error of Thiessen (%)	Kriging (mm/hr)	% error of Kriging (%)	Trend (mm/hr)	% error of Trend (%)	Inverse Distance Weighted (I-D-W) (mm/hr)	% error of (I-D-W) (%)	Spline (mm/hr)	% error of Spline (%)
1	27	6.75	9.29	9.59	3.23	10.06	8.29	9.30	0.11	10.11	8.83	9.24	-0.54
2	35	8.75	6.45	7.94	23.10	7.01	8.68	6.85	6.20	8.53	32.25	7.13	10.54
3	28	7.00	2.32	2.14	-7.76	2.51	8.19	2.55	9.91	4.02	73.28	2.83	21.98
4	36	9.00	13.58	13.08	-3.68	12.96	-4.57	13.99	3.02	12.56	-7.51	13.71	0.96
5	14	3.50	14.00	14.28	2.00	13.96	-0.29	14.00	0.00	13.17	-5.93	14.00	0.00
6	23	5.75	5.65	7.04	24.60	5.72	1.24	6.02	6.55	7.38	30.62	5.96	5.49
7	13	3.25	11.92	11.61	-2.60	12.00	0.67	12.02	0.84	11.72	-1.68	11.98	0.50
8	23	5.75	18.21	16.95	-6.92	16.26	-10.71	18.90	3.79	14.38	-21.03	19.13	5.05
9	19	4.75	0.73	0.84	15.07	0.56	-23.29	0.07	-90.41	1.56	113.70	0.57	-21.92
10	6	1.50	2.16	1.50	-30.56	1.85	-14.35	1.67	-22.69	2.65	22.69	1.78	-17.59
11	23	5.75	15.86	14.95	-5.74	15.55	-1.95	15.44	-2.65	14.39	-9.27	15.69	-1.07
12	17	4.25	4.58	4.00	-12.66	4.59	0.22	5.01	9.39	4.86	6.11	4.48	-2.18
13	8	2.00	1.87	1.37	-26.74	1.64	-12.30	1.51	-19.25	2.09	11.76	1.58	-15.51
14	14	3.50	9.00	8.50	-5.56	8.85	-1.67	9.20	2.22	9.71	7.89	8.75	-2.78
15	10	2.50	2.79	3.00	7.53	2.74	-1.79	2.82	1.08	3.49	25.09	2.67	-4.30
16	4	1.00	11.25	12.25	8.89	11.20	-0.44	11.39	1.24	11.59	3.02	11.17	-0.71
17	12	3.00	16.50	15.91	-3.58	15.70	-4.85	16.63	0.79	14.07	-14.73	16.92	2.55
18	12	3.00	0.33	0.08	-75.76	0.20	-39.39	-0.13	-139.39	0.74	124.24	0.29	-12.12
19	17	4.25	3.76	3.35	-10.90	3.90	3.72	4.05	7.71	4.34	15.43	3.98	5.85
20	18	4.50	12.33	12.33	0.00	12.29	-0.32	12.53	1.62	12.10	-1.87	12.33	0.00
21	18	4.50	5.72	6.55	14.51	5.74	0.35	6.10	6.64	6.32	10.49	5.89	2.97
22	31	7.75	1.22	1.35	10.66	1.09	-10.66	0.97	-20.49	2.24	83.61	1.36	11.48
23	11	2.75	8.63	12.00	39.05	8.80	1.97	9.15	6.03	9.69	12.28	8.80	1.97
24	19	4.75	4.52	2.57	-43.14	4.63	2.43	4.60	1.77	4.65	2.88	4.46	-1.33
Volume of Rainfall (mm-km^2/hr)			855.73	856.84		844.41		869.48		878.49		872.89	
Root Mean Square Error					1.04		0.51		0.36		1.30		0.31
No. of Closest Estimation					3		9		5		1		7

APPENDIX E

TABLE E.2 — Artificial Event No. 2: Gaussian Distributed Rainfall, Centred at (305250, 6259250)

Sub-Catchment No. (no.)	No. of Cell (no.)	Area (km^2)	Actual (mm/hr)	Thiessen (mm/hr)	% error of Thiessen (%)	Kriging (mm/hr)	% error of Kriging (%)	Trend (mm/hr)	% error of Trend (%)	Inverse Distance Weighted (I-D-W) (mm/hr)	% error of (I-D-W) (%)	Spline (mm/hr)	% error of Spline (%)
1	27	6.75	28.18	27.29	-3.16	28.96	2.77	29.41	4.36	31.08	10.29	28.09	-0.32
2	35	8.75	28.37	30.25	6.63	28.43	0.21	28.76	1.37	31.54	11.17	28.51	0.49
3	28	7.00	17.39	14.67	-15.64	17.12	-1.55	17.23	-0.92	19.99	14.95	17.82	2.47
4	36	9.00	30.61	30.50	-0.36	30.72	0.36	31.44	2.71	32.14	5.00	30.99	1.24
5	14	3.50	41.92	40.42	-3.58	40.97	-2.27	42.68	1.81	39.35	-6.13	41.64	-0.67
6	23	5.75	30.47	33.08	8.57	29.39	-3.54	29.70	-2.53	31.24	2.53	30.41	-0.20
7	13	3.25	44.38	43.30	-2.43	43.55	-1.87	43.15	-2.77	42.26	-4.78	44.06	-0.72
8	23	5.75	40.47	44.34	9.56	40.63	0.40	41.65	2.92	40.56	0.22	41.62	2.84
9	19	4.75	10.52	12.63	20.06	10.69	1.62	10.44	-0.76	14.24	35.36	10.70	1.71
10	6	1.50	17.33	16.33	-5.77	17.25	-0.46	17.18	-0.87	18.71	7.96	17.50	0.98
11	23	5.75	48.30	47.00	-2.69	47.45	-1.76	47.64	-1.37	44.77	-7.31	48.01	-0.60
12	17	4.25	29.23	28.00	-4.21	28.51	-2.46	28.76	-1.61	28.03	-4.11	29.11	-0.41
13	8	2.00	17.12	15.75	-8.00	16.94	-1.05	17.39	1.58	17.31	1.11	17.09	-0.18
14	14	3.50	40.85	37.50	-8.20	39.34	-3.70	39.30	-3.79	37.84	-7.37	40.81	-0.10
15	10	2.50	21.79	22.89	5.05	21.20	-2.71	22.47	3.12	21.68	-0.50	21.67	-0.55
16	4	1.00	45.50	46.25	1.65	44.36	-2.51	43.78	-3.78	43.18	-5.10	45.41	-0.20
17	12	3.00	45.41	45.08	-0.73	45.01	-0.88	45.68	0.59	42.79	-5.77	45.67	0.57
18	12	3.00	8.16	6.66	-18.38	7.96	-2.45	8.37	2.57	9.38	14.95	8.15	-0.12
19	17	4.25	24.82	22.17	-10.68	23.75	-4.31	25.89	4.31	23.13	-6.81	24.62	-0.81
20	18	4.50	43.50	44.33	1.91	42.86	-1.47	43.34	-0.37	41.99	-3.47	43.48	-0.05
21	18	4.50	30.61	30.00	-1.99	29.01	-5.23	31.49	2.87	27.96	-8.66	30.52	-0.29
22	31	7.75	12.80	12.29	-3.98	12.33	-3.67	13.65	6.64	15.04	17.50	12.84	0.31
23	11	2.75	37.90	46.00	21.37	36.68	-3.22	38.58	1.79	36.76	-3.01	38.14	0.63
24	19	4.75	23.94	17.73	-25.94	23.68	-1.09	25.15	5.05	22.72	-5.10	23.99	0.21
Volume of Rainfall (mm-km^2/hr)			3206.47	3183.30		3159.87		3237.69		3234.73		3216.72	
Root Mean Square Error					2.70		0.79		0.86		2.16		0.30
No. of Closest Estimation					1		3		2		2		17

APPENDIX E

TABLE E.3 — Artificial Event No. 3: Gaussian Distributed Rainfall, Centred at (302250, 6259250)

Sub-Catchment No. (no.)	No. of Cell (no.)	Area (km^2)	Actual (mm/hr)	Thiessen (mm/hr)	% error of Thiessen (%)	Kriging (mm/hr)	% error of Kriging (%)	Trend (mm/hr)	% error of Trend (%)	Inverse Distance Weighted (I-D-W) (mm/hr)	% error of (I-D-W) (%)	Spline (mm/hr)	% error of Spline (%)
1	27	6.75	13.14	12.40	-5.63	13.64	3.81	13.56	3.20	15.68	19.33	12.75	-2.97
2	35	8.75	19.20	18.71	-2.55	18.71	-2.55	19.04	-0.83	19.33	0.68	19.12	-0.42
3	28	7.00	17.71	14.92	-15.75	16.98	-4.12	17.97	1.47	16.93	-4.40	18.36	3.67
4	36	9.00	10.72	10.75	0.28	11.86	10.63	10.93	1.96	13.23	23.41	10.56	-1.49
5	14	3.50	19.64	18.57	-5.45	18.99	-3.31	20.60	4.89	19.19	-2.29	19.42	-1.12
6	23	5.75	25.13	25.34	0.84	23.05	-8.28	23.94	-4.74	22.31	-11.22	25.46	1.31
7	13	3.25	25.53	25.53	0.00	24.44	-4.27	24.86	-2.62	24.36	-4.58	25.36	-0.67
8	23	5.75	14.17	18.39	29.78	16.34	15.31	14.78	4.30	18.66	31.69	14.58	2.89
9	19	4.75	15.36	17.52	14.06	15.55	1.24	16.81	9.44	17.16	11.72	15.91	3.58
10	6	1.50	20.50	20.33	-0.83	19.59	-4.44	21.09	2.88	19.57	-4.54	21.22	3.51
11	23	5.75	23.52	23.73	0.89	22.99	-2.25	23.51	-0.04	22.72	-3.40	23.45	-0.30
12	17	4.25	26.88	27.00	0.45	25.02	-6.92	25.65	-4.58	24.85	-7.55	26.98	0.37
13	8	2.00	20.87	20.00	-4.17	19.91	-4.60	21.62	3.59	19.60	-6.09	21.13	1.25
14	14	3.50	29.00	26.50	-8.62	26.43	-8.86	27.07	-6.66	24.13	-16.79	28.72	-0.97
15	10	2.50	23.60	23.79	0.81	21.75	-7.84	23.84	1.02	20.78	-11.95	23.50	-0.42
16	4	1.00	28.50	26.75	-6.14	26.43	-7.26	26.91	-5.58	25.32	-11.16	27.99	-1.79
17	12	3.00	19.58	20.58	5.11	20.83	6.38	19.88	1.53	21.19	8.22	20.27	3.52
18	12	3.00	13.08	11.66	-10.86	13.23	1.15	14.36	9.79	13.15	0.54	13.30	1.68
19	17	4.25	23.47	21.82	-7.03	21.34	-9.08	23.68	0.89	20.27	-13.63	23.02	-1.92
20	18	4.50	23.94	24.66	3.01	23.17	-3.22	23.62	-1.34	23.04	-3.76	23.82	-0.50
21	18	4.50	24.83	22.55	-9.18	22.26	-10.35	24.52	-1.25	20.79	-16.27	24.09	-2.98
22	31	7.75	16.45	15.06	-8.45	15.58	-5.29	17.71	7.66	15.79	-4.01	16.47	0.12
23	11	2.75	25.81	27.00	4.61	23.50	-8.95	25.19	-2.40	22.70	-12.05	25.06	-2.91
24	19	4.75	18.73	14.94	-20.23	18.14	-3.15	19.15	2.24	17.41	-7.05	18.33	-2.14
Volume of Rainfall ($mm\text{-}km^2/hr$)			2143.39	2095.74		2077.52		2155.48		2096.41		2141.73	
Root Mean Square Error					1.73		1.48		0.88		2.39		0.42
No. of Closest Estimation					4		1		5		1		13

APPENDIX E

TABLE E.4 — Artificial Event No. 4: Gaussian Distributed Rainfall, Centred at (299250, 6259250)

Sub-Catchment No. (no.)	No. of Cell (no.)	Area (km^2)	Actual (mm/hr)	Thiessen (mm/hr)	% error of Thiessen (%)	Kriging (mm/hr)	% error of Kriging (%)	Trend (mm/hr)	% error of Trend (%)	Inverse Distance Weighted (I-D-W) (mm/hr)	% error of (I-D-W) (%)	Spline (mm/hr)	% error of Spline (%)
1	27	6.75	4.44	4.25	-4.28	7.19	61.94	4.12	-7.21	6.31	42.12	4.27	-3.83
2	35	8.75	9.62	8.97	-6.76	9.75	1.35	9.87	2.60	9.49	-1.35	9.64	0.21
3	28	7.00	13.60	11.53	-15.22	12.06	-11.32	13.96	2.65	11.97	-11.99	13.61	0.07
4	36	9.00	2.61	2.66	1.92	6.43	146.36	2.53	-3.07	4.28	63.98	2.57	-1.53
5	14	3.50	6.78	7.00	3.24	7.98	17.70	7.23	6.64	7.59	11.95	7.23	6.64
6	23	5.75	15.47	14.95	-3.36	12.97	-16.16	15.29	-1.16	13.02	-15.84	15.54	0.45
7	13	3.25	10.92	11.46	4.95	10.39	-4.85	11.10	1.65	10.85	-0.64	11.22	2.75
8	23	5.75	3.47	5.47	57.64	7.47	115.27	3.72	7.20	6.65	91.64	3.14	-9.51
9	19	4.75	16.68	17.05	2.22	14.21	-14.81	17.06	2.28	15.75	-5.58	16.26	-2.52
10	6	1.50	18.16	18.16	0.00	14.74	-18.83	18.10	-0.33	16.01	-11.84	17.82	-1.87
11	23	5.75	8.34	8.91	6.83	8.96	7.43	8.60	3.12	8.68	4.08	8.29	-0.60
12	17	4.25	18.41	19.00	3.20	15.14	-17.76	17.78	-3.42	16.97	-7.82	18.50	0.49
13	8	2.00	18.87	18.12	-3.97	15.44	-18.18	18.78	-0.48	16.86	-10.65	18.60	-1.43
14	14	3.50	15.42	14.78	-4.15	12.87	-16.54	14.87	-3.57	12.38	-19.71	15.45	0.19
15	10	2.50	19.00	18.29	-3.74	15.35	-19.21	18.74	-1.37	15.83	-16.68	19.02	0.11
16	4	1.00	13.00	11.75	-9.62	11.51	-11.46	13.01	0.08	11.51	-11.46	13.20	1.54
17	12	3.00	6.00	6.41	6.83	8.50	41.67	6.02	0.33	7.80	30.00	5.71	-4.83
18	12	3.00	15.50	14.33	-7.55	13.77	-11.16	15.86	2.32	14.31	-7.68	15.33	-1.10
19	17	4.25	16.76	16.41	-2.09	13.95	-16.77	16.70	-0.36	14.53	-13.31	16.93	1.01
20	18	4.50	9.72	10.33	6.28	9.83	1.13	9.74	0.21	9.69	-0.31	9.83	1.13
21	18	4.50	14.94	14.05	-5.96	12.81	-14.26	15.03	0.60	13.00	-12.99	15.28	2.28
22	31	7.75	15.77	14.29	-9.38	13.57	-13.95	16.25	3.04	13.71	-13.06	15.82	0.32
23	11	2.75	12.90	12.00	-6.98	11.58	-10.23	12.87	-0.23	11.41	-11.55	13.13	1.78
24	19	4.75	11.00	9.47	-13.91	11.27	2.45	11.19	1.73	10.93	-0.64	11.18	1.64
Volume of Rainfall ($mm\text{-}km^2/hr$)			1242.48	1207.04		1205.17		1250.58		1191.60		1242.92	
Root Mean Square Error					0.94		2.41		0.29		1.81		0.22
No. of Closest Estimation					3		0		8		2		11

APPENDIX E

TABLE E.5 — Artificial Event No. 5: Gaussian Distributed Rainfall, Centred at (296250, 6259250)

Sub-Catchment No. (no.)	No. of Cell (no.)	Area (km^2)	Actual (mm/hr)	Thiessen (mm/hr)	% error of Thiessen (%)	Kriging (mm/hr)	% error of Kriging (%)	Trend (mm/hr)	% error of Trend (%)	Inverse Distance Weighted (I-D-W) (mm/hr)	% error of (I-D-W) (%)	Spline (mm/hr)	% error of Spline (%)
1	27	6.75	0.37	0.59	59.46	0.51	37.84	0.03	-91.89	1.10	197.30	0.60	62.16
2	35	8.75	2.17	1.68	-22.58	1.98	-8.76	2.15	-0.92	2.04	-5.99	1.83	-15.67
3	28	7.00	5.03	3.75	-25.45	4.48	-10.93	5.13	1.99	4.14	-17.69	4.52	-10.14
4	36	9.00	0.02	0.00	-100.00	0.11	450.00	0.21	950.00	0.47	2250.00	-0.17	-950.00
5	14	3.50	0.85	0.57	-32.94	0.65	-23.53	0.75	-11.76	1.04	22.35	0.64	-24.71
6	23	5.75	4.56	3.78	-17.11	4.02	-11.84	4.66	2.19	3.64	-20.18	3.98	-12.72
7	13	3.25	2.00	2.00	0.00	1.87	-6.50	1.94	-3.00	1.97	-1.50	1.90	-5.00
8	23	5.75	0.08	0.47	487.50	0.38	375.00	0.64	700.00	0.92	1050.00	0.01	-87.50
9	19	4.75	8.89	8.78	-1.24	8.54	-3.94	8.82	-0.79	7.77	-12.60	9.00	1.24
10	6	1.50	7.66	8.50	10.97	7.31	-4.57	7.66	0.00	6.92	-9.66	7.65	-0.13
11	23	5.75	1.21	1.52	25.62	1.29	6.61	1.03	-14.88	1.53	26.45	1.38	14.05
12	17	4.25	6.11	6.00	-1.80	5.61	-8.18	5.83	-4.58	5.47	-10.47	5.66	-7.36
13	8	2.00	8.62	8.62	0.00	8.09	-6.15	8.01	-7.08	7.67	-11.02	8.32	-3.48
14	14	3.50	3.85	3.71	-3.64	3.42	-11.17	3.56	-7.53	2.94	-23.64	3.35	-12.99
15	10	2.50	7.59	6.80	-10.41	6.98	-8.04	6.98	-8.04	6.18	-18.58	7.16	-5.67
16	4	1.00	2.50	2.00	-20.00	2.50	0.00	2.49	-0.40	2.18	-12.80	2.46	-1.60
17	12	3.00	0.66	1.00	51.52	1.00	51.52	0.84	27.27	1.37	107.58	0.92	39.39
18	12	3.00	9.00	9.00	0.00	8.84	-1.78	9.04	0.44	8.29	-7.89	9.02	0.22
19	17	4.25	5.70	5.35	-6.14	5.21	-8.60	5.31	-6.84	4.95	-13.16	5.22	-8.42
20	18	4.50	1.66	1.66	0.00	1.60	-3.61	1.59	-4.22	1.74	4.82	1.50	-9.64
21	18	4.50	4.33	3.88	-10.39	3.92	-9.47	3.99	-7.85	3.98	-8.08	3.76	-13.16
22	31	7.75	7.41	6.87	-7.29	7.16	-3.37	7.20	-2.83	6.35	-14.30	7.26	-2.02
23	11	2.75	2.90	2.00	-31.03	2.65	-8.62	2.68	-7.59	2.77	-4.48	2.38	-17.93
24	19	4.75	3.00	3.05	1.67	3.04	1.33	2.96	-1.33	3.51	17.00	2.82	-6.00
Volume of Rainfall (mm-km^2/hr)			391.68	366.68		371.38		383.27		366.60		368.35	
Root Mean Square Error					0.50		0.34		0.28		0.72		0.33
No. of Closest Estimation					7		5		9		1		3

APPENDIX F

TABLE F.1 — Real Event on 5 November 92

Sub-Catchment No. (no.)	No. of Cell (no.)	Area (km^2)	Mean (mm/hr)	Thiessen (mm/hr)	% diff. of Thiessen from Mean (%)	Kriging (mm/hr)	% diff. of Kriging from Mean (%)	Trend (mm/hr)	% diff. of Trend from Mean (%)	Inverse Distance Weighted (mm/hr)	% diff. of (I-D-W) from Mean (%)	Spline (mm/hr)	% diff. of Spline from Mean (%)
1	27	6.75	10.55	9.05	-14.19	13.07	23.93	11.19	6.11	10.33	-2.05	9.09	-13.81
2	35	8.75	12.95	12.73	-1.71	13.12	1.30	13.98	7.94	12.87	-0.63	12.06	-6.89
3	28	7.00	17.99	23.02	27.97	13.84	-23.06	16.99	-5.55	18.38	2.18	17.71	-1.55
4	36	9.00	9.44	9.04	-4.22	12.67	34.24	8.77	-7.08	9.84	4.26	6.87	-27.21
5	14	3.50	10.46	8.71	-16.70	12.34	18.02	10.50	0.42	10.50	0.42	10.23	-2.16
6	23	5.75	12.90	11.80	-8.51	13.56	5.13	13.68	6.06	13.55	5.06	11.90	-7.74
7	13	3.25	14.52	15.96	9.92	13.19	-9.16	12.13	-16.46	15.18	4.55	16.14	11.16
8	23	5.75	8.36	8.20	-1.91	12.59	50.60	8.56	2.39	10.04	20.10	2.41	-71.17
9	19	4.75	15.09	15.66	3.75	14.35	-4.93	13.55	-10.23	15.14	0.30	16.77	11.10
10	6	1.50	14.20	14.42	1.53	14.29	0.62	14.19	-0.08	14.29	0.62	13.82	-2.69
11	23	5.75	12.94	14.15	9.32	12.07	-6.75	11.66	-9.92	12.79	-1.19	14.05	8.54
12	17	4.25	11.49	9.00	-21.66	13.55	17.95	14.24	23.96	10.79	-6.08	9.86	-14.17
13	8	2.00	14.04	14.69	4.61	14.27	1.62	13.75	-2.08	14.17	0.91	13.33	-5.07
14	14	3.50	13.62	13.11	-3.74	12.88	-5.43	13.87	1.84	13.73	0.81	14.51	6.53
15	10	2.50	12.70	11.25	-11.40	14.12	11.20	14.58	14.82	12.61	-0.69	10.93	-13.92
16	4	1.00	14.92	16.62	11.36	12.33	-17.38	13.82	-7.40	15.04	0.78	16.81	12.64
17	12	3.00	9.48	8.88	-6.35	11.71	23.50	9.80	3.35	10.39	9.58	6.63	-30.08
18	12	3.00	13.45	13.67	1.67	14.19	5.53	11.56	-14.03	13.55	0.77	14.26	6.05
19	17	4.25	12.46	10.94	-12.20	12.92	3.69	15.23	22.23	12.09	-2.97	11.12	-10.75
20	18	4.50	12.42	13.33	7.34	11.77	-5.22	12.36	-0.47	12.13	-2.32	12.50	0.66
21	18	4.50	13.13	13.39	1.95	12.15	-7.49	15.10	14.97	12.57	-4.29	12.46	-5.13
22	31	7.75	12.72	12.00	-5.65	13.78	8.35	13.65	7.33	12.26	-3.60	11.90	-6.43
23	11	2.75	13.73	16.00	16.50	11.85	-13.72	14.36	4.56	13.10	-4.62	13.36	-2.72
24	19	4.75	12.65	13.11	3.60	12.10	-4.38	12.80	1.15	12.46	-1.53	12.80	1.15
Volume of Rainfall (mm-km^2/hr)			1373.23	1381.63		1425.30		1397.75		1381.58		1279.90	
Root Mean Square Error					1.54		1.88		1.33		0.53		1.77

APPENDIX F

TABLE F.2 — Real Event on 6 November 92

Sub-Catchment No. (no.)	No. of Cell (no.)	Area (km^2)	Mean (mm/hr)	Thiessen (mm/hr)	% diff. of Thiessen from Mean (%)	Kriging (mm/hr)	% diff. of Kriging from Mean (%)	Trend (mm/hr)	% diff. of Trend from Mean (%)	Inverse Distance Weighted (mm/hr)	% diff. of (I-D-W) from Mean (%)	Spline (mm/hr)	% diff. of Spline from Mean (%)
1	27	6.75	50.27	47.28	-5.95	44.46	-11.56	55.24	9.88	46.91	-6.69	57.47	14.32
2	35	8.75	38.44	39.00	1.45	44.24	15.08	42.98	11.80	42.48	10.50	23.51	-38.84
3	28	7.00	32.92	37.89	15.11	41.41	25.81	28.48	-13.48	39.06	18.67	17.74	-46.11
4	36	9.00	48.32	53.33	10.36	44.64	-7.62	48.31	-0.03	51.67	6.92	43.67	-9.63
5	14	3.50	49.06	44.36	-9.57	44.40	-9.49	54.14	10.36	49.30	0.50	53.08	8.20
6	23	5.75	37.85	39.39	4.07	42.17	11.42	40.32	6.53	43.50	14.93	23.86	-36.96
7	13	3.25	59.06	62.62	6.02	47.31	-19.90	55.91	-5.34	61.12	3.48	68.36	15.74
8	23	5.75	34.57	41.52	20.09	44.13	27.64	31.67	-8.40	46.36	34.09	9.19	-73.42
9	19	4.75	29.25	28.89	-1.24	37.71	28.91	23.73	-18.88	30.73	5.05	25.20	-13.85
10	6	1.50	31.34	31.33	-0.04	38.33	22.29	27.88	-11.05	34.69	10.68	24.49	-21.87
11	23	5.75	54.00	61.06	13.07	43.38	-19.67	52.97	-1.91	52.79	-2.24	59.80	10.74
12	17	4.25	42.34	43.00	1.55	39.16	-7.52	43.47	2.66	42.47	0.30	43.62	3.01
13	8	2.00	32.60	30.75	-5.69	37.73	15.72	30.79	-5.56	32.39	-0.66	31.36	-3.82
14	14	3.50	54.69	55.57	1.62	41.79	-23.58	55.00	0.57	53.10	-2.90	67.97	24.29
15	10	2.50	37.52	37.10	-1.12	37.10	-1.12	39.92	6.40	35.55	-5.25	37.93	1.09
16	4	1.00	61.04	69.25	13.45	42.56	-30.28	58.81	-3.66	60.29	-1.23	74.30	21.72
17	12	3.00	32.61	31.67	-2.88	43.38	33.03	32.27	-1.04	39.49	21.11	16.23	-50.23
18	12	3.00	25.82	22.58	-12.53	35.86	38.91	22.04	-14.63	24.69	-4.36	23.91	-7.38
19	17	4.25	37.12	32.00	-13.80	36.41	-1.92	46.80	26.07	33.24	-10.46	37.16	0.10
20	18	4.50	46.43	51.67	11.30	42.34	-8.80	47.23	1.73	45.95	-1.03	44.94	-3.20
21	18	4.50	42.67	41.72	-2.22	38.23	-10.40	51.69	21.15	38.38	-10.05	43.31	1.51
22	31	7.75	28.30	22.87	-19.18	37.04	30.89	30.82	8.91	26.93	-4.83	23.83	-15.79
23	11	2.75	50.46	64.00	26.84	38.80	-23.10	54.17	7.36	46.97	-6.91	48.34	-4.19
24	19	4.75	34.32	30.24	-11.88	38.07	10.94	37.35	8.84	32.51	-5.26	33.41	-2.64
Volume of Rainfall (mm-km^2/hr)			4464.01	4581.55		4523.36		4596.99		4602.11		4016.03	
Root Mean Square Error					4.84		8.37		4.05		3.94		9.62